Journal of
Medicinal Chemistry

Subscriber access provided by BIU Pharmacie | Faculté de Pharmacie, Université Paris V

Article

Synthesis and pharmacological characterization of conformationally restricted retigabine analogues as novel neuronal Kv7 channels activators

Carmine Ostacolo, Francesco Miceli, Veronica Di Sarno, Piera Nappi, Nunzio Iraci, Maria Virginia Soldovieri, Tania Ciaglia, Paolo Ambrosino, Vincenzo Vestuto, Anna Lauritano, Simona Musella, Giacomo Pepe, Manuela Giovanna Basilicata, Michele Manfra, Diego Romano Perinelli, Ettore Novellino, Alessia Bertamino, Isabel M. Gomez-Monterrey, Pietro Campiglia, and Maurizio Taglialatela

J. Med. Chem., **Just Accepted Manuscript** • DOI: 10.1021/acs.jmedchem.9b00796 • Publication Date (Web): 09 Dec 2019

Downloaded from pubs.acs.org on December 9, 2019

Just Accepted

"Just Accepted" manuscripts have been peer-reviewed and accepted for publication. They are posted online prior to technical editing, formatting for publication and author proofing. The American Chemical Society provides "Just Accepted" as a service to the research community to expedite the dissemination of scientific material as soon as possible after acceptance. "Just Accepted" manuscripts appear in full in PDF format accompanied by an HTML abstract. "Just Accepted" manuscripts have been fully peer reviewed, but should not be considered the official version of record. They are citable by the Digital Object Identifier (DOI®). "Just Accepted" is an optional service offered to authors. Therefore, the "Just Accepted" Web site may not include all articles that will be published in the journal. After a manuscript is technically edited and formatted, it will be removed from the "Just Accepted" Web site and published as an ASAP article. Note that technical editing may introduce minor changes to the manuscript text and/or graphics which could affect content, and all legal disclaimers and ethical guidelines that apply to the journal pertain. ACS cannot be held responsible for errors or consequences arising from the use of information contained in these "Just Accepted" manuscripts.

is published by the American Chemical Society. 1155 Sixteenth Street N.W., Washington, DC 20036

Published by American Chemical Society. Copyright © American Chemical Society. However, no copyright claim is made to original U.S. Government works, or works produced by employees of any Commonwealth realm Crown government in the course of their duties.

Synthesis and pharmacological characterization of conformationally restricted retigabine analogues as novel neuronal Kv7 channels activators

Carmine Ostacolo,[†,#] Francesco Miceli[¶,#], Veronica Di Sarno[‡,#], Piera Nappi[¶], Nunzio Iraci[‡], Maria Virginia Soldovieri[§], Tania Ciaglia[‡], Paolo Ambrosino[¥], Vincenzo Vestuto[‡], Anna Lauritano[¶], Simona Musella[⊥], Giacomo Pepe[‡], Manuela G. Basilicata[‡], Michele Manfra[□], Diego Romano Perinelli[□], Ettore Novellino[†], Alessia Bertamino[‡], Isabel M. Gomez-Monterrey[†], Pietro Campiglia[‡,], Maurizio Taglialatela[¶,*].*

† Department of Pharmacy, University Federico II of Naples, Via D. Montesano 49, 80131, Naples, Italy

¶ Department of Neuroscience, Reproductive Sciences and Dentistry, University Federico II of Naples, Via Pansini, 5, 80131, Naples, Italy

‡ Department of Pharmacy, University of Salerno, Via G. Paolo II 132, 84084, Fisciano, Salerno, Italy

§Department of Medicine and Health Science V. Tiberio, University of Molise, Via F. de Sanctis, 86100, Campobasso, Italy

¥ Department of Science and Technology (DST), University of Sannio, Via Port'Arsa 11, 82100, Benevento Italy;

□ Department of Science, University of Basilicata, Via dell'Ateneo Lucano 10, 85100 Potenza, Italy

□ School of Pharmacy, University of Camerino, Via Gentile III da Varano, 62032, Camerino (MC), Italy

⊥ European Biomedical Research Center (EBRIS), Via Salvatore de Renzi, 3, 84125 Salerno (SA), Italy

ABSTRACT

Kv7 K^+ channels represent an attractive pharmacological targets for the treatment of different neurological disorders, including epilepsy. In this paper, 42 conformationally restricted analogues of the prototypical Kv7 activator retigabine have been synthesized and tested by electrophysiological patch-clamp experiments as Kv7 agonists. When compared to retigabine (0.93±0.43 μM), the EC_{50}s for Kv7.2 current enhancements by compound **23a** (0.08±0.04 μM) was lower, whereas no change in potency was observed for **24a** (0.63±0.07 μM). In addition, compared to retigabine, **23a** and **24a** showed also higher potency in activating heteromeric Kv7.2/Kv7.3 and homomeric Kv7.4 channels**.** Molecular modeling studies provided new insights into the chemical features required for optimal interaction at the binding site. Stability studies evidenced improved chemical stability of **23a** and **24a** in comparison with retigabine. Overall, the present results highlight that the N5-alkylamidoindole moiety provides a suitable pharmacophoric scaffold for the design of chemically-stable, highly-potent and selective Kv7 agonists.

INTRODUCTION

Epilepsy is one of the most common neurological disorders affecting approximately 1% of the worlwide population. Although several classes of antiepiletic drugs are available for clinical use, about one third of patients do not benefit from currently-available medications; thus, drugs with novel mechanisms of actions might significantly reduce this figure.[1]

The K_v7 (KCNQ) subfamily of K^+ channels comprises five members, each showing a distinct tissue distribution and physiological roles.[2] $K_v7.2$ and $K_v7.3$ are the most abundant K_v7 subunits in the central and peripheral nervous system; heteromeric channels composed of $K_v7.2$ and $K_v7.3$ subunits are thought to underlie a K^+ current, named M-current (I_{KM}), whose activation reduces neuronal excitability by driving the membrane potential to values close to the equilibrium potential for K^+ ions, thus limiting repetitive firing and causing spike frequency adaptation. The critical role exerted by I_{KM} in controlling neuronal excitability is also highlighted by the observation that mutations in the genes encoding for $K_v7.2$ and $K_v7.3$ are responsible for a wide spectrum of epileptic diseases ranging from Benign Familial Neonatal Seizures to severe epileptic encephalopathies, and that drugs acting as Kv7 activators are potent anticonvulsants in humans.[3] Retigabine is the proptotype Kv7 activator, recognizing a hydrophobic pocket located in the pore domain;[4] within this cavity, H-bond interactions are established between the carbamate group of retigabine and a tryptophan residue in the channel pore (W236 in Kv7.2, W265 in Kv7.3).[5] Retigabine has been approved as an add-on treatment for drug-resistant partial onset seizures with or without secondary generalisation in people aged 18 or older, and has been on the market since 2011; however, because of a low benefit/risk ratio, clinical use of retigabine has been declining over the years, leading to its discontinuation in 2017. Several drawbacks are likely responsible for the limited clinical efficacy of retigabine which can be summarized as follows: a. Poor selectivity for Kv7 subtypes. Indeed, activation of Kv7.4/5 channels expressed in genitourinary smooth muscle cells seems responsible for one of the most frequently-reported side effect, namely urinary retention; b. Short half-life. Retigabine is metabolized by phase-II enzymes (acetylation and N-glucuronidation), with little involvement of the cytochrome P450

system. Consequently, retigabine has fast clearance kinetics ($t_{1/2}$ ~ 6-8 hours), and requires three-times-a-day dosing;[6] c. Poor brain penetration. Because of its limited lipophilicity (Log P= 3.08), the brain-plasma concentration ratio of retigabine is rather low, thus requiring posological schemes at relatively high doses;[7] d. Chemical instability.One of the main clinical concern over retigabine is its tendency to cause retinal and muco-cutaneous blue-gray discoloration;[8] although the mechanism for this toxic effects remains poorly understood, one hypothesis is that light exposure may cause photodegradation and oxidation of retigabine's aniline ring, which may lead to dimer formation, partly in conjuction with melanin, which would be responsible for the abnormal pigmentation light-exposed tissues.[9]. To possibly overcome some of these limitations, we have designed and synthesized a small library of 42 novel conformationally-restricted retigabine derivatives, and characterized some of these compounds with respect to: potency, selectivity, chemical stability, and in vitro pharmacokinetics. In addition, molecular modeling studies were performed to identify the chemical features required for optimal interaction between the syntetized compounds and Kv7 channels. Noteworthy, in view of the previously-mentioned removal from the market of retigabine, and of the even more recent withdrawal of the marketing authorization for flupirtine, the precursor of retigabine used as a non-opioid analgesic, several naturally-occurring or synthetic small molecules with heterogeneous chemical scaffolds acting as Kv7 activators have been recently described.[10] In particular molecules bearing indoline and indole scaffolds and acting as Kv7 activators have been previously described in a patent by Valeant Pharmaceuticals;[11] nonetheless, a comprehensive description of their structure-activity relationships and a detailed pharmacological characterization of these molecules in terms of pharmacodynamics, metabolism and photostability is lacking.

RESULT AND DISCUSSION

Design and Chemistry

A new library of structural analogues of the Kv7 agonist retigabine was synthesized introducing a conformational restriction of retigabine (**I**) scaffold aimed at increasing the potency and the metabolic and photochemical stability by blocking the labile 4-NH_2 and removing the 2-NH_2 of benzene-1,2,4-triamine scaffold.[12] By this strategy, indoline (**A**), indole (**B**) and tetrahydronaphthalene (**C**) derivatives were designed and synthesized (Figure 1). Moreover, the designed structures allow extensive and chemically accessible modifications to investigate structure-activity relationships. The indoline derivatives (series **A**, Figure 1) were designed maintaining the substituted benzyl group at the N-1 position while varying the nature of both the R1 chain and the linker X on the amino group at position C-5. At this position, we have chosen a series of linker groups characterized by different electrostatic potential, electron density distribution, and N-X rotation energy profiles, such as amide, sulphonamide, urea, thiourea and guanidine, which could mimic the retigabine pattern HB acceptor-HB donor-aromatic ring (Figure S1 and Table S1).

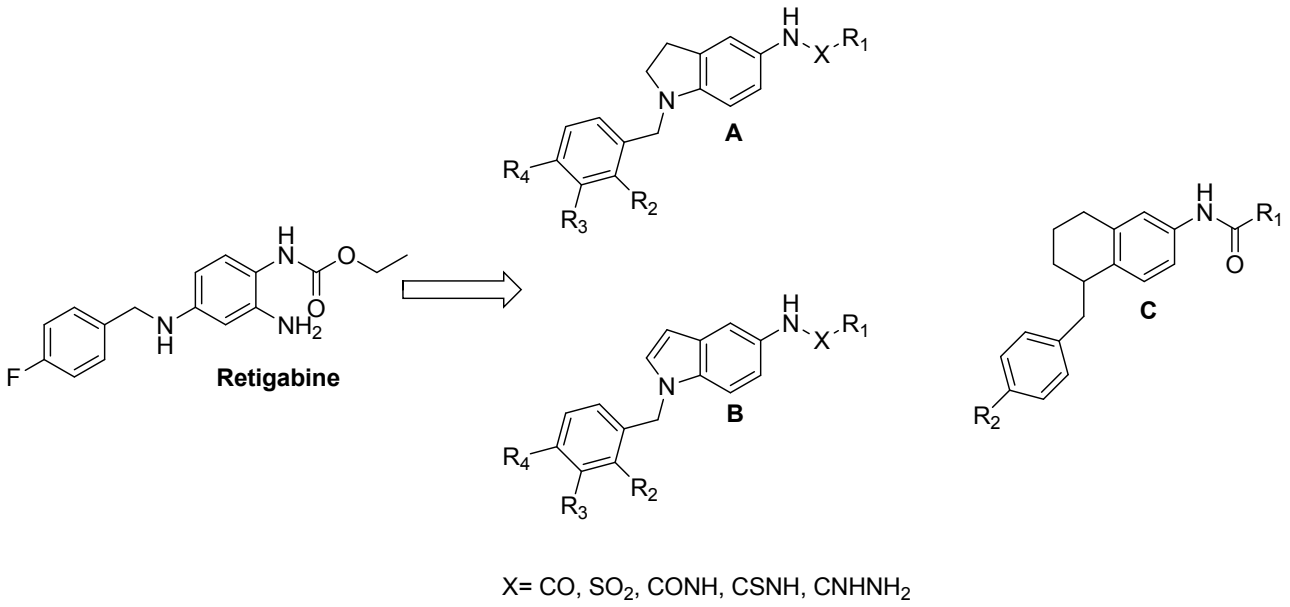

Figure 1. Structures of retigabine and its newly synthesized analogues

The first series of indoline analogues was synthesized according to the following scheme 1.

Scheme 1: Synthesis of 1-(4-fluorobenzyl)-5-substituted indoline derivatives **4a-b**, **5a-b**, **6**, **7**, **8a-i** and **9a-c**.

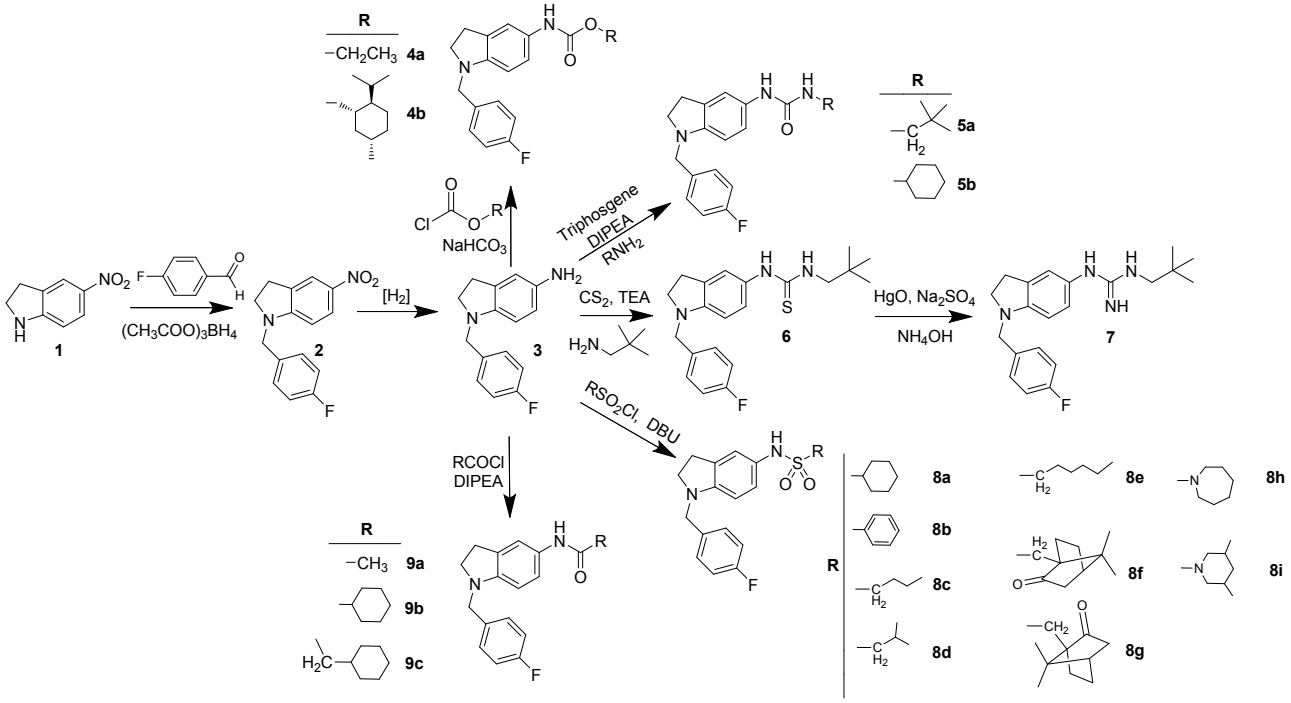

Starting from 5-nitroindoline (**1**) a reductive amination at the N-1 led to the corresponding 1-(4-fluorobenzyl)-5-nitroindoline (**2**) that, upon continuous flow hydrogenation to the corresponding amine (**3**), was used in the next steps. Reaction of **3** with ethyl or menthyl chloroformate in alkaline media gave the corresponding carbamate derivatives **4a** and **4b**. Urea derivatives **5a** and **5b** were prepared by one-pot reaction of **3** with triphosgene and 2,2-dimethylpropan-1-amine or cyclohexylamine, using DIPEA as base. On the other hand, treatment of **3** with CS_2 and 2,2-dimethylpropan-1-amine using TEA as base lead to the thiourea analogue of **5a** 1-(1-(4-fluorobenzyl)indolin-5-yl)-3-neopentylthiourea (**6**). Derivative **6** was converted to the corresponding carbodiimmide by reaction with HgO and then reacted with NH_4OH to give the guanidine derivative **7**. Finally, coupling of intermediate **3** with different sulfonyl chlorides at the presence of DBU led to the sulfonamide derivatives **8a-i**, while coupling with acyl chlorides using DIPEA as base led to the amide derivatives **9a-c**. A second series of indoline analogues, investigating the influence of N-1 substituents on the pharmacological activity, was synthesized according to schemes 2 and 3.

Scheme 2: Synthesis of 1-benzyl-5-cyclohexanesulfonamido indoline derivatives **13a-g.**

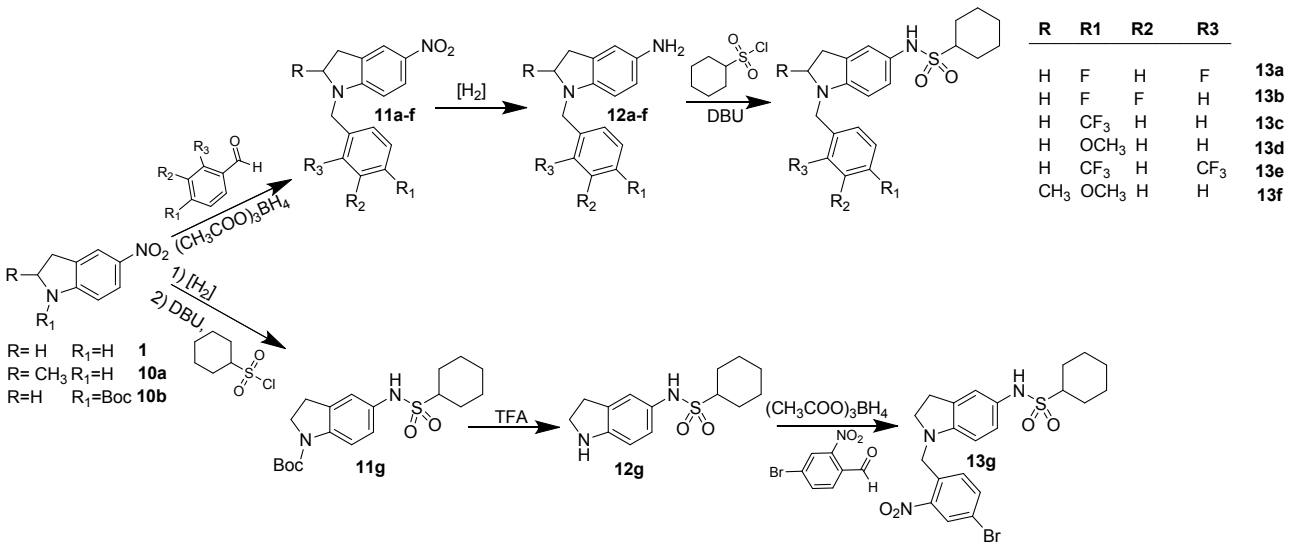

5-nitroindoline (**1**) or 2-methyl-5-nitroindoline (**10**) were derivatized by reductive amination using differently functionalized aldehydes, giving intermediates **11a-f**. Continuous flow hydrogenation of these intermediates led to the amines **12a-f** that were converted to the corresponding cyclohexylsulfonamides (**13a-f)**. Due to the lability of the 4-bromo-2-nitrobenzyl group to the hydrogenation conditions, final product **13g** was obtained using a different synthetic approach. The N-1 position of 5-nitroindoline (**1**) was protected as tert-butoxycarbonyl derivative obtaining the intermediate tert-butyl 5-nitroindoline-1-carboxylate (**10b).** The nitro group of compound **10b** was reduced to the corresponding amine (**11g**) and coupled with cyclohexane sulfonyl chloride, as previously described, before removal of the Boc protecting group by trifluoroacetic acid (TFA). The intermediate **12g**, thus obtained, underwent to reductive amination using 4-bromo-2-nitrobenzaldehyde. Functionalization of the N-1 was also attained by reaction of **1** with 4-chlorobenzoylchlorides, 2-(4-chlorophenyl)acetyl chloride and 1-(2-bromoethyl)-4-fluorobenzene to give intermediates **14a-b** and **17** (Scheme 3). These intermediates were reduced by continuous flow hydrogenation and converted to the corresponding sulfonamides **16a-b** and **19** by coupling with cyclohexanesulfonyl chloride (scheme 3).

Scheme 3: Synthesis of 1-acyl-5-cyclohexanesulfonamido (**16a-b)** and 1-alkyl-5-cyclohexanesulfonamido (**19)** indoline derivatives.

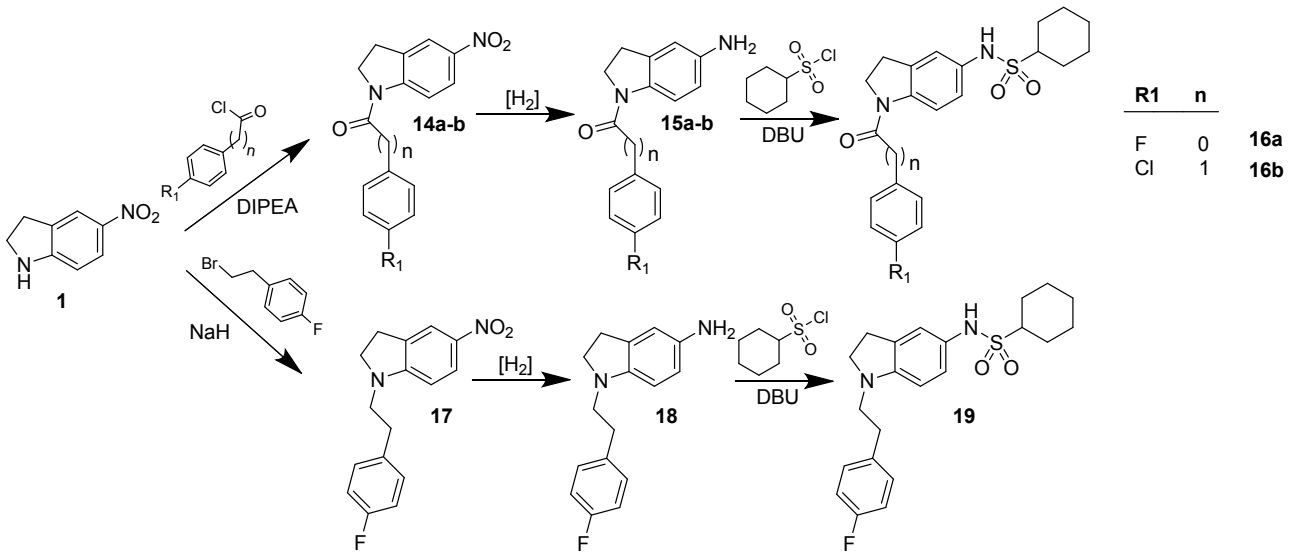

Indole analogues (**B**, figure 1) were synthesized according to scheme 4. Intermediate **20b** was obtained starting from 4-hydroxybenzaldehyde, that reacted with methoxymethyl chloride (MOMCl) to give 4-(methoxymethoxy)benzaldehyde (**19a**). The protected aldehydes was reduced to the corresponding alcohol (**20a**) using $NaBH_4$ and then subjected to iodination affording 1-(iodomethyl)-4-(methoxymethoxy)benzene (**20b**). Nucleophilic displacements of **20** or commercially available 4-substitued benzyl halides by 5-nitroindole in strong basic medium provided the nitro intermediates **21a-d,** which were reduced to the corresponding substituted amino indole derivatives **22a-d**, as previously described. Coupling of these intermediates with acyl chlorides afforded the final alkyl amide derivatives **23a-b, 24a** and **25a**. Removal of the methoxymethyl group from derivative **23b** by TFA led to **24b**. On the other hand, reaction of amine intermediates **22a-d** with cyclohexanesulfonylchloride gave final sulfonamides **23c**, **23d** and **26a**, while reaction with 2-cyclohexylethane-1-sulfonyl chloride (**20d**) led to the sulfonamide derivative **27a**. For the synthesis of **28a**, intermediate **22a** was reacted with chloroacetyl chloride and then subjected to nucleophilic displacement by n-butylamine. Alkylation of the secondary amine on the side chain by reductive amination with formaldehyde gave final product **29a**.

Scheme 4: Synthesis of 1-benzyl-5-amido (**23a-25a**, **23b-24b**, **28a-29a**) and 1-benzyl-5-cyclohexanesulfonamido (**23c-23d**, **26a-27a**) indole derivatives.

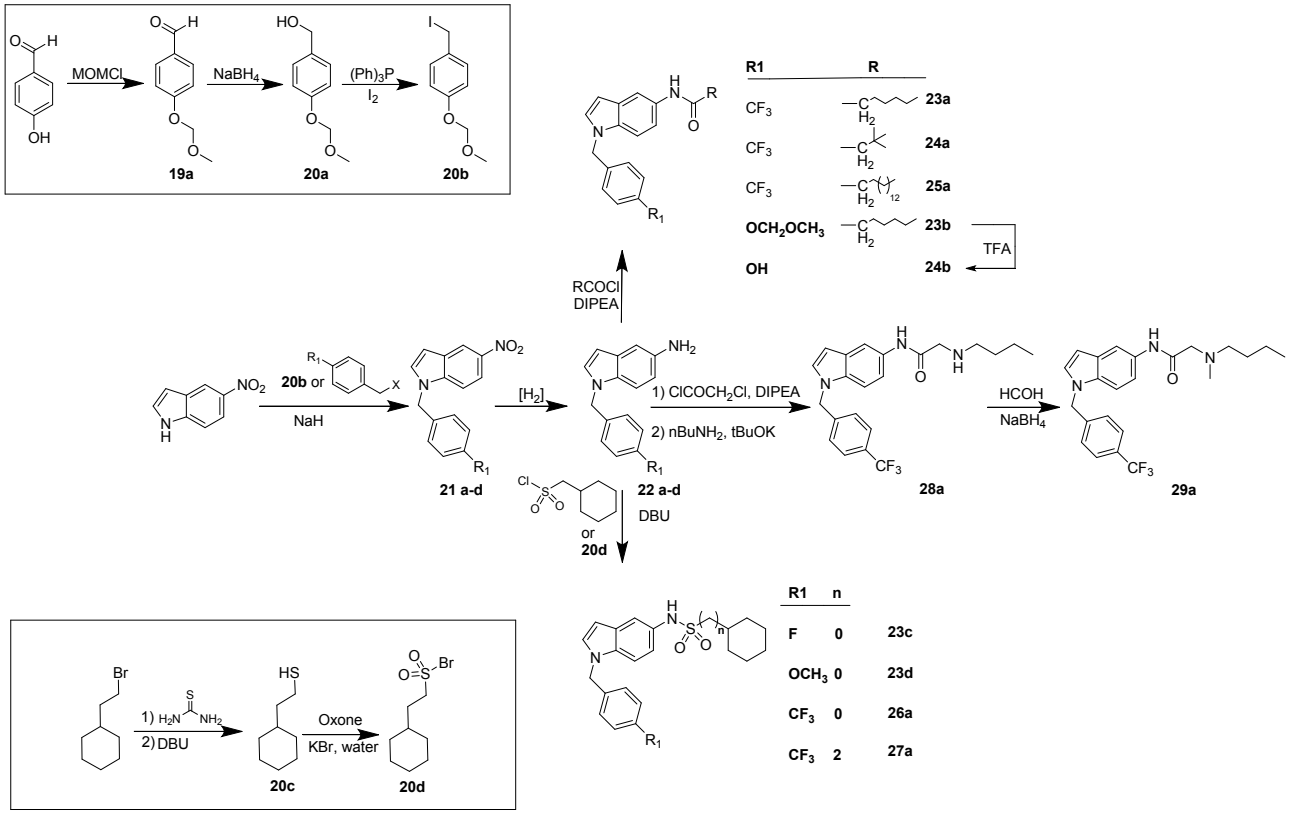

Tetrahydronaphthalene analogues (**C**, figure 1) were synthesized as depicted in scheme 5. Reaction of **30** with heptanoyl chloride and DIPEA, gave the amide intermediate **31**, which was reduced to the tetrahydronaphthol derivative **32** using $NaBH_4$ as reducing agent. Intermediate **32** was subjected to a modified Wittig reaction by formation of the corresponding phosphonium salt, followed by reaction with 4-(trifluoromethyl)benzaldehyde, giving the geometric isomers **33a** and **33b**.[13] Saturation of the double bond in **33a** and/or **33b** using ammonium formate and Pd/C as catalyst gave final compound **34** as racemic mixture.

Scheme 5: Synthesis of (R,S)-N-(5-(4-(trifluoromethyl)benzyl)-5,6,7,8-tetrahydronaphthalen-2-yl)heptanamide (**34**).

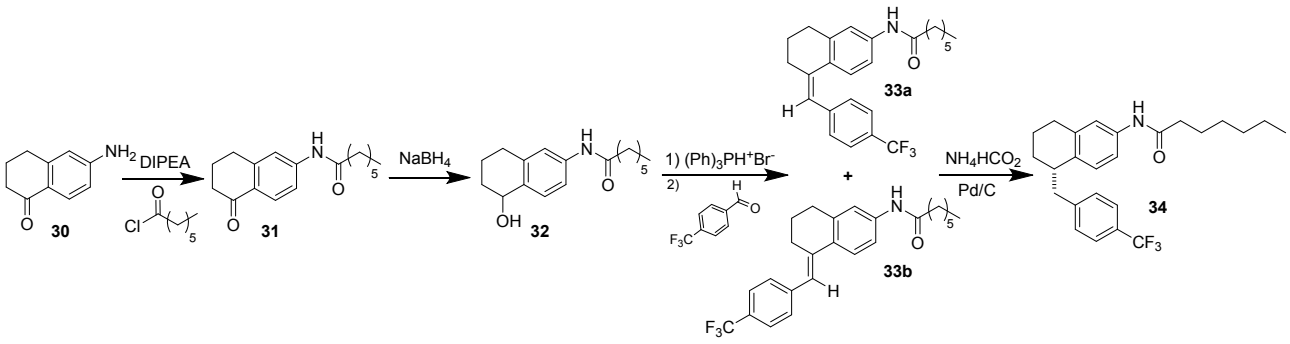

Effects of the retigabine derivatives on Kv7.2 channels expressed in CHO mammalian cells.

To assess the effects of these novel retigabine derivatives on Kv7.2 currents, and to identify compounds more active than retigabine we performed whole-cell patch-clamp electrophysiological experiments in mammalian CHO cells transiently transfected with Kv7.2 cDNA. The effect of the synthesized compounds was investigated at a single concentration (10 μM), using a ramp protocol in which Kv7.2 currents were activated by a 3-second voltage ramps from -80 to +20 mV. We used 10 μM of each compound given that this concentration exerts maximal efficacy in the case of retigabine, the comparator drug (see below). Moreover, most drug screening efforts performed in search of novel Kv7 modulators use a 10 μM compound concentration.[14]

Ramp-evoked currents were analysed by measuring the currents at -40 mV (a membrane potential value close to the activation threshold) and at 0 mV (a membrane potential value at which Kv7.2 conductance is almost completely saturated), and the effect of each compound was expressed as the ratio between current amplitude in the presence (A_2, B_2, I_{drug}) and absence (A_1, B_1, I_{CTL}) of the drug at these two membrane voltages (Figure 2 a-b, Table S2). Measuring drug effects at both -40 mV and 0 mV membrane potential values allowed to formulate distinct predictions on the potential effects of these compounds. In fact, the reference compound retigabine is described as a Kv7 activator because it exerts two main effects on Kv7.2 channel function: one is a leftward shift in the activation gating, the other being an increase in the maximal current at more depolarized potentials where conductance is saturated. Therefore, drug-induced current enhancement at -40 mV, a membrane potential value close to the current activation threshold, is likely to result in membrane hyperpolarization and

inhibition of action potential firing. On the other hand, drug-induced current enhancement at 0 mV, may reduce sustained neuronal depolarization during trains of action potentials and cause spike frequency adaptation. Therefore, measurements performed at both membrane potential values are likely to predict different profiles of mechanism of actions of a Kv7 activator. Using this method, drugs showing I_{drug}/I_{CTL} >1 are considered as enhancers, drugs whose I_{drug}/I_{CTL} is < 1 are blockers and drugs whose I_{drug}/I_{CTL} is = 1 are considered ineffective.

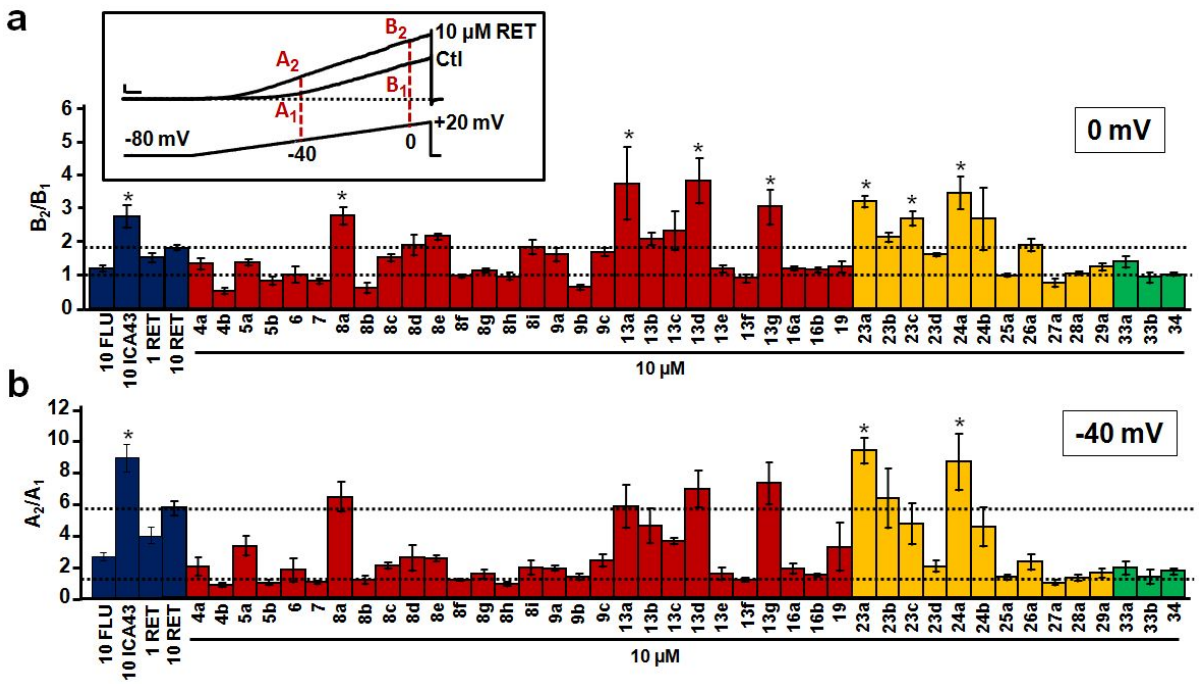

Figure 2. Effect of synthesized compounds on Kv7.2 current in comparison with retigabine. a-b. Representation of the ratio between current amplitude in the presence (A_2, B_2) and absence (A_1, B_1) of each of the indicatedcompounds (10 µM) calculated at 0 mV (a) and at -40 mV (b). The inset shows the protocol used to evaluate drug activity on Kv7.2 currents. Current scale, 400 pA; time scale, 0.2 s. Histograms are colored according to the following scheme: blue represents available Kv7 activators, such as retigabine (RET) at 1 and 10 µM, Flupirtine (FLU) at 10 µM, and ICA27243 (ICA43) at 10 µM; red represents indoline derivatives, yellow represents indole derivatives and green represents tetrahydronaphthalene derivatives. Each data point is expressed as the mean ± standard error of the mean (SEM) of at least 3 cells recorded in at least 2 independent transfections; the precise number of cells included in the analysis for each compound is specified in Table S2. * indicates values significantly different ($p < 0.05$) from retigabine (10 µM).

The effect of each newly synthesized compounds was compared to that of retigabine.[15] In this cellular assay, retigabine showed a ratio I_{drug}/I_{CTL} at -40 mV of about 6, whereas at 0 mV the I_{drug}/I_{CTL} ratio

was about 2 (Figure 2, a-b), suggesting that retigabine is more active at negative potentials than positive potentials, as previously described.[15,16] In order to further validate our screening assay we also evaluated the effects of a lower concentration (1 μM) of retigabine, as well as those of two additional Kv7 activators, namely flupirtine (FLU) and ICA-27243 (ICA43), two compounds showing lower and higher activity, respectively, than retigabine on Kv7.2 channels when the three compounds were compared at the 10 μM concentration.[17] The results obtained suggest that our screening assay is able to discriminate compounds with different activity on Kv7.2 currents, both at -40 mV and 0 mV (Figure 2).

Of the 42 compounds tested at the single concentration of 10 μM, seven (**8a**, **13a**, **13d**, **13g**, **23a**, **23c**, and **24a**) were able to increase Kv7.2 currents more than retigabine ($p<0.05$) at 0 mV; among these, only two (**23a** and **24a**) also increased Kv7.2 currents more than retigabine at -40 mV ($p<0.05$) (Figure 2 A-B). Given that activity at both -40 mV and 0 mV is predictive of a wider spectrum of pharmacological effects on neuronal excitability needed for novel anticonvulsant/analgesic compounds acting as Kv7 activators, **23a** and **24a** were selected for further analysis.

To compare the kinetics of onset and offset of the Kv7.2-activating effects and the potency of the two most active compounds **23a** and **24a** with those of retigabine, time-course experiments at increasing drug concentrations (0.01-10 μM) were performed. As shown in figure 3a and 3b, retigabine dose-dependently increased Kv7.2 currents with a fast ON kinetics; indeed, upon application of 10 μM of retigabine witha fast solution exchange apparatus, maximal steady-state levels were achieved in about 10 seconds. Similarly, currents returned to basal values after about 10 seconds upon retigabine removal from the bath. By contrast, the kinetics of onset and offset of both **23a** and **24a** appeared significantly slower. In particular, upon exposure to 10 μM **23a,** more than 200 seconds were needed to reach maximal steady-state current levels; little (if any) current recovery was observed upon 10 μM **23a** removal from the perfusion solution for at least 200 seconds. Similar, although slightly faster onset and recovery kinetics were observed upon exposure and removal, respectively, of 10 μM **24a**. It seems likely that the slower wash-in and wash-out kinetics shown by **23a** and **24a** when compared

to retigabine may be ascribed to the enhanced hydrophobicity of both newly-synthesized compounds, whose logPs were 6.83 and 5.58, respectively, both values significantly higher than that of retigabine (logP of 3.08). Given the higher hydrophobicity of **23a** and **24a** when compared to that of retigabine, the self-aggregating propensity of all three compounds was further evaluated using pyrene fluorescence spectroscopy measurements.[18] The results obtained, shown in Figure S2, revealed that the ratio of the pyrene fluorescence intensity peaks at λ372 nm (I) and λ383 nm (III) for **23a** and **24a** decreased as a function of drug concentration (1-100 μM), indicating an increase of hydrophobicity in the microenvironment sensed by the probe; these data are consistent with the hypothesis that **23a** and **24a** show the typical behaviour of amphiphilic self-assembling molecules forming supramolecular aggregates (micelles) in the nanometric range. By contrast, no change in the pyrene I/III fluorescence ratio was observed in the presence of retigabine. These findings suggest that the slow ON/OFF kinetics of compounds **23a** and **24a** (with the respect to those of retigabine) may correlate with their increased hydrophobicity. Although we don't know yet whether this physico-chemical property translates into significant changes in distribution and metabolism in vivo, and whether it represents a potential hurdle for in vivo application, it should be mentioned that one of the major limitation of retigabine is its rather poor brain penetration and short half-life, requiring 3 times-a-day administration.[7] Both these pharmacokinetic drawbacks might be improved by the increased hydrophobicity shown by **23a** and **24a**.

The EC_{50}s of **23a** and **24a** on Kv7.2 current activation (calculated as described in the Methods section and depicted in Fig. 3C) showed that **23a** was about 12 times more potent than retigabine, while no statistically-significant difference was observed between retigabine and **24a** (Figure 3D).

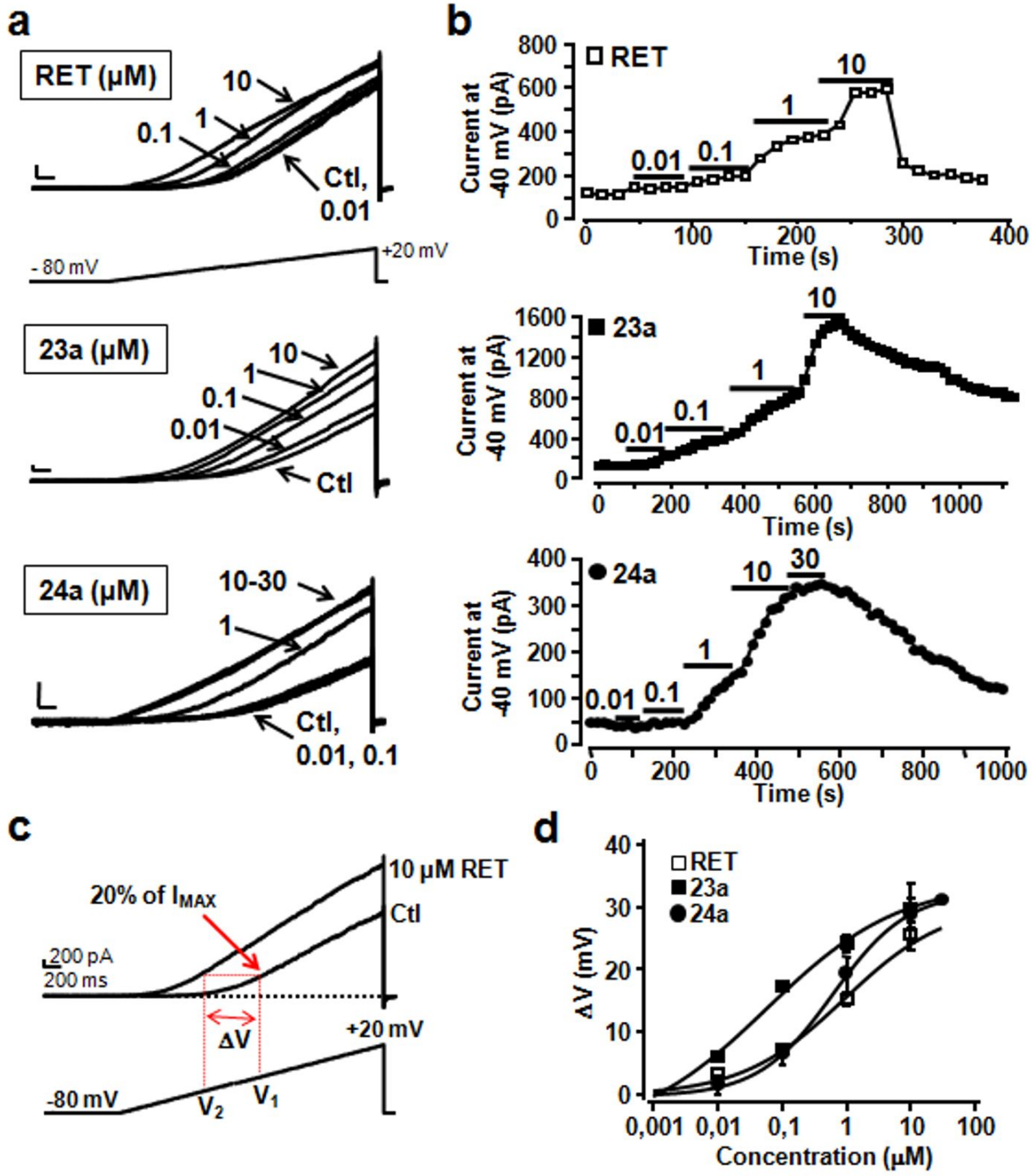

Figure 3. Effect of retigabine, 23a and 24a on ramp-evoked Kv7.2 current. a. Representative whole-cell current traces from Kv7.2 channels activated by the indicated ramp protocol recordedin control conditions and upon exposure to 0.01-10 μM retigabine (RET), **23a** and **24a**. **b.** Time courses of Kv7.2 current potentiation by retigabine (RET), **23a** and **24a**. The steady-state amplitudes of the peak currents at -40 mV were plotted as a function of time. The bars on top of the plot indicate the duration of drug application. Current scale, 200 pA; time scale, 0.2 s. c. Protocol used to calculate ΔV (V_2-V_1) at 20% of current peak value for controls (V_1) and after RET exposure (V_2). d. Dose-response curve for **RET**-, **23a**-, and **24a**-induced ΔV shift.

The voltage ramp-protocol used in the previously-described experiments did not allow us to precisely define the effect of the drugs on the steady-state properties of the Kv7.2 current; therefore, in the next experiments, we compared the effect of 0.03 μM retigabine and **23a** on Kv7.2 channels activated by constant voltage pulses (Figure 4 a-b**)**. While 0.03 μM retigabine failed to enhance maximal Kv7.2 currents and to modify their voltage-dependence, the same concentration of **23a** doubled Kv7.2 maximal conductance (Figure 4c) and caused a leftward shift of about 18 mV in the half-activation voltage ($V_{1/2}$) of Kv7.2 currents (Figure 4); in fact, the $V_{½}$ vaues were -20.1±1.2 mV, -24.4±1.8 mV and -38.2±2.0 mV for control (Ctl), 0.03 μM RET, and 0.03 μM **23a**, respectively (Figure 4d).

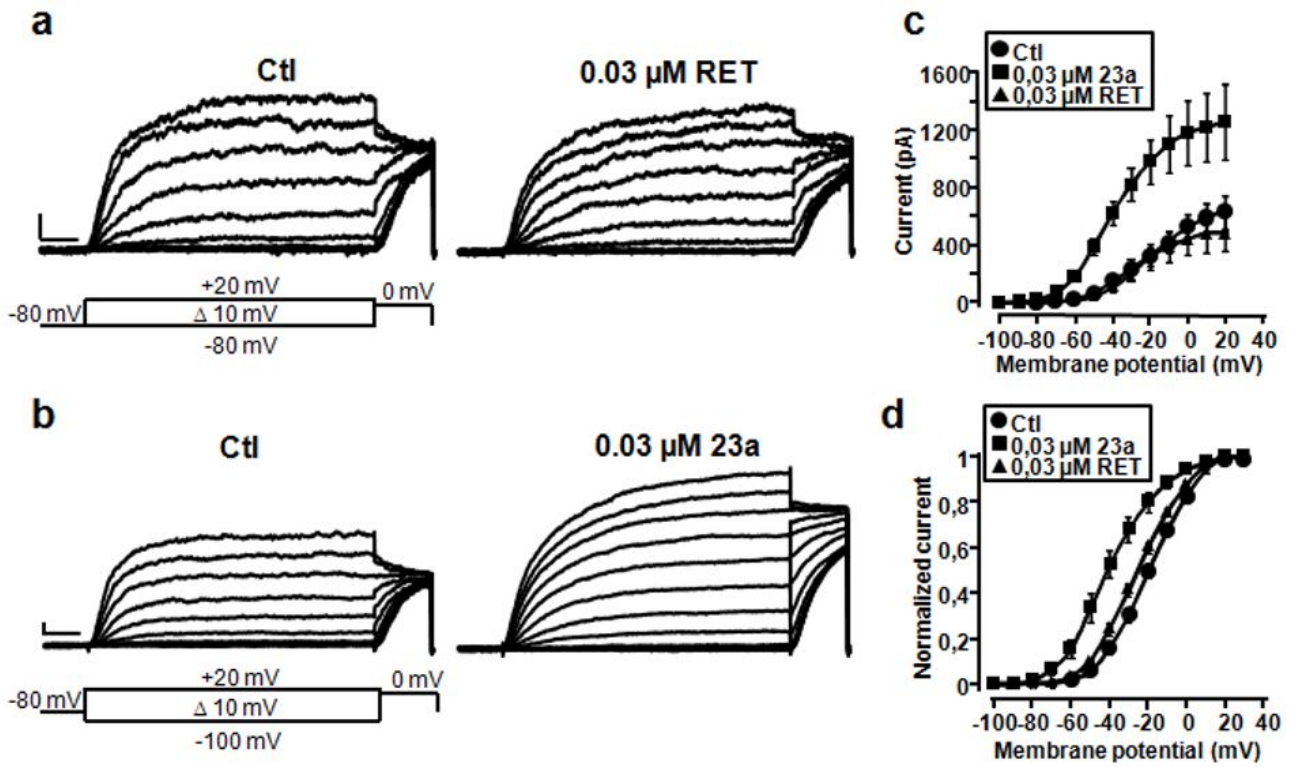

Figure 4. Effect of retigabine and 23a on Kv7.2 currents activated by constant voltage pulses. a-b. Representative macroscopic current traces recorded from a CHO cell expressing Kv7.2 homomeric channels in response to the indicated voltage protocol before (left) and after (right) application of 0.03 μM RET (**a**) or **23a** (**b**). Current scale, 100 pA; time scale, 0.2 s. **c**. Kv7.2 current/voltage curves before and after application of 0.03 μM RET or **23a**. **d.** Normalized Kv7.2 conductance/voltage curves before and after application of RET or **23a**. Continuous lines represent fits of the experimental data to a double Boltzmann distribution.

Small molecules can activate Kv7 channels throught different molecular mechanisms. Among these, retigabine activates Kv7.2 channels by recognizing a hydrophobic pocket located between the cytoplasmic parts of the S5 and the S_6 transmembrane domains in the open channel configuration; within this cavity, an H-bond is established between the carbamate group of retigabine and the aromatic side chain of a tryptophan present at the intracellular end of the S_5 helix (W236 in the Kv7.2 sequence). Substitution of this tryptophan with smaller and less hydrophobic leucine largely prevents the ability of retigabine to activate neuronal Kv7 subunits. [5b, 5c] By contrast, a second group of compounds, belonging to benzamides (ICA-27243 and ICA-069673) appears to recognize a poket located in the voltage sensing domain (VSD; region between the S_1 and the S_4 transmembrane domains).[19] In particular, two specific aminoacid positions in the S_3 segment of the Kv7.2 VSD (A181 and F168) seem to be relevant to confer current sensitivity to activation by benzamides.[19b]

To define the structural determinants for Kv7.2 current enhancement by **23a** and **24a**, and in particular whether these molecules required the presence of W236 in S_5 or of F168 in S_3, we examined the effect of **23a** and **24a** on retigabine-insensitive Kv7.2 W236L and on ICA-insensitive Kv7.2 F168L mutant channels. Application of 10 μM **23a** or **24a**, similarly to retigabine, failed to enhance Kv7.2 W236L currents; whereas ICA-27243 strongly activated Kv7.2 W236L currents (Figure 5 a-b). By contrast, application of 10 μM of retigabine, of **23a** or of **24a** increased Kv7.2 F168L currents, whereas ICA-27243 was ineffective. These results strongly suggest that W236 exerts a critical influence on retigabine, **23a** and **24a** binding within the pore hydrophobic pocket (Figure 5 c-d). Consistent with this hypothesis, **23a** (similarly to retigabine itself) failed to affect homomeric Kv7.1 currents where the 236 position is naturally occupied by a leucine residue (Figure S3).

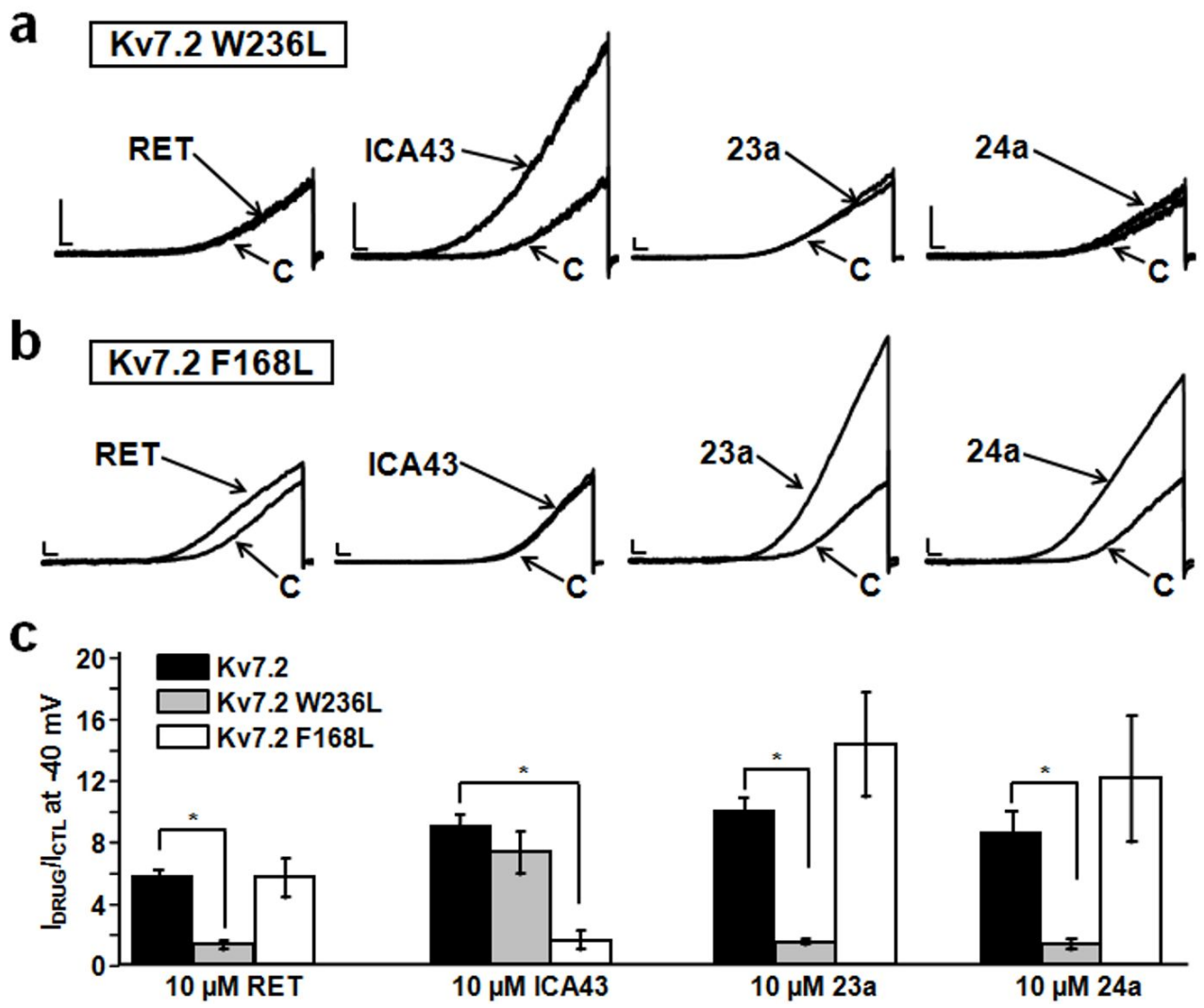

Figure 5. The W236 residue in Kv7.2 exerts a critical influence on **23a** and **24a** abilty to activate Kv7.2 currents. **a-b.** Representative traces of whole-cell ramp-evoked currents from Kv7.2 W236L (**a**) and Kv7.2 F168L (**b**) channels upon applicatio of 10 µM retigabine (RET), ICA 27243 (ICA43), **23a** and **24a. c.** Quantification of the effects of the indicated compounds on Kv7.2, W236L and Kv7.2 F168L currents; data are expressed as the ratio between current amplitude at -40 mV in the presence and absence of 10 µM drugs (I_{DRUG}/I_{CTL}). Each data point is expressed as the mean ± standard error of the mean (SEM) of at least 3 cells recorded in at least 2 independent transfections. * indicates values significantly different ($p < 0.05$) from respective controls.

Characterization of the selectivity profile for channels formed by different Kv7 subunits.

Considering that I_{KM} is mainly formed by heteromeric assembly of Kv7.2 and Kv7.3 subunits, in subsequent experiments we evaluated the activity of **23a** and **24a** on Kv7.2/Kv7.3 heteromeric currents. Similarly to Kv7.2, **23a** and **24a** dose-dependently (0.01-10 µM) increased Kv7.2/Kv7.3 with both compounds showing higher potency when compared to retigabine; also, when compared to retigabine, both **23a** and **24a** were more potent in activating homomeric Kv7.4 channels, whereas

only **24a** was more potent than the reference compound in activating homomeric Kv7.5 channels (Table 1).

In conclusion, the selectivity profile for **23a** was Kv7.2=Kv7.4=Kv7.2/Kv7.3>Kv7.5>>Kv7.3>>Kv7.1; while for the **24a** was Kv7.4>Kv7.5= Kv7.2=Kv7.2/Kv7.3=Kv7.3>>Kv7.1.

Table 1. EC_{50} and induced ΔV shift of retigabine and compounds **23a** and **24a** over different Kv7 channels.

Target channel	ΔV (mV)[a]			EC_{50} (μM)		
	RET	23a	24a	RET	23a	24a
Kv7.2	-25.37±1.23	-29.47±2.03	-30.01±3.81	0.93±0.43 (12)	0.08±0.04$^{\$}$ (15-20)	0.63±0.07 (6-9)
Kv7.2/Kv7.3	-26.81±1.93	-25.45±2.91	-20.00±2.48	1.72±0.41 (8)	0.21±0.14$^{\$}$ (6-8)	0.34±0.06$^{\$}$ (9-10)
Kv7.3	-39.88±5.13 (30 μM)	-26.25±4.60 (30 μM)	-21.40±6.18* (30 μM)	3.90±1.70 (6)	10.5±6.00† (7-9)	0.92±0.64 (6)
Kv7.4	-15.19±1.97	-32.85±2.97**	-24.43±5.39	1.98±0.84 (7)	0.10±0.02$^{\$}$ (6-7)	0.08±0.20$^{\$}$ (6)
Kv7.5	-21.95±5.40	-25.6±4.9	-19.7±3.6	0.80±0.24 (3)	1.07±0.12 (4)	0.35±0.14 (4)

The number of recordings is indicated in brackets. [a] All three drugs were used at 10 μM concentration, unless otherwise indicated; * $p<0.05$ vs ΔV of RET on Kv7.3 channels; ** $p<0.05$ vs ΔV of RET on Kv7.4 channels; $^{\$}$ $p<0.05$ vs EC_{50} of RET; † $p<0.05$ vs EC_{50} of 23a on Kv7.2 channels

Molecular Modeling

We used pharmacophore modelling to get insight into the chemical features of our novel Kv7 channel activators. In particular, using Phase [20] on an active set (composed by molecules showing more than 4 I_{drug}/I_{ctl} at -40 mV) and on an inactive set (Table S3), we obtained the pharmacophore model A (Figure 6a).

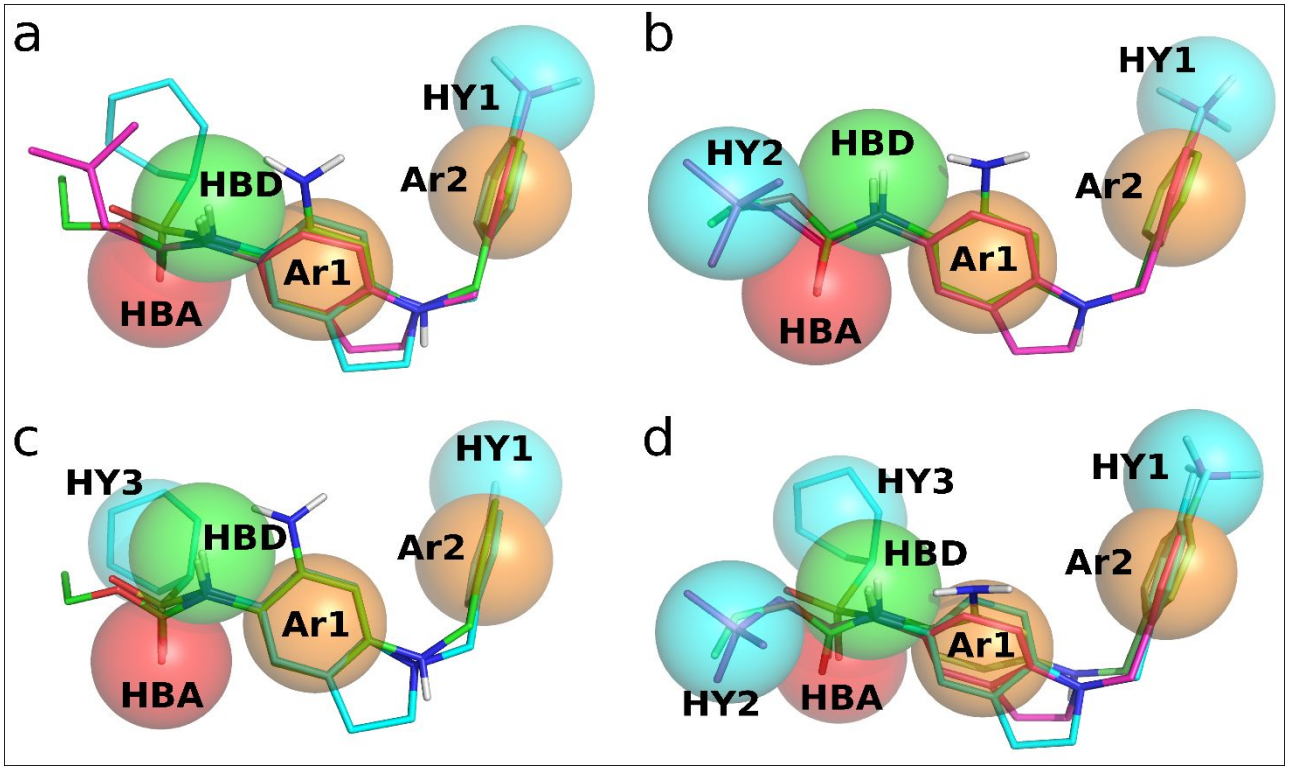

Figure 6. Pharmacophore models developed on the basis of our novel Kv7 channel activators. Pharmacophore features are color-coded as follows: Hydrophobic (HY – cyan), Aromatic (Ar – orange), Hydrogen Bond Donor (HBD – green), Hydrogen Bond Acceptor (HBA – red). Panel a) Model A with compounds **24a** and **8a** depicted in magenta and cyan sticks, respectively. Panel b) Model B with compound **24a** depicted in magenta sticks. Panel c) Model C with compound **8a** depicted in cyan sticks. Panel d) Model D with compounds **24a** and **8a** depicted in magenta and cyan sticks, respectively. **Retigabine** is depicted as reference, in every panel, in green sticks.

The model is composed by 5 pharmacophore features, a hydrogen bond acceptor (HBA), a hydrogen bond donor (HBD), a hydrophobic region (HY1) and two aromatic regions (Ar1 and Ar2). Despite the evident influence of the R1 substituent (see figure 1) on the activity, model A does not present any feature focused on these substituents. We thought this may be due to the different geometries of the sulfonamide and amide moieties of the molecules belonging to the active set. We thus developed two separate models for amides and sulfonamides. Removing the sulfonamide derivatives from the active set we obtained model B (Figure 6b). On the opposite, by keeping sulfonamides only we obtained model C (Figure 6c).

As evident from their superposition (Figure S4), the two models share features Ar1, Ar2, HY1, HBA and HBD, with almost identical coordinates (RMSD=0.51Å). We superimposed models B and C to

model A to get model D, (Figure 6d) that inherits Ar1, Ar2, HY1, HBA and HBD from model A, HY2 from model B and HY3 from model C. The hydrogen bond interaction with W236, whose importance has been proven for other channel modulators[5a] as well as for **23a** in this study, is represented in the models by the HBA feature. The finding of the two additional hydrophobic locations HY2 and HY3 could explain the great variety of substitutions tolerated at position 5, as well as the possibility of linking the HY2/3 substituent at 5-NH_2 with geometrically different linkers.

Indeed, despite the most potent molecules herein reported have an amide HBA-HBD moiety, the sulfonamide one is of great interest for this and for future investigations. It can mimic the HBA-HBD-Ar pattern of model D in different conformations and address the substituent at position 5 toward HY2 or HY3, due to its larger HBA surface and to the rotation/energy profile of the bond connecting HBA and HBD (Figure S1). For instance, compounds **8a** and **23a** are able to fit, in different conformations, both HY2 and HY3 (Figure 7). The sulfonamide derivative docks the substituent preferentially into HY3 (Figure 7b) but in a slightly higher energy conformation (ΔE_{intra}= 1.49 kcal/mol) the substituent can be addressed towards HY2. (Figure 7a) On the opposite, the amide compound **23a** preferentially addresses its aliphatic chain toward HY2, (Figure 7a) but, in another low energy conformation (ΔE_{intra}= 1.10 kcal/mol), due to the flexibility of the n-hexane moiety, the chain can fit into HY3. (Figure 7b).

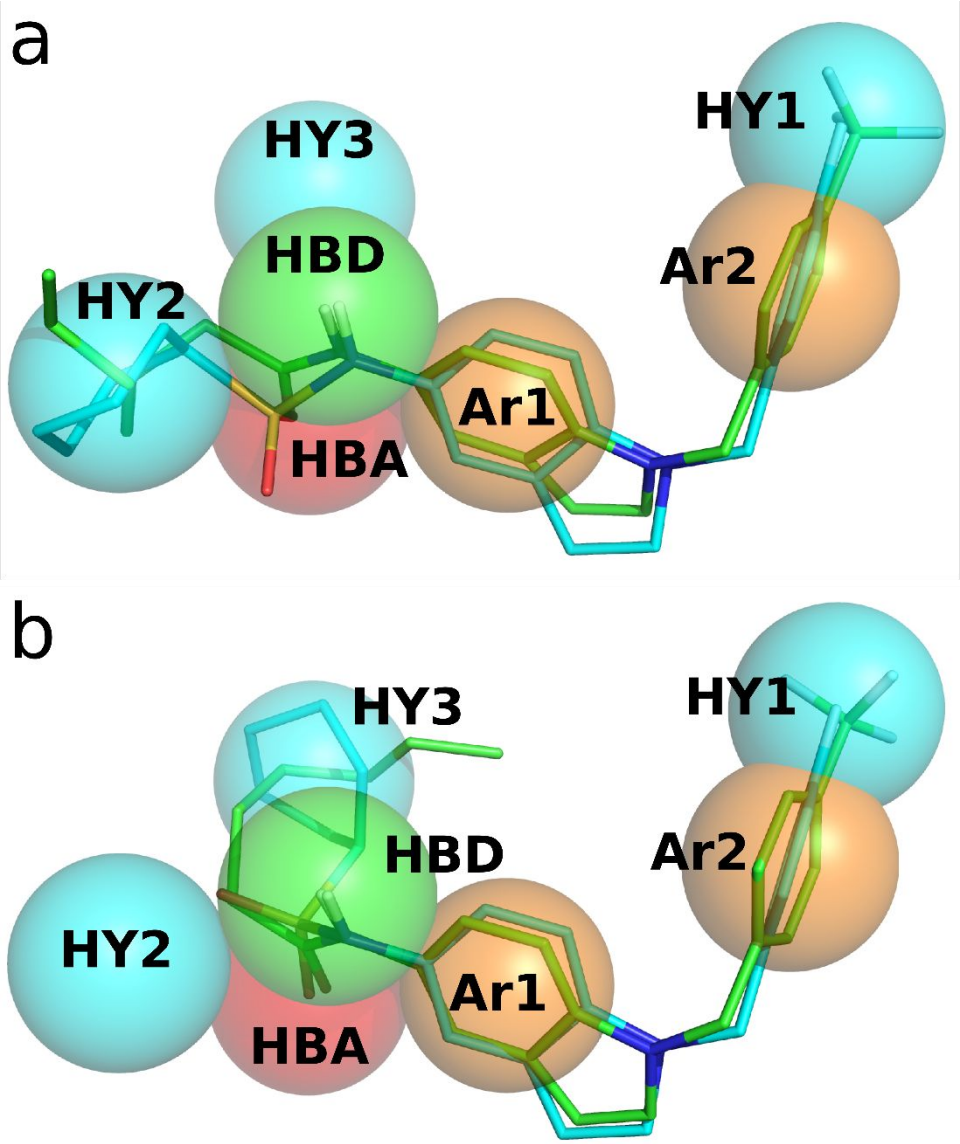

Figure 7. Compounds **23a** (green sticks) and **8a** (cyan sticks) fitting feature HY2 (panel a) and HY3 (panel b). Pharmacophore features are color-coded as follows: Hydrophobic (HY – cyan), Aromatic (Ar – orange), Hydrogen Bond Donor (HBD – green), Hydrogen Bond Donor (HBD – green).

HY2 and HY3 could probably indicate a whole, larger and flexible pocket on Kv7.2, where more flexible compounds could bind in different conformations, interacting with more protein residues. This may be achieved by the flexibility of the substituent in the case of **23a**, or of the sulfonamide linker in the case of **8a**. Homology modeling of the Kv7.2 219-325 region is in agreement with the existence of two hydrophobic sites separated by W236, this critical residue appears indeed surrounded, on two sides, by several hydrophobic residues that could be the counterpart of HY1 and

HY2/3 on the channel protein (Figure 8). Addressing the binding mode of our inhibitors, and their optimization by structure-based studies, is our next goal, although previously reported studies [5a, 21] have already provided very interesting clues on the binding mode of retigabine and other Kv7 channels modulators.

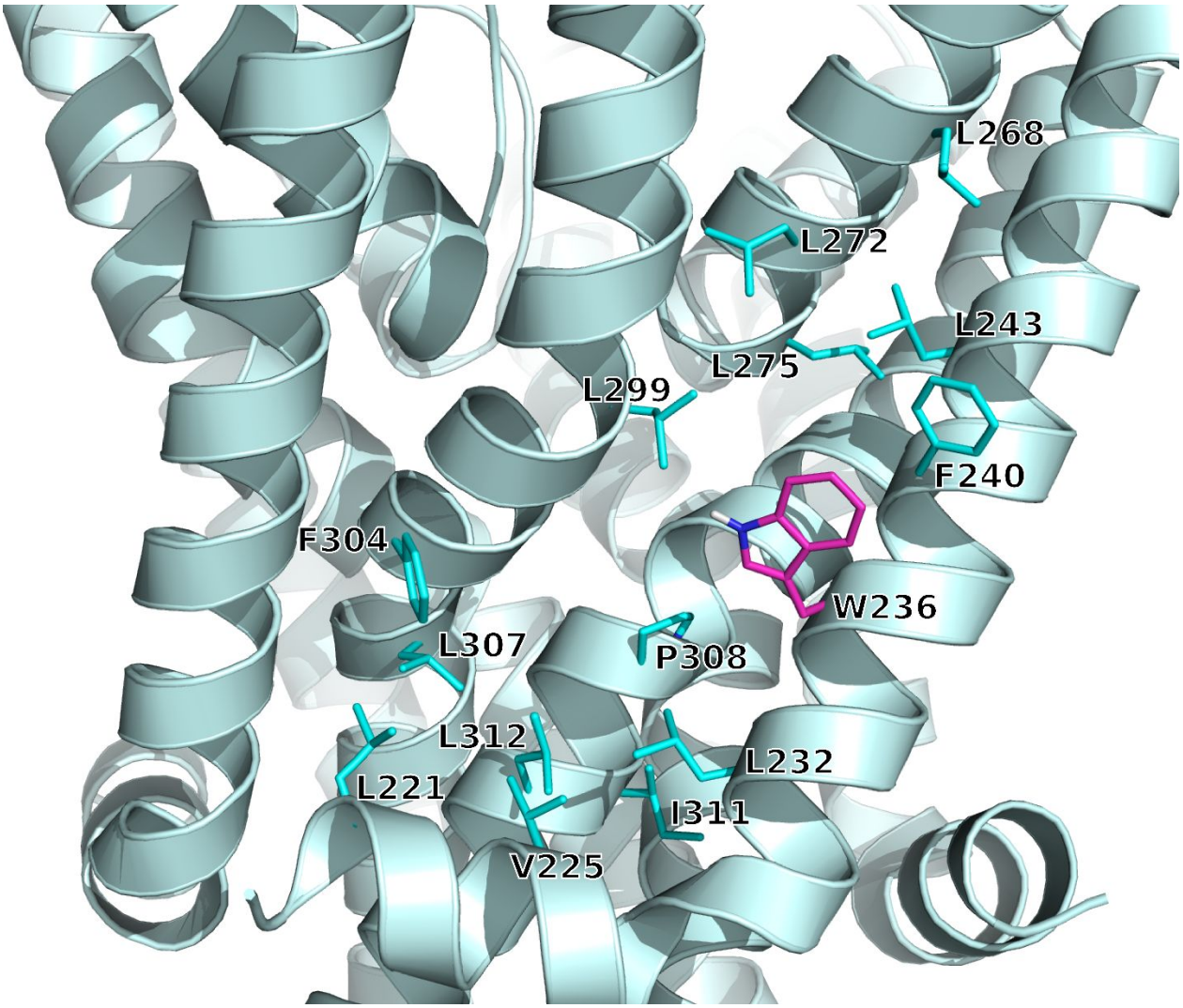

Figure 8. Kv modulators binding region modeled by homology with the CryoEM structure of Xenopus KCNQ1 channel (PDB id: 5vms). W236 (magenta sticks) is surrounded by several hydrophobic residues (cyan sticks) that could host chemical features HY1 and HY2/3.

Structure-activity relationship analysis

Compounds **5a**, **6**, and **7** show the activity rank that would be expected on the basis of their potential hydrogen bonding strength with the W236 side chain, with the urea moiety of **5a** showing higher efficacy than the guanidine of **7** and the thiourea of **6**.

The compounds bearing non-branched substituents at 5-NH_2 give clues about the HY2/3 feature. While in the amide series a six membered chain gives an optimal activity (**23a**, **23b**, **24b**), in the sulfonamide series, it does not (**8e**). Substitutions of a methylene group of **23a** by nitrogen, as in compounds **28a** and **29a**, increase hydrophilicity of the chain that would fall into HY2 and result detrimental to the activity. Compounds with longer (**25a**) or bulkier (**8f-8g**) chains show a loss in activity that could be due to steric clashes with the target protein. Even the substitution of the cyclohexyl substituent of **8a** with an aromatic ring (**8b**), is detrimental to the activity. Interesting SAR clues are also evidenced for the substituents at N-1 position. Derivatization of the N-1 by acyl groups, with its subsequent change in geometry and misfitting of HY1, is responsible for a markedly reduced activation of the channel (compounds **16a** and **16b**). On the other side, N-1 benzyl derivatives are among the most active compounds (compounds **8a**, **23a-d** and **24a-b**), while the substitution of the benzyl moiety with a phenylethyl group is not tolerated (compound **19**). Both electron-withdrawal and electron-donating groups were used to decorate N-1 benzyl moiety. In accordance with previous reports, electron-withdrawal substituents exert positive effects on the channel activation (compounds **13g**, **23a**, **24a**).[9a] Nevertheless, we found that also some electron-donating groups such as hydroxy and alkoxy groups are suitable substituents in the para position of the N-1 benzyl moiety (compounds **13d**, **23b**, **23d** and **24b**). In addition, we found some differences in efficacy between the indoline and the indole series when some specific para substituents were used to decorate the N-1 benzyl group. For instance, the p-trifluoromethyl group is effective in improving efficacy for the indole series (compound **23a**) while penalizing the activity for the indoline series (compound **13c**). At the opposite, the p-methoxy substituent is responsible for a remarkable increase in efficacy in the indoline series (compound **13b**) when compared to fluorine, but decreases efficacy in the indole series (compound

23d). These differences are actually difficult to be explained by the data we collected so far; synthesis of more derivatives and future target-based study could provide further clues. It can be speculated that in our model, the N-1 benzyl moiety falls within the AR2/HY1 region, thus an electron withdrawing group might be able to improve hydrophobic interactions in these regions. On the other side, N-1 benzyl substituents, might be also involved in more specific interactions in the HY1 region, such as hydrogen or halogen bonds, justifying the apparent conflicting results. However, the para position appears to be the preferred position for the N-1 benzyl substituents. Multiple substitution in different positions are well tolerated, but do not significantly influence efficacy (derivatives **13a-b**, **13c-e** and **13g**).

Retigabine and its conformationally restricted analogues **4a** and **9a** are able to fit six out of the seven chemical features required by the pharmacophore model. Despite this, the activity of retigabine is significantly higher. This may be explained by the lack of a primary amine in compounds **4a** and **9a**, corresponding to the 2-NH_2 of retigabine, that probably exerts supplementary interactions at the receptor site that **4a** and **9a** do not properly compensate with additional hydrophobic interactions at HY2/3 as the most potent compound of these series do.

Finally, tetrahydronaphthalene derivatives **33a**, **33b** and **34**, were totally inactive when tested over Kv7.2 channels. Considering that these molecules bear the substituents conferring enhanced efficacy in the A and B chemiotypes, the lack of activity has to be attributed to the tetrahydronaphthalene scaffold. This hypothesis is consistent with molecular modeling data showing that the different central core and the double bond of **33a** and **33b** indeed hamper the fitting within the Ar2-HY1 region.

Photostability assays

Retigabine chemical photoinstability is a well-known characteristic of the molecule, likely leading to some important adverse events observed during chronic long-term therapy, such as blue-gray discololoration of skin, mucosae, and, possibly, retina[8,9a,22]. Two main impurities, corresponding to C5-C5 and C5-N retigabine dimers, likely obtained by oxidative self-coupling of two quinone diimine

tautomers, have been foud in retigabine batches.[23] Retigabine dimer formation, which is favoured in aqueous media under UV radiation,[23] is reponsible for the change in color of retigabine aqueous solutions from colourless to red/dark blue when left on air, and for the previously mentioned retinal and muco-cutaneous side effects.[8,9a] More recently, phenazinium, phenazine and benzimidazole dimers of retigabine with high melanin affinity have been identified by matrix-assisted laser desorption/ionization imaging mass spectrometry in corneal tissue.[24] Given these premises, all synthesized derivatives were subjected to photostability assays. Initially, an UV quartz cuvette containing an aqueous solution of retigabine (100 μg/mL) was irradiated in a black-box UV analyzer at wavelenghts of 254 nm (UV-B) and 365 nm (UV-A) for 6 hours. At predetermined intervals (2, 4 and 6 hours) aliquots were withdrawn and analyzed by HPLC. The molecule showed high photostability under these experimental conditions with negligible degradation after 6 hours (about 5%, data not shown). By contrast, exposure to visible light led to a remarkable and significant photodegradation of retigabine; as a matter of fact, about 47,33±4,03% of retigabine was degraded after 6 hours of drug exposition to artificial daylight lamp. Quantitatively similar results were obtained upon direct exposure of retigabine to natural solar light (43.5±4.3% degradation at 6 hours). We then decided to further investigate the photodegradative behaviour of retigabine by analysing the corresponding by-products. As shown in figure S5 the HPLC profile of photodegraded retigabine batches is mainly characterized by the presence of two additional peaks with a retention time of 5.98 and 14.39 minutes. Running HPLC/MS analysis of these peaks we were able to detect the mass spectra only for the late eluting peak (14.39 minutes), putatively identified as the retigabine adduct ethyl (2,4-bis((4-fluorobenzyl)amino)phenyl)carbamate (Figure S6). The peak eluting at 5.98 minutes was undetectable by mass spectrometry, in accordance with a previous report showing the occurrence of non-identified retigabine impurity at shorter retention times.[22] Thus, we decided to analyse the unknown peak using a GC/MS method, leading to the identification of 4-fluorobenzaldehyde as the main by-product in retigabine photodegradation (Figure S7). The result was further confirmed by comparison with the HPLC trace of pure 4-fluorobenzaldehyde (Figure S8)

and is consistent with a photooxidative C-N bond cleavage mechanism widely described in literature.[25] The proposed mechanism justifies the reason why visible light is more effective in inducing retigabine photodegradation[25c] and corroborate the hypothesis concerning the molecular structure of the peak eluting at 14.39 minutes. Considering that Groseclose and Castellino [24] found that the typical absorbance of retigabine photoinduced dimers is 550 nm, we decided to set the same wavelength for the UV detection, evidencing some additional byproducts with a retention time between 7.00 and 10.00 minutes. HPLC/MS/MS analysis of the most abundant peak lead to the putative identification of a dimer with a mass peak of 601.2357 m/z and a serie of MS/MS peaks roughly corresponding to some of the previously reported phenazinium dimers (Figure S9).[24] Thereafter, the most active synthesized derivatives, namely derivatives **8a**, **13a**, **13d**, **23a** and **24a**, were subjected to the photostability assay. Results obtained are reported in Table 2.

Table 2: Photoinduced degradation of retigabine and its analogues under solar lighting. Results are expressed as percentage of degradation±SD

Derivative	Time (h)		
	2	*4*	*6*
Retigabine	9.65±6.93%	25.16±7.31%	47.33±4.03%
8a	45.29±7.35%	86.87±10.54%	≥99%
13a	33.46±6.50%	81.72±1.12%	≥99%
13d	37.51±7.25%	84.66±4.12%	≥99%
23a	1.36±0.89%	5.82±2.05%	9.15±2.91%
23c	6.46±1.78%	15.78±1.97%	23.11±1.84%
24a	0.96±0.64%	6.62±2.17%	8.45±1.99%

Our results indicate that the N-(1-benzyl)indolin-5-yl)sulfonamide derivatives **8a**, **13a** and **13d** are even less stable than retigabine. At 6h degradation is almost complete and only traces of the starting molecules are detectable by HPLC analysis. This is likely due to the sulfonyl activation of the *p*-quinone diimine intermediate[26] representing the starting product in the degradative pattern for retigabine-like by-products. We perfomed HPLC/MS analysis for derivative **8a** to further investigate

the photodegradation pattern for this series of indolin-5-yl sulfonamides (Figure S10), but no significant mass peaks were identified. On the other side, GC/MS analysis revealed, also for **8a**, the presence of 4-fluorobenzaldehyde as the main photooxidation by-product, evidencing a similar photogradative pathway with retigabine (Figure S10). Increased photostability was attained turning to the N-(1-(4-fluorobenzyl)-1H-indol-5-yl)sulfonamide scaffold, as for **23c**, probably due to the improved delocalization of the π-electrons of the indole ring. Finally, derivatives **23a** and **24a**, obtained by replacement of the sulfonamide with a carboxamide moiety, were the most photostable retigabine analogues, showing less than 10% of degradation after the 6 hours time-course.

In vitro metabolism

In vitro metabolism assays were performed using the S9 fraction of human liver microsomes as model. Compounds **23a** and **24a** were selected for this study due to the potency and efficacy shown as Kv 7.2 agonists and to their inherent photostability. The phase I metabolism of these derivatives was initially investigated, in comparison with retigabine. In our assay, only a very small extent (3.11±0.21%) of retigabine undergoes phase I metabolism, a result consistent with available data.[6] Instead, derivative **23a** was found to undergo extensive (48.71±2.47 %) phase I metabolism. This is likely due to the fact that indole moiety is naturally prone to cytochrome metabolism [27], and the long and lipophilic side chain further decrease the metabolic stability of the compound. [28] In fact, when the lipophilicity of the side chain is decreased, as for derivative **24a,** an improved Phase I metabolic stability is attained (17.30±1.74% of degradation). Next, retigabine and the more stable to Phase I metabolism **24a** underwent to UDP-glucuronsyltransferases (UGT) and N-acyl transferase (NAT) activity evaluation. Retigabine was metabolized in 11.41±2.73% in UGT activity assays and in 12.68±1.94% in NAT activity assays, in agreement with the literature [12b, 29]. Compound **24a** displayed increased stability in both assays, being metabolized by 7.42±1.81% in UGT activity assays and 3.41±0.62% in NAT activity assays. Collectively, these results highlight a good in vitro metabolic

stability for compound **24a**, especially during Phase II metabolism, making **24a** a potential candidate for *in vivo* metabolic and pharmacokinetic studies.

CONCLUSIONS

Activation of Kv7 channels effectively suppresses neuronal hyperexcitability, a common feature of different neuropsychiatric disorders such as epilepsy,[30] neuropathic pain,[31] amyotrophic lateral sclerosis [32] and many others.[33] For these reasons, identification of Kv7 channels modulators showing improved pharmacokinetic and pharmacodynamic properties over existing compounds represents an attractive research topic in medicinal chemistry; this issue is even more pressing in the light of the recent market withdrawal of retigabine and flupirtine, the only two clinically approved drugs acting as Kv7 activators. In fact, the analgesic flupirtine was found to cause drug-induced liver injury in rare but fatal cases, whereas prolonged use of the antiepileptic retigabine led to muco-cutanous and retinal discoloration. Several efforts have been previously made in search for the structure-activity relationships regulating retigabine binding and actions at Kv7.2 and Kv7.3 channels. Results obtained so far describe the retigabine binding site as a central hydrophilic core flanked by two hydrophobic pockets. The most important chemical interaction evidenced is represented by a hydrogen bond between the carbamate group of retigabine as donor and a specific, highly conserved, triptophan residue (W265 in Kv7.3, W236 in Kv7.2) as acceptor. This H-bond has been considered as critically responsible to confer retigabine its ability to control Kv7 channel gating [5a, 21, 34] and is the reason why retigabine is inactive over cardiac Kv7.1 channels, in which this specific triptophan is substituted by a leucine residue. Previous investigations also provided evidence that the use of electron-withdrawing group in the para position of benzylamino substituents at C-4 of retigabine is able to increase potency and efficacy over Kv7.2/7.3 heterotetramers,[9a] while introduction of a fluorine atom in position 3 of the benzene-1,2,4-triamine core modulated selectivity among Kv7 channel subtypes.[35] Nevertheless, a systematic investigation of the structural determinants required for Kv7 channel modulation is still missing. In the present paper we have investigated the Kv7-opening ability of a series of constrained

retigabine analogues carrying specific substitutions in critical positions, thus generating a pharmacophore model. Our results further highlight the pivotal role of the H-bonding with W236 in Kv7.2 channel activation, but also reveal the possibility of using H-bond donor groups different from carbamate, such as amide and sulfonamide. It is worth of note that the replacement of the benzyl group at the N-4 position of retigabine (N-1 position in our derivatives) is hardly tolerated. When different substituents are used, the efficacy of the compound is always decreased in our series. Moreover, we found that the N-1 benzyl moiety tolerate multiple substitutions, regardless of the electron-withdrawing or electron-donating properties of the substituents. Previous results have led to the hypothesis of the existence of a narrow hydrophobic pocket accommodating the N-1 benzyl moiety exerting a specific interaction in the para-position. In addition, by the present data we may suppose the existence of a larger hydrophobic pocket (HY2 and HY3 region of the pharmacophore model), able to accommodate a wide range of hydrophobic substituents. Notably, some substituents at the position C-1 of retigabine (corresponding to the C-5 position in our derivatives) were also studied by Kumar et al.,[9a] who demonstrated that while lipophilic isopropyl chain improved potency by about 2/3 times, more hydrophilic substituents were not tolerated, suggesting the existence of a hydrophobic pocket. In agreement with this hypothesis, our results also highlight that changes in lipophilicity at C-5 also modify the kinetics of onset and offset of Kv7.2 channel activation; in fact, when compared to retigabine (log P=3.08), more lipophilic **23a** (logP=6.83) and **24a** (logP=5.58) both displayed slower kinetics. These results are in good agreement with recently published studies concerning flupirtine analogues.[36] Mostly important, we found that the type of substituents in position C-5 of the indole series influences selectivity between Kv7.2 and Kv7.3 channels. In particular, long and flexible carbon chains as in derivative **23a** are required for Kv7.2 selectivity. Furthermore, both indole derivatives **23a** and **24a** showed selectivity for Kv7.4 channels. Finally, we found that some of the most active derivatives show a dramatic improvement in photostability in comparison with retigabine. Further investigations are needed to optimize metabolic properties of synthesized

compounds, but the preliminary results obtained seem highly promising for the development of a new class of Kv7 channel modulators.

Experimental section

General. All reagents and solvents used were purchased from Sigma-Aldrich (Milan, Italy), unless otherwise stated. Reactions were carried out with magnetic stirring in round-bottomed flasks unless otherwise noted. Moisture-sensitive reactions were conducted in oven-dried glassware under nitrogen stream, using freshly distilled solvents. Pre-coated glass silica gel plates (F254, 0.25 mm, VWR International) were used for TLC analysis of reaction mixtures, while crude products were purified by an automated flash chromatography system (Isolera Spektra one, Biotage, Uppsala, Sweden) coupled with an APCI mass detector (Dalton 2000, Biotage), using pre-loaded silica gel cartridges (SNAP KP-Sil, Biotage). Continuous flow hydrogenation reactions were conducted using the H-cube hydrogenation reactor (ThalesNano, Budapest, Hungary) equipped with pre-loaded Pd/C 10% cartridges (30 mm, ThalesNano). NMR spectra were recorded on Varian Mercury 400 MHz and on a Bruker Avance 400 MHz and 300 MHz apparatus, at room temperature. Chemical shifts were reported in δ values (ppm) relative to internal Me_4Si, for ^1H and ^{13}C NMR, and $CClF_3$ for ^{19}F NMR. J values were reported in hertz (Hz). ^1H-NMR and ^{19}F NMR peaks were described using the following abbreviations: s (singlet), d (doublet), t (triplet) and m (multiplet). HR-MS spectra were recorded by LTQ-Orbitrap-XL-ETD mass spectrometer (Thermo Scientific, Bremen, Germany), equipped with an ESI source. Analytical RP-HPLC analysis of final products was performed to confirm ≥95% purity using the instrumentation and the UHPLC PDA conditions described below.

General procedure A: reductive amination reaction.

Reductive aminations were performed following the procedure previously described,[37] using 5-nitroindoline (**1**), 2-methyl-5-nitroindoline (**10**) or tert-butyl 5-nitroindoline-1-carboxylate (**10b**)

as starting materials and commercially available aldehydes. Briefly, to a solution of the aldehyde (1.0 eq) in DCM:CH_3COOH (5:1 v/v) 2.0 equivalents of **1**, **10** or **10b** were added and the mixture was warmed to reflux for 1.5h. After addition of 1.8 equivalents of sodium triacetoxyborohydride the mixture was refluxed for further 3-5h. After cooling to room temperature, aqueous solution of NaOH (1N) was added. The organic layer was separated and further extracted with NaOH 1N. After drying over Na_2SO_4, the organic phase was concentrated in vacuo. Intermediates thus obtained were purified by flash chromatography using linear gradients of n-hexane/ethyl acetate as mobile phase.

General procedure B: Continuous flow hydrogenation.

Reduction of 5-nitroindoline and 5-nitroindole derivatives was achieved by continuous flow hydrogenation using the H-Cube hydrogenator and commercially available Pd/C 10% cartridges as catalyst. Starting material was dissolved in a mixture of THF/CH_3OH (1:1, v:v) at a final concentration of 0.1M and was pumped at a flow rate of 1.0 mL/min. Temperature was set at 30°C while the hydrogen inlet pressure was set at 10 bar. After completion, the reaction solution was evaporated *in vacuo* and the obtained products used in the following step without further purification.

General procedure C: Synthesis of sulfonamides

Indolin-5-amino and 1H-indol-5-amino intermediates (1.0 eq) were dissolved in dry DCM under a nitrogen positive pressure. To this solution 1.2 equivalents of 1,5-diazabiciclo(5.4.0)undec-7-ene (DBU) were added. The reaction mixture was stirred at room temperature for 15 minutes, then 1.5 equivalents of the proper sulfonyl chloride were added. The mixture was stirred for further 2h. The reaction was then washed with a saturated solution of $NaHCO_3$ and brine. The organic phase was extracted, dried over anhydrous $NaSO_4$, filtered and concentrated *in vacuo*. Crude products were purified using a linear gradient of n-exane/ethyl acetate.

General procedure D: Synthesis of amides

Indolin-5-amino and 1H-indol-5-amino intermediates (1.0 eq) were dissolved in dry DCM under a nitrogen positive pressure and added, under stirring, with 1.2 equivalents of N,N-Diisopropylethylamine (DIPEA). The mixture was cooled to 0°C and added dropwise with a solution of the proper acyl chloride or acyl bromide (1.2 eq) in DCM. The solution was allowed to cool to room temperature and stirred for further 30 minutes. The reaction was then washed with a saturated solution of $NaHCO_3$ and brine. The organic phase was extracted, dried over anhydrous $NaSO_4$, filtered and concentrated in vacuo. Crude products were purified using a linear gradient of n-exane/ethyl acetate.

General procedure E: Synthesis of N-1 substitued 5-nitro indoline and 5-nitro-1H-indole derivatives.

The reactions were performed following the procedure described before.[38] Briefly, 5-nitroindoline (**1)** or 5-nitro-1H-indole (**20**) (1.0 eq) were dissolved in dry DCM/DMF (2/1 v/v) under stirring, at 0 °C. To this solution, 1.2 equiv of NaH were added portionwise and the mixture stirred for 30 min at 0 °C. Then, a solution of of the proper alkyl halide (1.2 eq) in dry DCM was added dropwise. The mixture was warmed to room temperature and stirred for 12 h. After quenching by 10% aqueous solution of citric acid and washing with brine, the organic layer was separated, dried over anhydrous Na_2SO_4 and evaporated in vacuo. Crude products were purified by flash chromatography coupled to mass spectrometry, using a linear gradient of n-exane/ethyl acetate.

1-(4-fluorobenzyl)-5-nitroindoline (2)

Synthesized according to the general procedure A using 5-nitroindoline (**1**) and 4-fluorobenzaldehyde as reagents. Intermediate **2** was isolated as a yellow powder in 65% yield. ^{1}H NMR ($CDCl_3$, 400 MHz): δ: 3.12 (t, 2H, CH_2, J = 8.6 Hz); 3.63 (t, 2H, CH_2, J = 8.6 Hz); 4.42 (s, 2H, CH_2); 6.37 (d, 1H, aryl, J = 8.1 Hz); 7.04-7.09 (m, 2H, aryl); 7.24-7.28 (m, 2H, aryl); 7.94 (s, 1H, aryl); 8.08 (d, 1H, aryl, J = 7.8 Hz). HR-MS *m/z*: calcd for $C_{19}H_{14}FN_2O_2$, [$(M+H)^+$]: 273.1034; found 273.1039

1-(4-fluorobenzyl)indolin-5-amine (3)

Synthesized from intermediate **2** according to the general procedure B. The product was obtained as a grey powder in 98% yield. ^{1}H NMR ($CDCl_3$, 400 MHz): δ: 2.98 (t, 2H, CH_2, J = 8.7 Hz); 3.18 (t, 2H, CH_2, J = 8.7 Hz); 3.35 (bs, 2H, NH_2); 4.12 (s, 2H, CH_2); 6.38 (d, 1H, aryl, J = 8.1 Hz); 6.47 (d, 1H, aryl, J = 8.2 Hz); 6.60 (s, 1H, aryl); 6.99-7.07 (m, 2H, aryl); 7.34-7.39 (m, 2H, aryl). HR-MS *m/z*: calcd for $C_{15}H_{16}FN_2$, [$(M+H)^+$]: 243.1292; found 243.1301

Ethyl (1-(4-fluorobenzyl)indolin-5-yl)carbamate (4a)

Intermediate **3** (1.0 eq) was dissolved in dry THF and stirred under nitrogen positive pressure. The solution was added with 1.1 equivalents of $NaHCO_3$ and the resulting suspension was cooled to 0°C in ice bath. To this suspension, 1.1 equivalents of ethyl chloroformate were added and the slurry was stirred at 0°C for further 30 minutes. After warming at room temperature, an equal volume of water was added and the solution was extracted three times with ethylacetate. Organic phases were dried over anhydrous $NaSO_4$, filtered and concentrated *in vacuo*. Final product was isolated as a white crystal in 72% yield and crystallized from n-hexane/diethyl ether. ^{1}H NMR ($CDCl_3$, 400 MHz): δ: 1.32 (t, 3H, CH_3, J = 7.1 Hz); 2.97 (t, 2H, CH_2, J = 8.2 Hz); 3.29 (t, 2H, CH_2, J = 8.2 Hz); 4.19-4.25 (m, 4H, CH_2); 6.37 (bs, 1H, NH); 6.45 (d, 1H, aryl, J = 8.3 Hz); 6.95 (d, 1H, aryl, J = 7.7 Hz); 7.04 (t, 2H, aryl, J = 8.4 Hz); 7.22 (bs, 1H, aryl); 7.32-7.36 (m, 2H, aryl). ^{13}C NMR ($CDCl_3$, 100 MHz) δ: 14.6; 28.6; 53.5; 53.9; 61.0; 107.0; 115.2; 115.4; 118.8; 119.3; 129.4; 131.0; 134.0; 149.3; 160.8; 163.3. ^{19}F NMR ($CDCl_3$, 376.3 MHz) δ: -(115.89-115.80) (m, 1F, CF) HR-MS *m/z*: calcd for $C_{18}H_{20}FN_2O_2$, [$(M+H)^+$]: 315.1503; found 315.1514

(1S,2R,5S)-2-isopropyl-5-methylcyclohexyl (1-(4-fluorobenzyl)indolin-5-yl)carbamate (4b)

Final product **4b** was synthesized according to the same procedure described above for **4a**, using the commercially available (1S)-(+)-menthyl chloroformate as reagent. The product was obtained as a white wax in 63% yield. $[\alpha]^{25}_{D}$: 32.67 ± 0.04 (c = 0.15, MeOH). ^{1}H NMR ($CDCl_3$, 400 MHz): δ: 0.83 (d, 3H, C*H*$_3$, *J* = 7.0 Hz); 0.93 (d, 6H, C*H*$_3$, *J* = 7.1 Hz); 0.99-1.16 (m, 2H, C*H*$_2$); 1.27-1.41 (m, 1H, C*H*$_2$); 1.49-1.56 (m, 1H, C*H*); 1.67-1.74 (m, 2H, C*H*$_2$); 1.94-2.02 (m, 1H, C*H);* 2.09-2.16 (m, 1H, C*H*$_2$); 2.96 (t, 2H, C*H*$_2$, *J* = 8.4 Hz); 3.27 (t, 2H, C*H*$_2$, *J* = 8.4 Hz); 4.18 (s, 2H, C*H*$_2$); 4.61-4.70 (m, 1H, C*H*); 6.35 (bs, 1H, NH); 6.42 (d, 1H, aryl, *J* = 8.5 Hz); 6.95 (d, 1H, aryl, *J* = 8.2 Hz); 7.03 (t, 2H, aryl, *J* = 8.7 Hz); 7.25 (bs, 1H, aryl); 7.31-7.36 (m, 2H, aryl). ^{13}C NMR ($CDCl_3$, 100 MHz) δ: 16.5; 20.8; 22.1; 23.6; 26.3; 28.6; 31.4; 34.3; 41.5; 47.4; 53.5; 53.9; 74.8; 107.1; 115.2; 115.4; 117.4; 118.9; 129.1; 129.4; 129.5; 131.0; 134.0; 154.0; 160.8; 163.3. ^{19}F NMR ($CDCl_3$, 376.3 MHz) δ: -(115.82-115.74) (m, 1F, C*F*) HR-MS *m/z*: calcd for $C_{26}H_{34}FN_2O_2$, $[(M+H)^+]$: 425.2599; found 425.2608

1-(1-(4-fluorobenzyl)indolin-5-yl)-3-neopentylurea (5a)

Triphosgene (1.0 eq) was dissolved in dry DCM, under nitrogen stream at 0°C. To the resulting mixture, a solution of 1.25 equivalents of 1-(4-fluorobenzyl)indolin-5-amine **(3)** and 2.6 equivalents of DIPEA dissolved in DCM were added dropwise in 5 minutes. The solution was maintained under stirring for further 5 minutes. Then, a solution of 2,2-dimethylpropan-1-amine (2.5 eq) and DIPEA (2.6 eq) in DCM was added dropwise. The reaction mixture was allowed to warm at room temperature, maintained under stirring overnight and quenched by adding an equal volume of water. The organic phase was washed with a saturated solution of $NaHCO_3$ and then with brine, before being dried over anhydrous Na_2SO_4, filtered and evaporated to dryness. The crude product was isolated as white crystal in 69% yield and crystallized from ethyl acetate. ^{1}H NMR ($CDCl_3$, 400 MHz): δ: 0.89 (s, 9H, 3 C*H*$_3$); 2.99 (t, 2H, C*H*$_2$, *J* = 8.3 Hz); 3.05 (d, 2H, C*H*$_2$, *J* = 6.3 Hz); 3.35 (t, 2H, C*H*$_2$, *J* = 8.3 Hz); 4.23 (s, 2H, C*H*$_2$); 4.71 (t, 1H, N*H*, *J* = 5.6 Hz); 5.98 (s, 1H, N*H*); 6.45 (d, 1H, aryl, *J* = 8.2 Hz);

6.92 (d, 1H, aryl, J = 8.2 Hz); 7.02-7.07 (m, 3H, aryl); 7.32-7.35 (m, 2H, aryl). ^{13}C NMR ($CDCl_3$, 100 MHz) δ: 27.2; 28.4; 32.2; 51.4; 53.0; 53.7; 107.1; 115.3; 115.5; 122.8; 125.0; 127.7; 129.40; 129.45; 131.5; 133.7; 150.9; 157.5; 160.9; 163.3 ^{19}F NMR ($CDCl_3$, 376.3 MHz) δ: -(115.55-115.34) (m, 1F, C*F*). HR-MS *m/z*: calcd for $C_{21}H_{27}FN_3O$, [$(M+H)^+$]: 356.2133; found 356.2148

1-cyclohexyl-3-(1-(4-fluorobenzyl)indolin-5-yl)urea (5b)

Final product **5b** was synthesized as described above for **5a**, using cyclohexylamine in place of 2,2-dimethylpropan-1-amine. Final product was obtained as a white crystal in 57% yield and crystallized from methanol. ^{1}H NMR (DMSO-d6, 400 MHz): δ: 1.08-1.34 (m, 5H, CH_2 and C*H*); 1.52-1.55 (m, 1H, C*H*); 1.63-1.67 (m, 2H, CH_2); 1.77-1.80 (m, 2H, CH_2); 2.82 (t, 2H, CH_2, J = 8.2 Hz); 3.14 (t, 2H, CH_2, J = 8.2 Hz); 3.39-3.43 (m, 1H, C*H*); 4.16 (s, 2H, CH_2); 5.85 (d, 1H, N*H, J* = 7.9 Hz); 6.47 (d, 1H, aryl, J = 8.4 Hz); 6.90 (d, 1H, aryl, J = 8.4 Hz); 7.14-7.19 (m, 3H, aryl); 7.37-7.41 (m, 2H, aryl); 7.86 (s, 1H, N*H*). ^{13}C NMR (DMSO-d6, 100 MHz) δ: 24.9; 25.8; 28.7; 33.6; 48.0; 53.3; 53.8; 107.0; 115.4; 115.6; 116.6; 117.7; 130.4; 130.5; 132.1; 135.1; 147.6; 155.3; 160.5; 162.9. ^{19}F NMR (DMSO-d6, 376.3 MHz) δ: -(116.04-115.96) (m, 1F, C*F*). HR-MS *m/z*: calcd for $C_{22}H_{27}FN_3O$, [$(M+H)^+$]: 368.2133; found 368.2139

1-(1-(4-fluorobenzyl)indolin-5-yl)-3-neopentylthiourea (6)

Starting from 1-(4-fluorobenzyl)indolin-5-amine **(3),** final compound **6** was obtained via isothiocyanate intermediate, followed by reaction with 2,2-dimethylpropan-1-amine slightly modifying a previously described procedure.[39] In our procedure, the use of benzene as solvent was avoided by replacing with dry toluene for the synthesis of the isothiocyanate intermediate, and dry DCM for the conversion of the isothiocyanate to thiourea. The final product was obtained as a grey powder in 54% yield and was crystallized form ethyl acetate. ^{1}H NMR ($CDCl_3$, 400 MHz): δ: 0.89 (s, 9H, CH_3); 2.99 (t, 2H, CH_2, J = 8.4 Hz); 3.39 (t, 2H, CH_2, J = 8.4 Hz); 3.48 (d, 2H, CH_2, J = 5.8

Hz); 4.25 (s, 2H, CH_2); 5.93 (t, 1H, N*H*, *J* = 7.4 Hz); 6.46 (d, 1H, aryl, *J* = 8.1 Hz); 6.90 (d, 2H, aryl, *J* = 9.4 Hz); 7.01-7.07 (m, 2H, aryl); 7.29-7.33 (m, 2H, aryl); 7.58 (s, 1H, N*H*). ^{13}C NMR ($CDCl_3$, 100 MHz) δ: 27.4; 28.2; 32.2; 52.5; 53.4; 56.4; 107.0; 115.3; 115.6; 123.3; 125.2; 126.1; 129.3; 132.0; 133.3; 152.1; 160.5; 163.7; 181.7. ^{19}F NMR ($CDCl_3$, 376.3 MHz) δ: -(115.25-115.18) (m, 1F, C*F*) HR-MS *m/z*: calcd for $C_{21}H_{27}FN_3S$, [$(M+H)^+$]: 372.1904; found 372.1911

1-(1-(4-fluorobenzyl)indolin-5-yl)-3-neopentylguanidine (7)

Final compound **7** was obtained from **6** via carbodiimide intermediate followed by reaction with 2,2-dimethylpropan-1-amine, using the procedure described by Plsikova et al.[40] The final product was obtained as white crystal in 40% yield and crystallized from methanol.

^{1}H NMR ($CDCl_3$, 400 MHz): δ: 0.97 (s, 9H, 3 CH_3); 2.93 (t, 2H, CH_2, *J* = 8.1 Hz); 2.99 (s, 2H, CH_2); 3.25 (t, 2H, CH_2, *J* = 8.1 Hz); 4.18 (s, 2H, CH_2); 6.47 (d, 1H, aryl, *J* = 8.1 Hz); 6.67 (d, 1H, aryl, *J* = 7.8 Hz); 6.77 (s, 1H, aryl); 7.04 (t, 2H, aryl, *J* = 8.5 Hz); 7.34-7.37 (m, 2H, aryl). ^{13}C NMR ($CDCl_3$, 100 MHz) δ: 27.3; 28.7; 53.5; 53.9; 54.1; 107.9; 115.1; 115.4; 120.8; 122.1; 129.5; 129.6; 131.5; 134.3; 148.5; 160.8; 163.2. ^{19}F NMR ($CDCl_3$, 376.3 MHz) δ: -(115.86-115.78) (m, 1F, C*F*). HR-MS *m/z*: calcd for $C_{21}H_{28}FN_4$, [$(M+H)^+$]: 355.2293; found 355.2300

N-(1-(4-fluorobenzyl)indolin-5-yl)cyclohexanesulfonamide (8a)

Final product **8a** was obtained from 1-(4-fluorobenzyl)indolin-5-amine **(3)** and cyclohexanesulfonyl chloride following the general procedure C. The product was isolated in 67% yield as a grey powder that crystallizes from n-hexane/diethyl ether. ^{1}H NMR ($CDCl_3$, 400 MHz): δ: 1.10-1.21 (m, 3H, CH_2 and C*H*); 1.47-1.60 (m, 3H, CH_2 and C*H*); 1.80-1.82 (m, 2H, CH_2); 2.08-2.11 (m, 2H, CH_2); 2.83-2.91 (m, 3H, CH_2 and C*H*); 3.25 (t, 2H, CH_2, *J* = 8.3 Hz); 4.12 (s, 2H, CH_2); 5.96 (s, 1H, N*H*); 6.31 (d, 1H, aryl, *J* = 8.2 Hz); 6.81 (d, 1H, aryl, *J* = 8.3 Hz); 6.93-6.98 (m, 3H, aryl); 7.22-7.25 (m, 2H, aryl). ^{13}C NMR ($CDCl_3$, 100 MHz) δ: 25.1; 26.4; 28.4; 53.0; 53.7; 59.3; 106.9; 115.3; 115.5; 121.4;

123.3; 126.5; 129.3; 129.4; 131.4; 133.7; 151.0; 160.9; 163.33. ^{19}F NMR ($CDCl_3$, 376.3 MHz) δ: -(114.71-114.63) (m, 1F, C*F*) HR-MS *m/z*: calcd for $C_{21}H_{26}FN_2O_2S$, [$(M+H)^+$]: 389.1694; found 389.1699; [$(M+Na)^+$]: 411.1513; found 411.1520

N-(1-(4-fluorobenzyl)indolin-5-yl)benzenesulfonamide (8b)

Final product **8b** was obtained from 1-(4-fluorobenzyl)indolin-5-amine **(3)** and benzenesulfonyl chloride following the general procedure C. The product was isolated in 70% yield as a grey powder that crystallizes from n-hexane/ethyl acetate. ^{1}H NMR ($CDCl_3$, 400 MHz): δ: 2.92 (t, 2H, CH_2, *J* = 8.0 Hz); 3.31 (t, 2H, CH_2, *J* = 8.0 Hz); 4.18 (s, 2H, CH_2); 6.20 (s, s, 1H, N*H*); 6.29 (d, 1H, aryl, *J* = 8.2 Hz); 6.61 (d, 1H, aryl, *J* = 6.8 Hz); 6.87 (s, 1H, aryl); 7.03 (t, 2H, aryl, *J* = 8.4 Hz); 7.28-7.31 (m, 3H, aryl); 7.46 (t, 2H, aryl, *J* = 7.3 Hz); 7.56 (t, 1H, aryl, *J* = 7.1 Hz); 7.74 (d, 2H, aryl, *J* = 7.4 Hz). ^{13}C NMR ($CDCl_3$, 100 MHz) δ: 28.2; 52.8; 53.6; 106.6; 115.3; 115.5; 122.6; 124.7; 125.7; 127.4; 128.8; 129.3; 129.4; 131.1; 132.6; 133.6; 139.4; 151.4; 160.9; 163.3. ^{19}F NMR ($CDCl_3$, 376.3 MHz) δ: -(115.53-115.46) (m, 1F, C*F*) HR-MS *m/z*: calcd for $C_{21}H_{20}FN_2O_2S$, [$(M+H)^+$]: 383.1224; found 383.1230

N-(1-(4-fluorobenzyl)indolin-5-yl)butane-1-sulfonamide (8c)

Final product **8c** was obtained from 1-(4-fluorobenzyl)indolin-5-amine **(3)** and butanesulfonyl chloride following the general procedure C. The product was isolated in 72% yield as an off-white powder that crystallizes from n-hexane/diethyl ether. ^{1}H NMR ($CDCl_3$, 400 MHz): δ: 0.94 (t, 3H, CH_3, *J* = 7.3 Hz); 1.38-1.49 (m, 2H, CH_2); 1.78-1.88 (m, 2H, CH_2); 2.95-3.06 (m, 4H, 2 CH_2); 3.34 (t, 2H, CH_2, *J* = 7.9 Hz); 4.21 (s, 2H, CH_2); 6.28 (s, 1H, N*H*); 6.40 (d, 1H, aryl, *J* = 8.2 Hz); 6.91 (d, 1H, aryl, *J* = 8.1 Hz); 7.02-7.07 (m, 3H, aryl); 7.30-7.35 (m, 2H, aryl). ^{13}C NMR ($CDCl_3$, 100 MHz) δ: 13.6; 21.5; 25.5; 28.3; 50.6; 52.9; 53.7; 106.9; 115.3; 115.5; 121.7; 123.7; 126.2; 129.3; 129.4;

131.5; 133.6; 151.2; 160.5; 163.7. ^{19}F NMR ($CDCl_3$, 376.3 MHz) δ: -(113.51-113.43) (m, 1F, C*F*) HR-MS *m/z*: calcd for $C_{19}H_{24}FN_2O_2S$, $[(M+H)^+]$: 363.1537; found 363.1545

N-(1-(4-fluorobenzyl)indolin-5-yl)-2-methylpropane-1-sulfonamide (8d)

Final product **8d** was obtained from 1-(4-fluorobenzyl)indolin-5-amine **(3)** and 2-methylpropane-1-sulfonyl chloride following the general procedure C. The product was isolated in 71% yield as an off-white powder that crystallizes from n-hexane/diethyl ether. ^{1}H NMR ($CDCl_3$, 400 MHz): δ: 1.08 (d, 6H, CH_3, J = 6.6 Hz); 2.26-2.31 (m, 1H, C*H*); 2.90 (d, 2H, CH_2 J = 6.3 Hz); 2.96 (t, 2H, CH_2, J = 8.2 Hz); 3.32 (t, 2H, CH_2, J = 8.2 Hz); 4.19 (s, 2H, CH_2); 6.18 (s, 1H, N*H*); 6.38 (d, 1H, aryl, J = 7.8 Hz); 6.88 (d, 1H, aryl, J = 7.4 Hz); 7.00-7.04 (m, 3H, aryl); 7.29-7.32 (m, 2H, aryl). ^{13}C NMR ($CDCl_3$, 100 MHz) δ: 21.3; 24.6; 27.6; 48.5; 53.9; 58.6; 58.8; 115.6; 115.8; 116.5; 118.7; 119.2; 126.5; 132.7; 132.8; 136.4; 136.7; 139.6; 162.4; 164.9. ^{19}F NMR ($CDCl_3$, 376.3 MHz) δ: -(114.75-114.68) (m, 1F, C*F*) HR-MS *m/z*: calcd for $C_{19}H_{24}FN_2O_2S$, $[(M+H)^+]$: 363.1537; found 363.1545

N-(1-(4-fluorobenzyl)indolin-5-yl)hexane-1-sulfonamide (8e)

Final product **8e** was obtained from 1-(4-fluorobenzyl)indolin-5-amine **(3)** and hexanesulfonyl chloride following the general procedure C. The product was isolated in 67% yield as a grey powder that crystallizes from ethyl acetate. ^{1}H NMR (CD_3OD, 400 MHz): δ: 0.91 (t, 3H, CH_3, J = 7.9 Hz); 1.28-1.34 (m, 4H, CH_2); 1.36-1.46 (m, 2H, CH_2); 1.75-1.82 (m, 2H, CH_2); 3.13-3.18 (m, 4H, 2 CH_2); 3.91 (t, 2H, CH_2, J = 8.2 Hz); 4.70 (s, 2H, CH_2); 7.18-7.27 (m, 3H, aryl); 7.33-7.35 (m, 2H, aryl); 7.49-7.52 (m, 2H, aryl). ^{13}C NMR (CD_3OD, 100 MHz) δ: 12.9; 22.0; 23.2; 27.6; 31.0; 51.1; 53.4; 53.9; 58.9; 115.8; 116.3; 118.9; 119.3; 126.1; 133.0; 135.7; 137.0; 140.2; 162.5; 165.0. ^{19}F NMR ($CDCl_3$, 376.3 MHz) δ: -(113.17-113.10) (m, 1F, C*F*) HR-MS *m/z*: calcd for $C_{21}H_{28}FN_2O_2S$, $[(M+H)^+]$: 391.1850; found 391.1862

1-((1S,4R)-7,7-dimethyl-2-oxobicyclo[2.2.1]heptan-1-yl)-N-(1-(4-fluorobenzyl)indolin-5-yl)methanesulfonamide (8f)

Final product **8f** was obtained from 1-(4-fluorobenzyl)indolin-5-amine **(3)** and (1S)-(+)-10-camphorsulfonyl chloride following the general procedure C. The product was isolated in 57% yield as a grey powder that crystallizes from n-hexane/ethyl acetate. $[\alpha]^{25}_{D}$: 37.50 ± 0.05 (c = 0.12, MeOH). ^{1}H NMR ($CDCl_3$, 400 MHz): δ: 0.92 (s, 3H, C*H*$_3$); 0.99 (s, 3H, C*H*$_3$); 1.47-1.52 (m, 1H, C*H*); 1.98-2.20 (m, 4H, C*H*$_2$ and 2 C*H*); 2.44-2.51 (m, 1H, C*H*); 2.81 (d, 1H, C*H*, *J* = 15.3 Hz); 2.98 (t, 2H, C*H*$_2$, *J* = 8.3 Hz); 3.28-3.36 (m, 4H, 2 C*H*$_2$); 3.44 (d, 1H, C*H*, *J* = 15.2 Hz); 4.21 (s, 2H, C*H*$_2$); 6.41 (d, 1H, aryl, *J* = 8.3 Hz); 6.94 (d, 1H, aryl, *J* = 8.3 Hz); 7.04 (t, 2H, aryl *J* = 8.7 Hz); 7.10 (s, 1H, aryl); 7.31-7.35 (m, 2H, aryl); 7.45 (s, 1H, N*H*). ^{13}C NMR ($CDCl_3$, 100 MHz) δ: 19.4; 19.9; 27.1; 27.8; 28.4; 42.9; 43.1; 48.1; 49.1; 53.0; 53.7; 59.8; 106.8; 115.3; 115.5; 121.9; 123.5; 127.7; 129.3; 129.4; 131.3; 133.8; 151.1; 160.9; 163.3; 217.5. ^{19}F NMR ($CDCl_3$, 376.3 MHz) δ: -(115.58-115.50) (m, 1F, C*F*) HR-MS *m/z*: calcd for $C_{25}H_{30}FN_2O_3S$, $[(M+H)^+]$: 457.1986; found 457.2001

1-((1R,4S)-7,7-dimethyl-2-oxobicyclo[2.2.1]heptan-1-yl)-N-(1-(4-fluorobenzyl)indolin-5-yl)methanesulfonamide (8g)

Final product **8g** was obtained from 1-(4-fluorobenzyl)indolin-5-amine **(3)** and (1R)-(−)-10-camphorsulfonyl chloride following the general procedure C. The product was isolated in 50% yield as a grey powder that crystallizes from n-hexane/ethyl acetate. $[\alpha]^{25}_{D}$: -38.10 ± 0.06 (c = 0.12, MeOH). ^{1}H NMR ($CDCl_3$, 300 MHz): δ: 0.92 (s, 3H, C*H*$_3$); 0.98 (s, 3H, C*H*$_3$); 1.47-1.52 (m, 1H, C*H*); 1.97-2.22 (m, 5H, 2 C*H*$_2$ and C*H*); 2.44-2.52 (m, 1H, C*H*); 2.80 (d, 1H, C*H*, *J* = 15.6 Hz); 2.97 (t, 2H, C*H*$_2$, *J* = 8.6 Hz); 3.32 (t, 2H, C*H*$_2$, *J* = 8.6 Hz); 3.43 (d, 1H, C*H*, *J* = 16.0 Hz); 4.21 (s, 2H, C*H*$_2$); 6.41 (d, 1H, aryl, *J* = 8.4 Hz); 6.93 (d, 1H, aryl, *J* = 8.4 Hz); 7.01-7.10 (m, 3H, aryl); 7.30-7.35 (m, 2H, aryl); 7.47 (s, 1H, N*H*). ^{13}C NMR ($CDCl_3$, 75 MHz) δ: 19.4; 20.0; 27.1; 27.7; 28.4; 42.9; 43.1; 48.1; 49.1; 53.0; 53.7; 59.8; 106.8; 115.3; 115.56; 121.8; 123.5; 127.7; 129.40; 129.44; 131.3;

133.8; 151.1; 160.9; 163.3; 217.5. ^{19}F NMR ($CDCl_3$, 376.3 MHz) δ: -(115.89-115.82) (m, 1F, C*F*). HR-MS *m/z*: calcd for $C_{25}H_{30}FN_2O_3S$, $[(M+H)^+]$: 457.1986; found 457.1995

N-(1-(4-fluorobenzyl)indolin-5-yl)azepane-1-sulfonamide (8h)

Final product **8h** was obtained from 1-(4-fluorobenzyl)indolin-5-amine **(3)** and azepane-1-sulfonyl chloride following the general procedure C. The product was isolated in 69% yield as an off-white powder that crystallizes from n-hexane/diethyl ether. ^{1}H NMR ($CDCl_3$, 400 MHz): δ: 1.56-1.59 (m, 4H, 2 CH_2); 1.68-1.70 (m, 4H, 2 CH_2); 2.97 (t, 2H, CH_2, *J* = 8.3 Hz); 3.29-3.34 (m, 6H, 3 CH_2); 4.21 (s, 2H, CH_2); 6.27 (s, 1H, NH); 6.41 (d, 1H, aryl, *J* = 8.3 Hz); 6.90 (d, 1H, aryl, *J* = 8.2 Hz); 7.02-7.06 (m, 3H, aryl); 7.31-7.34 (m, 2H, aryl). ^{13}C NMR ($CDCl_3$, 100 MHz) δ: 26.9; 28.4; 29.1; 48.9; 53.1; 53.7; 106.8; 115.2; 115.5; 121.4; 123.5; 127.4; 129.4; 129.5; 131.1; 133.8; 150.8; 160.9; 163.3. ^{19}F NMR ($CDCl_3$, 376.3 MHz) δ: -(115.58-115.51) (m, 1F, C*F*). HR-MS *m/z*: calcd for $C_{21}H_{27}FN_3O_2S$, $[(M+H)^+]$: 404.1803; found 404.1876

N-(1-(4-fluorobenzyl)indolin-5-yl)-3,5-dimethylpiperidine-1-sulfonamide (8i)

Final product **8i** was obtained as a conformers mixture (A:B, 4:1) from 1-(4-fluorobenzyl)indolin-5-amine **(3)** and 3,5-dimethylpiperidine-1-sulfonyl chloride following the general procedure C. The product was isolated in 65% yield as an off-white powder that crystallizes from ethyl acetate. ^{1}H NMR (CD_3OD, 400 MHz): δ: (**A**) = 0.60-0.69 (m, 1H, C*H*); 0.88 (s, 3H, CH_3); 0.90 (s, 3H, CH_3); 1.56-1.60 (m, 2H, CH_2,); 1.75 (d, 2H, CH_2, *J* = 12.9 Hz); 2.24 (t, 2H, CH_2, *J* = 11.7 Hz); 3.12 (bs, 2H, CH_2); 3.66-3.69 (m, 2H, CH_2); 3.86 (bs, 2H, CH_2); 4.66 (s, 2H, CH_2); 7.17-7.24 (m, 5H, aryl); 7.46-7.49 (m, 2H, aryl). (**B**) = 0.88 (s, 3H, CH_3); 0.90 (s, 3H, CH_3); 1.37 (t, 2H, CH_2, *J* = 5.7 Hz); 1.75 (d, 2H, CH_2, *J* = 12.9 Hz); 1.89-1.91 (m, 2H, CH_2); 2.83-2.88 (m, 2H, CH_2); 3.12 (bs, 2H, CH_2); 3.22-3.26 (m, 2H, CH_2); 3.86 (bs, 2H, CH_2); 4.66 (s, 2H, CH_2); 7.17-7.24 (m, 5H, aryl); 7.46-7.49 (m, 2H, aryl). ^{13}C NMR (CD_3OD, 100 MHz) δ: (**A** + **B**) = 17.2; 17.8; 26.7; 27.6; 30.8; 38.0; 41.3;

52.4; 52.6; 53.9; 58.7; 58.8; 115.6; 115.8; 118.4; 118.8; 132.8; 132.9; 136.5; 162.5; 164.9. ^{19}F NMR ($CDCl_3$, 376.3 MHz) δ: -(116.04-116.12) (m, 1F, C*F*). HR-MS *m/z*: calcd for $C_{22}H_{29}FN_3O_2S$, [$(M+H)^+$]: 418.1959; found 418.1964

N-(1-(4-fluorobenzyl)indolin-5-yl)acetamide (9a)

Final product **9a** was obtained from 1-(4-fluorobenzyl)indolin-5-amine **(3)** and acetyl chloride following the general procedure D. The product was isolated in 84% yield as a white powder that crystallizes from n-hexane/diethyl ether. ^{1}H NMR (CD_3OD, 400 MHz) δ: 2.09 (s, 3H, CH_3); 2.91 (t, 2H, CH_2, *J* = 8.2 Hz); 3.24 (t, 2H, CH_2, *J* = 8.2 Hz); 4.20 (s, 2H, CH_2); 6.50 (d, 1H, aryl, *J* = 8.4 Hz); 7.04-7.12 (m, 3H, aryl); 7.27 (s, 1H, aryl); 7.37-7.40 (m, 2H, aryl). ^{13}C NMR (CD_3OD, 100 MHz) δ: 22.2; 28.0; 52.9; 53.5; 106.8; 114.6; 114.8; 118.0; 119.9; 129.3; 129.5; 130.5; 134.32; 134.35; 149.5; 160.9; 163.3; 169.9. ^{19}F NMR (CD_3OD, 376.3 MHz) δ: -(117.98-118.06) (m, 1F, C*F*). HR-MS *m/z*: calcd for $C_{17}H_{18}FN_2O$, [$(M+H)^+$]: 285.1398; found 285.1405

N-(1-(4-fluorobenzyl)indolin-5-yl)cyclohexanecarboxamide (9b)

Final product **9b** was obtained from 1-(4-fluorobenzyl)indolin-5-amine **(3)** and cyclohexanecarbonyl chloride following the general procedure D. The product was isolated in 79% yield as a white powder that crystallizes from ethyl acetate. ^{1}H NMR ($CDCl_3$, 400 MHz): δ: 1.22-1.38 (m, 3H, CH_2); 1.50-1.71 (m, 3H, CH_2); 1.84-1.87 (m, 2H, CH_2); 1.95-1.98 (m, 2H, CH_2); 2.18-2.24 (m, 1H, C*H*); 2.96 (t, 2H, CH_2, *J* = 8.2 Hz); 3.28 (t, 2H, CH_2, *J* = 8.2 Hz); 4.19 (s, 2H, CH_2); 6.42 (d, 1H, aryl, *J* = 8.3 Hz); 7.01-7.06 (m, 4H, aryl); 7.31-7.35 (m, 2H, aryl); 7.39 (s, 1H, N*H*). ^{13}C NMR ($CDCl_3$, 100 MHz) δ: 25.8; 28.6; 29.8; 46.4; 53.3; 53.8; 106.8; 115.2; 115.4; 118.4; 119.8; 129.0; 129.5; 133.97; 134.0; 149.5; 160.8; 163.3;174.1. $_{19}$F NMR ($CDCl_3$, 376.3 MHz) δ: -(115.73-115.81) (m, 1F, CF); HR-MS *m/z*: calcd for $C_{22}H_{26}FN_2O$, [$(M+H)^+$]: 353.2024; found 353.2031

2-cyclohexyl-N-(1-(4-fluorobenzyl)indolin-5-yl)acetamide (9c)

Final product **9c** was synthesized starting from 1-(4-fluorobenzyl)indolin-5-amine **(3)** and 2-cyclohexylacetyl chloride following the general procedure D. The product was isolated in 81% yield as a white powder that crystallizes from methanol. ^{1}H NMR (DMSO-d6, 400 MHz): δ: 0.92-1.00 (m, 2H, C*H*$_2$); 1.11-1.27 (m, 3H, C*H*$_2$); 1.60-1.74 (m, 5H, C*H*$_2$); 2.11 (d, 2H, C*H*$_2$, J = 7.0 Hz); 2.85 (t, 2H, C*H*$_2$, *J* = 8.3 Hz); 3.18 (t, 2H, C*H*$_2$, J = 8.3 Hz); 4.20 (s, 2H, C*H*$_2$); 6.51 (d, 1H, aryl, *J* = 8.4 Hz); 7.12-7.19 (m, 3H, aryl); 7.34-7.40 (m, 3H, aryl); 9.48 (s, 1H, N*H*). ^{13}C NMR (DMSO-d6, 100 MHz) δ: 26.1; 26.4; 28.6; 33.0; 35.4; 44.6; 52.8; 53.5; 107.3; 115.4; 115.6; 117.5; 119.0; 130.2; 130.4; 130.5; 130.7; 134.90; 134.92; 148.7; 160.5; 163.0; 170.0. ^{19}F NMR ($CDCl_3$, 376.3 MHz) δ: -(115.99-115,91) (s, 1F, C*F*).HR-MS *m/z*: calcd for $C_{23}H_{28}FN_2O$, [(M+H)$^+$]: 367.2186; found 367.2195

tert-butyl 5-nitroindoline-1-carboxylate (10b)

5-nitroindoline (1, 1.0 eq) was dissolved in DCM and added with 2.0 equivalents of TEA and 2.0 equivalents of di-tert-butyl dicarbonate. The mixture was refluxed overnight under stirring. Upon cooling to room temperature the mixture was extracted three times with aqueous 2N HCl. The organic phase was dried over anhydrous Na_2SO_4, filtered and evaporated under vacuum. Crude product was purified by silica gel chromatography using a linear gradient of n-hexane/ethyl acetate as mobile phase. After flash-chromatographic purification, tert-butyl 5-nitroindoline-1-carboxylate (**10b**) was obtained as an orange crystal in 64% yield. ^{1}H NMR ($CDCl_3$, 400 MHz) δ: 1.47 (s, 9H, Boc); 2.93 (t, 2H, C*H*$_2$, *J* = 8.0 Hz); 3.76-3.90 (m, 4H, C*H*$_2$ and N*H*$_2$); 6.42-6.47 (m, 2H, aryl); 7.57 (bs, 1H, aryl). HR-MS *m/z*: calcd for $C_{13}H_{19}N_2O_2$, [(M+H)$^+$]: 235.1441; found 235.1452

1-(2,4-difluorobenzyl)-5-nitroindoline (11a)

Synthesized according to the general procedure A using 5-nitroindoline (**1**) and 2,4-difluorobenzaldehyde as reagents. Intermediate **11a** was obtained as a yellow powder in 72% yield.

^{1}H NMR ($CDCl_3$, 400 MHz): δ: 3.12 (t, 2H, CH_2, J = 8.4 Hz); 3.66 (t, 2H, CH_2, J = 8.4 Hz); 4.45 (s, 2H, CH_2); 6.40 (d, 1H, aryl, J = 8.5 Hz); 6.85-6.91 (m, 2H, aryl); 7.21-7.28 (m, 1H, aryl); 7.93 (s, 1H, aryl); 8.08 (d, 1H, aryl, J = 6.5 Hz). HR-MS *m/z*: calcd for $C_{15}H_{13}F_2N_2O_2$, [(M+H)$^+$]: 291.0940; found 291.0951

1-(3,4-difluorobenzyl)-5-nitroindoline (11b)

Synthesized according to the general procedure A using 5-nitroindoline (**1**) and 3,4-difluorobenzaldehyde as reagents. Intermediate **11b** was obtained as a yellow powder in 60% yield. ^{1}H NMR ($CDCl_3$, 400 MHz): δ: 3.14 (t, 2H, CH_2, J = 8.4 Hz); 3.64 (t, 2H, CH_2, J = 8.4 Hz); 4.40 (s, 2H, CH_2); 6.35 (d, 1H, aryl, J = 8.6 Hz); 7.00-7.22 (m, 3H, aryl); 7.96 (s, 1H, aryl); 8.08 (d, 1H, aryl, J = 6.2 Hz). HR-MS *m/z*: calcd for $C_{15}H_{13}F_2N_2O_2$, [(M+H)$^+$]: 291.0940; found 291.0952

5-nitro-1-(4-(trifluoromethyl)benzyl)indoline (11c)

Synthesized according to the general procedure A using 5-nitroindoline (**1**) and 4-(trifluoromethyl)benzaldehyde as reagents. Intermediate **11c** was obtained as a yellow powder in 76% yield. ^{1}H NMR ($CDCl_3$, 400 MHz): δ: 3.14 (t, 2H, CH_2, J = 8.5 Hz); 3.67 (t, 2H, CH_2, J = 8.5 Hz); 4.51 (s, 2H, CH_2); 6.33 (d, 1H, aryl, J = 8.3 Hz); 7.41 (d, 2H, aryl, J = 12.0 Hz); 7.63 (d, 2H, aryl, J = 12.0 Hz); 7.92 (s, 1H, aryl); 8.03 (d, 1H, aryl, J = 6.5 Hz). HR-MS *m/z*: calcd for $C_{16}H_{14}F_3N_2O_2$, [(M+H)$^+$]: 323.1002; found 323.1010

1-(4-methoxybenzyl)-5-nitroindoline (11d)

Synthesized according to the general procedure A using 5-nitroindoline (**1**) and p-anisaldehyde as reagents. Intermediate **11d** was isolated as a yellow powder in 72% yield. ^{1}H NMR ($CDCl_3$, 400 MHz): δ: 3.07 (t, 2H, CH_2, J = 8.4 Hz); 3.62 (t, 2H, CH_2, J = 8.4 Hz); 3.83 (s, 3H, CH_3); 4.39 (s, 2H, CH_2); 6.37 (d, 1H, aryl, J = 8.4 Hz); 6.90 (d, 2H, aryl, J = 9.8 Hz); 7.20 (d, 2H, aryl, J = 9.8 Hz); 7.93

(s, 1H, aryl); 8.08 (d, 1H, aryl, J = 6.6 Hz). HR-MS *m/z*: calcd for $C_{16}H_{17}N_2O_3$, [$(M+H)^+$]: 285.1234; found 185.1284

1-(2,4-bis(trifluoromethyl)benzyl)-5-nitroindoline (11e)

Synthesized according to the general procedure A using 5-nitroindoline (**1**) and 2,4-bis(trifluoromethyl)benzaldehyde as reagents. Intermediate **11e** was obtained as a yellow powder in 58% yield. ^{1}H NMR ($CDCl_3$, 400 MHz): δ: 3.22 (t, 2H, CH_2, J = 8.4 Hz); 3.75 (t, 2H, CH_2, J = 8.4 Hz); 4.70 (s, 2H, CH_2); 6.25 (d, 1H, aryl, J = 8.6 Hz); 7.61 (d, 1H, aryl, J = 8.6 Hz); 7.81 (d, 1H, aryl, J = 8.9 Hz); 7.97-8.05 (m, 3H, aryl). HR-MS *m/z*: calcd for $C_{17}H_{13}F_6N_2O_2$, [$(M+H)^+$]: 391.0876; found 391.0884

1-(4-methoxybenzyl)-2-methyl-5-nitroindoline (11f)

Synthesized according to the general procedure A using 2-methyl-5-nitroindoline (**10a**) and p-anisaldehyde as reagents. Intermediate **11f** was isolated as a yellow powder in 72% yield. ^{1}H NMR (CDCl3, 400 MHz): δ: 1.33 (d, 3H, CH_3, J= 7.4 Hz); 2.67-2.75 (m, 1H, C*H*); 3.20-3.28 (m, 1H, C*H*); 3.81-3.91 (m, 4H, C*H* and CH_3); 4.20 (d, 1H, C*H*, J=14.7 Hz), 4.43 (d, 1H, C*H*, J=14.7 Hz); 6.88 (d, 2H, aryl, J=10.1 Hz); 7.10 (s, 1H, aryl); 7.51 (d, 2H, aryl, J=12.0 Hz); 7.84 (d, 2H, aryl, J=8.5 Hz). HR-MS m/z: calcd for $C_{17}H_{19}N_2O_3$, [$(M+H)^+$]: 299.1390; found 299.1401

tert-butyl 5-(cyclohexanesulfonamido)indoline-1-carboxylate (11g)

tert-butyl 5-nitroindoline-1-carboxylate (**10b**), synthesized according to the procedure described in supplementary materials, was reduced to the corresponding tert-butyl 5-aminoindoline-1-carboxylate by the general procedure B. The amine intermediate was reacted, without further purification, with cyclohexanesulfonyl chloride, following the general procedure C and giving **11g** in 54% yield as a grey solid. ^{1}H NMR ($CDCl_3$, 400 MHz): δ: 1.12-1.26 (m, 3H, CH_2 and C*H*); 1.27-1.74 (m, 12H, Boc

and CH_2); 1.83-1.90 (m, 2H, CH_2); 2.07-2.17 (m, 2H, CH_2); 2.86-2.95 (m, 1H, C*H*); 3.07 (t, 2H, CH_2, *J* = 8.6 Hz); 3.96 (t, 2H, CH_2, *J* = 8.6 Hz); 6.99-3.07 (m, 1H, aryl); 7.14 (s, 1H, aryl); 7.37 (bs, 1H, aryl); 7.76 (bs, 1H, N*H*). HR-MS *m/z*: calcd for $C_{19}H_{29}N_2O_4S$, [(M+H)$^+$]: 381.1843; found 381.1849.

1-(2,4-difluorobenzyl)indolin-5-amine (12a)

Synthesized according to the general procedure B. Intermediate **12a** was isolated as a grey powder in 97% yield. ^{1}H NMR ($CDCl_3$, 400 MHz): δ: 2.92 (t, 2H, CH_2, *J* = 8.7 Hz); 3.23-3.32 (m, 4H, CH_2 and NH_2); 4.18 (s, 2H, CH_2); 6.41 (d, 1H, aryl, *J* = 6.4 Hz); 6.49 (d, 1H, aryl, *J* = 6.4 Hz); 6.61 (s, 1H, aryl); 6.81-6.90 (m**,** 2H, aryl); 7.40-7.48 (m, 1H, aryl). HR-MS *m/z*: calcd for $C_{15}H_{15}F_2N_2$, [(M+H)$^+$]: 261.1198; found 261.1205.

1-(3,4-difluorobenzyl)indolin-5-amine (12b)

Synthesized according to the general procedure B. Intermediate **12b** was isolated as an off-white powder in 98% yield. ^{1}H NMR ($CDCl_3$, 400 MHz): δ: 2.93 (t, 2H, CH_2, *J* = 8.5 Hz); 3.03 (bs, 2H, NH_2); 3.20 (t, 2H, CH_2, *J* = 8.5 Hz); 4.11 (s, 2H, CH_2); 6.28 (d, 1H, aryl, *J* = 6.4 Hz); 6.35 (d, 1H, aryl, *J* = 7.2 Hz); 6.51 (s, 1H, aryl); 7.09-7.27 (m, 3H, aryl). HR-MS *m/z*: calcd for $C_{15}H_{15}F_2N_2$, [(M+H)$^+$]: 261.1198; found 261.1205.

1-(4-(trifluoromethyl)benzyl)indolin-5-amine (12c)

Synthesized according to the general procedure B. Intermediate **12c** was isolated as a white powder in 95% yield. ^{1}H NMR ($CDCl_3$, 400 MHz): δ: 2.94 (t, 2H, CH_2, *J* = 8.6 Hz); 3.21-3.27 (m, 4H, CH_2 and NH_2); 4.21 (s, 2H, CH_2); 6.35 (d, 1H, aryl, *J* = 8.9 Hz); 6.48 (d, 1H, aryl, *J* = 8.9 Hz); 6.63 (s, 1H, H-4); 7.54 (d, 2H, aryl, *J* = 5.7 Hz); 7.62 (d, 2H, aryl, *J* = 6.1 Hz). HR-MS *m/z*: calcd for $C_{16}H_{16}F_3N_2$, [(M+H)$^+$]: 293.1260; found 293.1269.

1-(4-methoxybenzyl)indolin-5-amine (12d)

Synthesized according to the general procedure B. Intermediate **12d** was isolated as a grey powder in 98% yield. ^{1}H NMR ($CDCl_3$, 400 MHz): δ: 2.88 (t, 2H, C*H*$_2$, *J* = 8.3 Hz); 3.17-3.23 (m, 4H, C*H*$_2$ and N*H*$_2$); 3.83 (s, 3H, C*H*$_3$); 4.10 (s, 2H, C*H*$_2$); 6.41 (d, 1H, aryl, *J* = 8.2 Hz); 6.47 (d, 1H, aryl, *J* = 9.2 Hz); 6.61 (s, 1H, aryl); 6.89 (d, 2H, aryl, *J* = 8.7 Hz); 7.31 (d, 2H, aryl, *J* = 8.7 Hz). HR-MS *m/z*: calcd for $C_{16}H_{19}N_2O$, [$(M+H)^+$]: 255.1492; found 255.1501.

1-(2,4-bis(trifluoromethyl)benzyl)indolin-5-amine (12e)

Synthesized according to the general procedure B. Intermediate **12e** was isolated as a white powder in 94% yield. ^{1}H NMR ($CDCl_3$, 400 MHz): δ: 2.71 (t, 2H, C*H*$_2$, *J* = 8.5 Hz); 3.37 (t, 2H, C*H*$_2$, *J* = 8.5 Hz); 3.50 (bs, 2H, N*H*$_2$); 4.40 (s, 2H, C*H*$_2$); 6.20 (d, 1H, aryl, *J* = 7.5 Hz); 6.48 (d, 1H, aryl, *J* = 7.4 Hz); 6.56 (s, 1H, aryl); 7.58 (d, 1H, aryl, *J* = 6.2 Hz); 7.95-8.02 (m, 2H, aryl). HR-MS *m/z*: calcd for $C_{17}H_{15}F_6N_2$, [$(M+H)^+$]: 361.1134; found 361.1140.

1-(4-methoxybenzyl)-2-methylindolin-5-amine (12f)

Synthesized according to the general procedure B. Intermediate **12f** was isolated as an off-white powder in 96% yield. ^{1}H NMR ($CDCl_3$, 400 MHz): δ: 1.33 (d, 3H, C*H*$_3$, J= 7.3 Hz); 2.52-2.62 (m, 1H, C*H*); 3.02-3.11 (m, 1H, C*H*); 3.35 (bs, 2H, N*H*$_2$); 3.84 (s, 3H, C*H*$_3$); 4.12 (d, 1H, C*H*$_2$, J=15.4 Hz), 4.30 (d, 1H, C*H*$_2$, J=15.4 Hz); 5.76 (d, 1H, aryl, J=3.8 Hz); 6.00 (d, 1H, aryl, J= 8.2 Hz); 6.82-6.90 (m, 3H, aryl) 7.29 (d, 2H, aryl, J=8.0 Hz); HR-MS *m/z*: calcd for $C_{17}H_{21}N_2O$, [$(M+H)^+$]: 269.1348; found 269.1351.

N-(indolin-5-yl)cyclohexanesulfonamide (12g)

Intermediate **11g** was dissolved in a solution of TFA in DCM (20% v:v) and stirred at room temperature for 45 minutes. The reaction was then diluted with DCM and extracted with water and

saturated solution of $NaHCO_3$. The organic phase was dried over anhydrous Na_2SO_4, filtered and evaporated under vacuum. Purification by flash chromatography gave **12g** as a grey solid in 90% yield ^{1}H NMR (CD_3OD, 400 MHz): δ: 1.18-1.31 (m, 2H, CH_2); 1.48-1.70 (m, 4H, 2 CH_2); 1.85-1.89 (m, 2H, CH_2); 2.11-2.17 (m, 2H, CH_2); 2.99-3.08 (m, 1H, C*H*); 3.31 (t, 2H, CH_2, *J* = 8.9 Hz); 3.86 (t, 2H, CH_2, *J* = 8.9 Hz); 7.28 (d, 1H, aryl, *J* = 6.8 Hz); 7.41-7.43 (m, 2H, aryl). HR-MS *m/z*: calcd for $C_{14}H_{21}N_2O_2S$, [$(M+H)^+$]: 281.1318; found 281.1326.

N-(1-(2,4-difluorobenzyl)indolin-5-yl)cyclohexanesulfonamide (13a)

Final product **13a** was synthesized according to the general procedure C. It was isolated in 71% yield as an off-white powder that crystallizes from n-hexane/ethyl acetate. ^{1}H NMR ($CDCl_3$, 400 MHz): δ: 1.21-1.26 (m, 3H, CH_2); 1.55-1.71 (m, 3H, CH_2); 1.88-1.91 (m, 2H, CH_2); 2.17-2.20 (m, 2H, CH_2); 2.95-3.02 (m, 3H, CH_2 and C*H*); 3.40 (t, 2H, CH_2, *J* = 8.3 Hz); 4.26 (s, 2H, CH_2); 6.21 (s, 1H, N*H*); 6.43 (d, 2H, aryl, *J* = 8.3 Hz); 6.82-6.93 (m, 3H, aryl); 7.07 (s, 1H, aryl); 7.34-7.40 (m, 1H, aryl). ^{13}C NMR ($CDCl_3$, 100 MHz) δ: 25.1; 26.4; 28.4; 46.5; 53.7; 59.3;103.6; 103.9; 104.1; 106.8; 111.13; 111.17; 111.34; 111.38; 115.0; 116.5; 120.75; 120.79; 120.90; 120.94; 121.29; 123.19; 123.23; 126.61; 126.71; 126.75; 130.72; 130.78; 130.81; 130.87; 131.3; 150.6; 159.63; 159.75; 160.98; 161.10; 162.1; 162.2; 163.45; 163.57. ^{19}F NMR ($CDCl_3$, 376.3 MHz) δ: -(113.98-113.91) (m, 1F, C*F*); -(115.54-115.46) (m, 1F, C*F*); HR-MS *m/z*: calcd for $C_{21}H_{25}F_2N_2O_2S$, [$(M+H)^+$]: 407.1599; found 407.1611; [$(M+Na)^+$]: 429.1419; found 429.1427

N-(1-(3,4-difluorobenzyl)indolin-5-yl)cyclohexanesulfonamide (13b)

Final product **13b** was synthesized according to the general procedure C. It was isolated in 68% yield as an off-white powder that crystallizes from n-hexane/ethyl acetate. ^{1}H NMR ($CDCl_3$, 400 MHz): δ: 1.20-1.31 (m, 3H, CH_2); 1.56-1.72 (m, 3H, CH_2); 1.89-1.92 (m, 2H, CH_2); 2.17-2.21 (m, 2H, CH_2); 2.92-2.96 (m, 1H, C*H*); 3.01 (t, 2H, CH_2, *J* = 8.3 Hz); 3.37 (t, 2H, CH_2, *J* = 8.3 Hz); 4.19 (s, 2H,

CH_2); 6.02 (s, 1H, N*H*); 6.36 (d, 1H, aryl, *J* = 8.3 Hz); 6.89 (d, 1H, aryl, *J* = 10.3 Hz); 7.08-7.23 (m, 4H, aryl). ^{13}C NMR ($CDCl_3$, 100 MHz) δ: 25.11; 25.14; 26.4; 28.4; 52.9; 53.9; 59.4; 106.9; 116. 4; 116.6; 117.2; 117.4; 121.4; 123.29; 123.39; 123.43; 123.46; 123.49; 126.8; 131.4; 150.7; ^{19}F NMR ($CDCl_3$, 376.3 MHz) δ: -(1137.54-137.43) (m, 1F, C*F*); -(139.98-139.87) (m, 1F, C*F*); HR-MS *m/z*: calcd for $C_{21}H_{25}F_2N_2O_2S$, [(M+H)$^+$]: 407.1599; found 407.1612; [(M+Na)$^+$]: 429.1419; found 429.1426

N-(1-(4-(trifluoromethyl)benzyl)indolin-5-yl)cyclohexanesulfonamide (13c)

Final product **13c** was synthesized according to the general procedure C. It was isolated in 68% yield as a white powder that crystallizes from n-hexane/ethyl acetate. ^{1}H NMR ($CDCl_3$, 400 MHz): δ: 1.20-1.31 (m, 3H, CH_2); 1.56-1.62 (m, 3H, CH_2); 1.70-1.72 (m, 2H, CH_2); 2.18-2.21 (m, 2H, CH_2); 2.92-2.98 (m, 1H, C*H*); 3.02 (t, 2H, CH_2, *J* = 8.3 Hz); 3.39 (t, 2H, CH_2, *J* = 8.3 Hz); 4.30 (s, 2H, CH_2); 6.14 (s, 1H, N*H*); 6.37 (d, 1H, aryl, *J* = 8.2 Hz); 6.91 (d, 1H, aryl, *J* = 8.2 Hz); 7.09 (s, 1H, aryl); 7.50 (d, 2H, aryl, *J* = 8.0 Hz); 7.63 (d, 2H, aryl, *J* = 8.0 Hz). ^{13}C NMR ($CDCl_3$, 100 MHz) δ: 20.36; 20.40; 21.6; 23.7; 48.7; 49.3; 54.6; 102.12; 116.6; 118.5; 120.74; 120.77; 120.81; 120.85; 122.1; 123.2; 124.7; 125.0; 126.6; 137.6; 146.1; ^{19}F NMR ($CDCl_3$, 376.3 MHz) δ: -63.21 (s, 3F, CF_3); HR-MS *m/z*: calcd for $C_{22}H_{26}F_3N_2O_2S$, [(M+H)$^+$]: 439.1662; found 439.1677; [(M+Na)$^+$]: 461.1481; found 461.1490

N-(1-(4-methoxybenzyl)indolin-5-yl)cyclohexanesulfonamide (13d)

Final product **13d** was synthesized according to the general procedure C. It was isolated in 68% yield as a grey powder that crystallizes from n-hexane/ethyl acetate. ^{1}H NMR ($CDCl_3$, 400 MHz): δ: 1.22-1.28 (m, 3H, CH_2); 1.57-1.72 (m, 3H, CH_2); 1.89-1.93 (m, 2H, CH_2); 2.17-2.21 (m, 2H, CH_2); 2.94-2.99 (m, 3H, H-3 and C*H*); 3.34 (t, 2H, H-2, *J* = 8.3 Hz); 3.83 (s, 3H, CH_3); 4.19 (s, 2H, CH_2); 5.93 (s, 1H, N*H*); 6.43 (d, 1H, H-7, *J* = 8.3 Hz); 6.88-6.92 (m, 3H, H-6 and aryl); 7.05 (s, 1H, H-4); 7.28

(d, 2H, aryl, *J* = 8.6 Hz). ^{13}C NMR ($CDCl_3$, 100 MHz) δ: 25.13; 25.15; 26.4; 28.4; 53.0; 53.5; 55.3; 59.2; 106.8; 113.9; 121.5; 123.5; 126.2; 129.1; 130.0; 131.5; 151.2; 158.9; HR-MS *m/z*: calcd for $C_{22}H_{29}F_3N_2O_3S$, [$(M+H)^+$]: 401.1893; found 401.1902; [$(M+Na)^+$]: 423.1718; found 423.1724

N-(1-(2,4-bis(trifluoromethyl)benzyl)indolin-5-yl)cyclohexanesulfonamide (13e)

Final product **13e** was synthesized according to the general procedure C. It was isolated in 65% yield as a white powder that crystallizes from n-hexane/ethyl acetate. ^{1}H NMR ($CDCl_3$, 400 MHz): δ: 1.20-1.31 (m, 3H, C*H*$_2$); 1.56-1.72 (m, 3H, C*H*$_2$); 1.90-1.92 (m, 2H, C*H*$_2$); 2.19-2.21 (m, 2H, C*H*$_2$); 2.93-2.99 (m, 1H, C*H*); 3.09 (t, 2H, H-3, *J* = 8.3 Hz); 3.50 (t, 2H, H-2, *J* = 8.3 Hz); 4.49 (s, 2H, C*H*$_2$); 6.17 (s, 1H, N*H*); 6.24 (d, 1H, H-7, *J* = 8.3 Hz); 6.89 (d, 1H, H-6, *J* = 9.2 Hz); 7.13 (s, 1H, H-4); 7.80 (d, 1H, aryl, *J* = 8.1 Hz); 7.87 (d, 1H, aryl, *J* = 8.1 Hz);7.96 (s, 1H, aryl). ^{13}C NMR ($CDCl_3$, 100 MHz) δ: 25.10; 25.14; 26.4; 28.6; 50.3; 54.5; 59.5; 106.7; 121.2; 121.4; 122.3; 123.1; 123.2; 123.31; 123.35; 125.0; 127.2; 128.5; 128.8; 128.9; 129.0; 129.5; 129.7; 130.0; 131.2; 141.7; 150.4; ^{19}F NMR ($CDCl_3$, 376.3 MHz) δ: -60.57 (s, 3F, C*F*$_3$), -62.80 (s, 3F, C*F*$_3$) HR-MS *m/z*: calcd for $C_{23}H_{25}F_6N_2O_2S$, [$(M+H)^+$]: 507.1535; found 507.1541; [$(M+Na)^+$]: 529.1355; found 529.1362

(S, R)-N-(1-(4-methoxybenzyl)-2-methylindolin-5-yl)cyclohexanesulfonamide (13f)

Final product **13f** was synthesized according to the general procedure C. It was isolated in 65% yield as a yellowish wax and was not crystallized. ^{1}H NMR ($CDCl_3$, 400 MHz): δ: 1.17-1.28 (m, 3H, C*H*$_2$); 1.33 (d, 3H, C*H*$_3$, J=8.0 Hz); 1.53-1.68 (m, 3H, C*H*$_2$); 1.84-1.86 (m, 2H, C*H*$_2$); 2.07-2.10 (m, 2H, C*H*$_2$); 2.60-2.66 (m, 1H, C*H*); 2.89-2.97 (m, 1H, C*H*); 3.10-3.16 (m, 1H, C*H*); 3.74-3.81 (m, 4H, C*H* and C*H*$_3$); 4.12 (d, 1H, C*H*, J=15.7 Hz), 4.36 (d, 1H, C*H*, J=15.7 Hz); 6.06 (s, 1H, N*H*); 6.23 (s, 1H, aryl); 6.39 (d, 1H, aryl, J=7.7 Hz); 6.87 (d, 2H, aryl, J= 8.7 Hz); 6.94 (d, 1H, aryl, J=7.7 Hz); 7.27 (d, 2H, aryl, J=8.7 Hz); ^{13}C NMR ($CDCl_3$, 100 MHz) δ: 19.55; 25.04; 26.29; 36.69; 49.64; 55.23; 59.62; 60.28; 99.67; 109.12; 113.89; 124.45; 125.65; 128.70; 130.24; 136.48; 153.47; 158.71 HR-

MS *m/z*: calcd for $C_{23}H_{31}N_2O_3S$, [(M+H)$^+$]: 415.2050; found 415.2059; [(M+Na)$^+$]: 437.1869; found 437.1874

N-(1-(4-bromo-2-nitrobenzyl)indolin-5-yl)cyclohexanesulfonamide (13g)

The final product **13g** was synthesized from **12g** and 4-bromo-2-nitrobenzaldehyde following the general procedure A. It was isolated in 71% yield as a yellowish solid that crystallizes form n-hexane/ethyl acetate ^{1}H NMR ($CDCl_3$, 400 MHz): δ: 1.20-1.31 (m, 3H, C*H*$_2$ and C*H*); 1.58-1.72 (m, 3H, C*H*$_2$ and C*H*); 1.89-1.93 (m, 2H, C*H*$_2$); 2.17-2.20 (m, 2H, C*H*$_2$); 2.91-2.99 (m, 1H, C*H*); 3.06 (t, 2H, C*H*$_2$, *J* = 8,3 Hz); 3.46 (t, 2H, H-2, *J* = 8.3 Hz); 4.54 (s, 2H, C*H*$_2$); 5.99 (s, 1H, N*H*); 6.26 (d, 1H, aryl, *J* = 8.3 Hz); 6.87 (d, 1H, aryl, *J* = 8.2 Hz); 7.10 (s, 1H, aryl); 7.59 (d, 1H, aryl, *J* = 8.3 Hz); 7.74 (d, 1H, aryl, *J* = 10.3 Hz); 8.21 (s, 1H, aryl). ^{13}C NMR ($CDCl_3$, 100 MHz) δ: 25.10, 25.13; 26.4; 28.5; 51.6; 54.7; 59.4; 106.8; 121.2; 121.4; 123.3; 127.2; 128.0; 131.2; 133.5; 136.5; 148.8; 150.4. HR-MS *m/z*: calcd for $C_{21}H_{25}BrN_3O_4S$, [(M+H)$^+$]: 494.0744; found 494.0755; [(M+Na)$^+$]: 516.0563; found 516.0570

(4-fluorophenyl)(5-nitroindolin-1-yl)methanone (14a)

To a solution of 5-nitro indoline (**1**, 1.0 eq) and DIPEA (1.2 eq) stirred at 0°C under nitrogen stream, was added dropwise a solution of 4-fluorobenzoyl chloride (1.2 eq) in DCM. The resulting mixture was allowed to warm to room temperature and stirred for further 2h. Then, the reaction was quenched by adding a saturated solution of $NaHCO_3$. The organic phase was extracted two more times with aqueous HCl 2N, dried over anhydrous Na_2SO_4, filtered and evaporated under vacuum. Crude product was purified by flash chromatography giving **14a** as a yellowish solid in 81% yield. ^{1}H NMR ($CDCl_3$, 400 MHz): δ: 3.24 (t, 2H, C*H*$_2$, *J* = 8.5 Hz); 4.21 (t, 2H, C*H*$_2$, *J* = 8.5 Hz); 7.16-7.19 (m, 2H, aryl); 7.60-7.64 (m, 2H, aryl); 7.79 (bs, 1H, aryl); 8.10-8.14 (m, 2H, aryl). HR-MS *m/z*: calcd for $C_{15}H_{12}FN_2O_3$, [(M+H)$^+$]: 287.0826; found 287.0833

2-(4-chlorophenyl)-1-(5-nitroindolin-1-yl)ethan-1-one (14b)

Intermediate **14b** was synthesized using the same procedure described above for **14a**, starting from 5-nitro indoline (**1**) and 2-(4-chlorophenyl)acetyl chloride. Flash chromatographic purification gave **14b** as a dark yellow solid in 79% yield. ^{1}H NMR ($CDCl_3$, 400 MHz): δ: 3.29 (t, 2H, CH_2, J = 8.3 Hz); 3.82 (s, 2H, CH_2);4.23 (t, 2H, CH_2, J = 8.3 Hz); 7.24 (d, 2H, aryl, J = 8.5 Hz); 7.36 (d, 2H, aryl, J = 8.5 Hz); 8.04 (s, 1H, aryl); 8.12 (d, 1H, aryl, J = 6.8 Hz); 8.33 (d, 1H, aryl, J = 7.2 Hz). HR-MS *m/z*: calcd for $C_{16}H_{14}ClN_2O_3$, [(M+H)$^+$]: 317.0687 and [(M+H)$^+$+2]: 319.0658; found 319.0690 and 319.0663

(5-aminoindolin-1-yl)(4-fluorophenyl)methanone (15a)

Prepared from **14a** using the general procedure B. After purification the product was isolated in 94% yield as a white solid. ^{1}H NMR ($CDCl_3$, 400 MHz): δ: 3.05 (t, 2H, CH_2, J = 8.6 Hz); 3.59 (bs, 2H, NH_2); 4.01 (t, 2H, CH_2, J = 8.6 Hz); 6.57-6.62 (m, 2H, aryl); 7.10-7.16 (m, 2H, aryl); 7.55-7.59 (m, 2H, aryl); 8.02 (bs, 1H, aryl). HR-MS *m/z*: calcd for $C_{15}H_{14}FN_2O$, [(M+H)$^+$]: 257.1085; found 257.1094

1-(5-aminoindolin-1-yl)-2-(4-chlorophenyl)ethanone (15b)

Prepared from **14b** using the general procedure B. After purification the product was isolated in 89% yield as a white solid. ^{1}H NMR ($CDCl_3$, 400 MHz): δ: 3.09 (t, 2H, CH_2, J = 8.4 Hz); 3.43 (bs, 2H, NH_2); 3.63 (s, 2H, CH_2); 4.09 (t, 2H, CH_2, J = 8.3 Hz); 7.20 (d, 2H, aryl, J = 8.3 Hz); 7.31 (d, 2H, aryl, J = 8.3 Hz); 7.49-7.54 (m, 2H, aryl); 7.73 (d, 1H, aryl, J = 6.9 Hz). HR-MS *m/z*: calcd for $C_{16}H_{16}ClN_2O$, [(M+H)$^+$]: 287.0946; found 287.0954

N-(1-(4-fluorobenzoyl)indolin-5-yl)cyclohexanesulfonamide (16a)

Synthesized by coupling intermediate **15a** with cyclohexylsulfonyl chloride as for the general procedure C. After purification, **16a** was obtained in 61% yield as a white solid that crystallizes from ethyl acetate. ^{1}H NMR (DMSO-d6, 400 MHz): δ: 1.06-1.24 (m, 3H, C*H*$_2$); 1.36-1.45 (m, 2H, C*H*$_2$); 1.58-1.60 (m, 1H, C*H*$_2$); 1.75-1.78 (m, 2H, C*H*$_2$); 2.00-2.03 (m, 2H, C*H*$_2$); 2.89-2.97 (m, 1H, C*H*); 3.07 (t, 2H, C*H*$_2$, *J* = 8.2 Hz); 4.00 (t, 2H, C*H*$_2$, *J* = 8.2 Hz); 7.04 (bs, 1H, aryl); 7.15 (s, 1H, aryl); 7.32 (t, 1H, aryl, *J* = 8.8 Hz);7.65-7.68 (m, 2H, aryl); 7.95 (bs, 1H, aryl); 9.65 (s, 1H, N*H*). ^{13}C NMR (DMSO-d6, 100 MHz) δ: 24.8; 25.2; 26.4; 28.3; 50.9; 59.1; 115.8; 116.0; 117.3; 118.9; 130.0; 130.1; 133.9; 134.5; 134.9; 139.4; 162.1; 164.6; 167.2; ^{19}F NMR (DMSO-d6, 376.3 MHz) δ: -(117.14-117.21) (m, 1F, C*F*).HR-MS *m/z*: calcd for $C_{21}H_{24}FN_2O_3S$, [(M+H)$^+$]: 403.1486; found 403.1495; [(M+Na)$^+$]: 425.1306; found 425.1316

N-(1-(2-(4-chlorophenyl)acetyl)indolin-5-yl)cyclohexanesulfonamide (16b)

Synthesized by coupling intermediate **15b** with cyclohexanesulfonyl chloride as for the general procedure C. After purification, **16b** was obtained in 57% yield as an off-white solid that crystallizes from ethyl acetate. ^{1}H NMR (DMSO-d6, 400 MHz): δ: 1.05-1.24 (m, 3H, C*H*$_2$); 1.34-1.43 (m, 2H, C*H*$_2$); 1.56-1.58 (m, 1H, C*H*); 1.73-1.76 (m, 2H, C*H*$_2$,); 1.98-2.01 (m, 12H, C*H*$_2$); 2.86-2.93 (m, 1H, C*H*); 3.14 (t, 2H, C*H*$_2$, *J* = 8.2 Hz); 3.83 (d, 2H, C*H*$_2$, *J* = 6.0 Hz);); 4.16 (t, 2H, C*H*$_2$, *J* = 8.2 Hz); 6.99 (d, 1H, aryl, *J* = 8.6 Hz); 7.12 (s, 1H, aryl); 7.25-7.33 (m, 3H, aryl); 7.38 (d, 1H, aryl, J=8.4 Hz); 7.94-7.98 (m, 1H, aryl); 9.59 (s, 1 H, N*H*). ^{13}C NMR (DMSO-d6, 100 MHz) δ: 24.8; 25.2; 26.4; 27.9; 41.5; 48.2; 59.1; 116.7; 117.41; 117.4; 119.1; 126.9; 128.6; 128.7; 129.9; 131.7; 132.0; 133.5; 134.4; 134.7; 135.6; 139.8; 162.8; 169.2; HR-MS *m/z*: calcd for $C_{22}H_{26}ClNO_3S$, [(M+H)$^+$]: 433.1347 and [(M+H)$^+$+2]: 435.1318; found 433.1342 and 435.1323

1-(4-fluorophenethyl)-5-nitroindoline (17)

Synthesized from 5-nitroindoline (1) following the general procedure E. The product was isolated in 68% yield as a yellowish solid. ^{1}H NMR ($CDCl_3$, 400 MHz): δ: 2.89 (t, 2H, CH_2, J = 6.7 Hz); 3.06 (t, 2H, CH_2, J = 8.4 Hz); 3.48 (t, 2H, CH_2, J = 6.7 Hz); 3.62 (t, 2H, CH_2, J = 8.4 Hz); 6.20 (d, 1H, CH_2, J = 8.6 Hz); 6.98-7.04 (m, 2H, aryl); 7.16-7.20 (m, 2H, aryl); 7.89 (s, 1H, aryl); 8.05 (d, 1H, aryl, J = 8.3 Hz). HR-MS *m/z*: calcd for $C_{16}H_{16}FN_2O_2$, [(M+H)$^+$]: 287.1190; found 287.1200

1-(4-fluorophenethyl)indolin-5-amine (18)

Prepared from **17** using the general procedure B for continuous flow hydrogenation. The intermediate was isolated in 92% yield as a white solid. ^{1}H NMR ($CDCl_3$, 400 MHz): δ: 2.79-2.96 (m, 4H, 2 CH_2); 3.26-3.49 (m, 6H, 2 CH_2 and NH_2); 6.23 (d, 1H, aryl, J = 8.5 Hz); 6.95-7.05 (m, 2H, aryl); 7.13-7.28 (m, 4H, aryl). HR-MS *m/z*: calcd for $C_{16}H_{18}FN_2$, [(M+H)$^+$]: 257.1449; found 257.1453

N-(1-(4-fluorophenethyl)indolin-5-yl)cyclohexanesulfonamide (19)

Obtained by coupling of **18** with cyclohexane sulfonyl chloride as for the general procedure C. The final product was isolated in 57% yield as an off-with solid that crystallizes in n-hexane/diethyl ether. ^{1}H NMR ($CDCl_3$, 400 MHz): δ: 1.19-1.30 (m, 3H, CH_2 and CH); 1.56-1.71 (m, 3H, CH_2 and CH); 1.89-1.92 (m, 2H, CH_2); 2.17-2.20 (m, 2H, CH_2); 2.85-3.00 (m, 5H, CH and 2 CH_2); 3.30 (t, 2H, CH_2, J = 7.9 Hz); 3.42 (t, 2H, CH_2, J = 8.3 Hz); 5.99 (s, 1H, NH); 6.35 (d, 1H, aryl, J = 8.3 Hz); 6.90 (d, 1H, aryl, J = 8.3 Hz); 6.99-7.04 (m, 3H, aryl); 7.20-7.23 (m, 2H, aryl). ^{13}C NMR ($CDCl_3$, 100 MHz) δ: 25.1; 26.4; 28.4; 32.8; 50.89; 50.90; 53.2; 59.2; 106.4; 115.19; 115.2; 115.4; 121.5; 123.5; 126.0; 130.0; 131.2; 135.3; 150.8; 160.3; 162.8; ^{19}F NMR ($CDCl_3$-d6, 376.3 MHz) δ: -(115.51-115.59) (m, 1F, CF); HR-MS *m/z*: calcd for $C_{22}H_{28}FN_2O_2S$, [(M+H)$^+$]: 403.1850; found 403.1862; [(M+Na)$^+$]: 425.1669; found 425.1675

4-(methoxymethoxy)benzaldehyde (19a)

4-hydroxybenzaldehyde (1.0 eq) was dissolved in dry dimethylformamide (DMF) and added with 1.2 equivalents of potassium tert-butoxide. After 5 minutes stirring at room temperature a solution of methoxymethyl chloride (MOMCl, 1.2 eq) in DMF was added dropwise. The mixture was stirred for 4h before being quenched by aqueous 2N HCl. The aqueous phase was extracted three times with DMC. The organic phases were collected, dried over anhydrous Na_2SO_4, filtered and evaporated. Purification of the crude product by flash chromatography gave **33** in 76% yield. ^{1}H NMR ($CDCl_3$, 400 MHz) δ: 3.44 (s, 3H, C*H*$_3$), 5.22 (s, 2H, C*H*$_2$), 7.12 (d, 2H, aryl, J= 8.0 Hz), 7.80 (d, 2H, aryl, J= 8.0 Hz l); 9.87 (s, 1H, OC*H*).

(4-(methoxymethoxy)phenyl)methanol (20a)

The reaction was A solution of **19a** (1.0 eq**)** in methanol was cooled in an ice bath and added portionwise with 3 equivalents of $NaBH_4$. The reaction warmed to room temperature and was maintained under stirring for 15 minutes. Aqueous 2N HCl was then slowly added to quench the excess of hydride. The aqueous phase was extracted with ethyl acetate and the resulting organic phase washed two times with brine, dried over anhydrous Na_2SO_4, filtered and evaporated *in vacuo*. After flash chromatographic purification, **20a** was obtained in 86% yield. ^{1}H NMR ($CDCl_3$, 400 MHz) δ: 2.83 (bs, 1H, OH), 3.48 (s, 3H, C*H*$_3$); 4.57 (s, 2H, C*H*$_2$), 5.16 (s, 2H, C*H*$_2$); 7.02 (d, 2H, aryl, J= 8.0 Hz); 7.27 (d, 2H, aryl, J= 8.0 Hz).

1-(iodomethyl)-4-(methoxymethoxy)benzene (20b)

Synthesized according to the procedure previously described.[41] Iodine (1.5 eq) was dissolved in dry DCM and added with 1.5 equivalents of triphenylphosphine. The solution was stirred for 1.5 hours and then added with 1.5 equivalents of imidazole, stitting for further 1 hour. Then alcohol **20a** was added to the resulting slurry, mantaining under stirring overnight. Then a saturated aqueous solution of $Na_2S_2O_3$ was added and the organic layer was further washed with brine. The organic layer was dryed over Na_2SO_4, filtered and concentrated in vacuo. Compound **20b** was obtained in 67% yield

after purification of the crude product by flash-chromatography using a linear gradient of n-hexane/ethyl acetate as mobile phase. ^{1}H NMR ($CDCl_3$, 400 MHz) δ: 3.50 (s, 3H, C*H*$_3$); 4.49 (s, 2H, C*H*$_2$), 5.19 (s, 2H, C*H*$_2$); 6.99 (d, 2H, aryl, J= 8.0 Hz); 7.34 (d, 2H, aryl, J= 8.0 Hz). HR-MS *m/z*: calcd for $C_9H_{11}IO_2$, [$(M+H)^+$]: 277.9804; found 277.9812;

2-cyclohexylethane-1-thiol (20c)

2-cyclohexylethane-1-thiol (**20c**) was synthesized according to Thuo et al.[42] from (2-bromoethyl)cyclohexane (2.0 mmol) that was dissolved in 20 mL of ethanol, added with thiourea (2.4 mmol) and heated to reflux overnight. Removal of the solvent led to an oil that was mixed with aqueous NaOH (6.0 mmol in 20 mL) and refluxed under magnetic stirring for 2 hours. After colling to room temperature the resulting solution was extracted three times with diethyl ether. The organic phases were collected, dried over Na_2SO_4, and concentrated in vacuo. After purification by flash chromatography eluting with n-hexane, intermediate 20c was isolated in 65% yield. ^{1}H NMR ($CDCl_3$, 400 MHz) δ: 0.79-088 (m, 2H, CH_2), 1.06-1.22 (m, 4H, 2 CH_2), 1.46 (q, 2H C*H*$_2$, J_1=7.2 Hz, J_2=15.2 Hz); 1.56-1.65 (m, 5H, CH and CH_2), 2.60 (t, 2H, CH_2, J=7.7 Hz).

2-cyclohexylethane-1-sulfonyl bromide (20d)

Compound **20c** was prepared in 75% yield as previously described.[43] Briefly, **20b** (1 mmol) was suspended in 5 mL of water and added with 1.0 mmol of KBr and 2.5 mmol of oxone. The reaction was stirred for 20 minutes and then extracted two times with ethyl acetate. The organic layers were collected, dyied over Na_2SO_4 and concentrated in vacuo. Crude product was purified by flash chromatography using n-hexane as eluent. ^{1}H NMR ($CDCl_3$, 400 MHz) δ: 0.79-0.95 (m, 2H, CH_2), 1.10-1.24 (m, 4H, 2 CH_2), 1.54-1.70 (m, 5H, CH and 2 CH_2), 1.76 (q, 2H, CH_2, J_1=6.7 Hz, J_2=16.1 Hz), 3.88 (q, 2H, CH_2, J_1=7.8 Hz, J_2=10.2 Hz). HR-MS *m/z*: calcd for $C_8H_{15}BrO_2S$, [$(M+H)^+$]: 253.9976; found 253.9984.

5-nitro-1-(4-(trifluoromethyl)benzyl)-1H-indole (21a)

Synthesized according to the general procedure E, starting from 5-nitro-1H-indole (**20**) and commercially available 1-(bromomethyl)-4-(trifluoromethyl)benzene. The intermediate was obtained in 71% yield as an orange solid ^{1}H NMR ($CDCl_3$, 400 MHz): δ: 5.44 (s, 2H, CH_2); 6.75 (d, 1H, aryl, J = 3.2 Hz); 7.18 (d, 2H, aryl, J = 8.4 Hz); 7.24 (d, 1H, aryl, J = 8.3 Hz); 7.31 (d, 1H, aryl, J = 4.0 Hz); 7.56 (d, 2H, aryl, J = 8.5 Hz); 8.04 (d, 1H, aryl, J = 8.2 Hz); 8.58 (s, 1H, aryl). HR-MS *m/z*: calcd for $C_{16}H_{12}F_3N_2O_2$, [$(M+H)^+$]: 321.0845; found 321.0254

1-(4-(methoxymethoxy)benzyl)-5-nitro-1H-indole (21b)

Synthesized according to the general procedure E, starting from 5-nitro-1H-indole (**20**) and 1-(iodomethyl)-4-(methoxymethoxy)benzene. The intermediate was obtained in 65% yield as a yellowish solid ^{1}H NMR ($CDCl_3$, 400 MHz) δ: 3.48 (s, 3H, CH_3); 5.17 (s, 2H, CH_2), 5.32 (s, 2H, CH_2); 6.73 (d, 1H, aryl, J= 3.5 Hz); 7.02 (d, 2H, aryl, J= 8.3 Hz); 7.09 (d, 2H, aryl, J= 8.4 Hz); 7.28 (d, 1H, aryl, J= 4.7 Hz); 7.34 (d, 1H, aryl, J= 8.2 Hz); 8.09 (d, 1H, aryl, J= 8.5 Hz); 8.61 (s, 1H, aryl). HR-MS *m/z*: calcd for $C_{17}H_{17}N_2O_4$, [$(M+H)^+$]: 313.1183; found 313.1201

1-(4-fluorobenzyl)-5-nitro-1H-indole (21c)

Synthesized according to the general procedure E, starting from 5-nitro-1H-indole (**20**) and commercially available 1-(bromomethyl)-4-fluorobenzene. The intermediate was obtained in 74% yield as an orange solid. ^{1}H NMR ($CDCl_3$, 400 MHz): δ: 5.36 (s, 2H, CH_2); 6.75 (d, 1H, aryl, J = 3.7 Hz); 7.01-7.13 (m, 4H, aryl); 7.28 (d, 2H, aryl, J = 4.2 Hz); 8.10 (d, 2H, aryl, J = 8.6 Hz); 8.63 (s, 1H, aryl). HR-MS *m/z*: calcd for $C_{15}H_{12}FN_2O_2$, [$(M+H)^+$]: 271.0805; found 271.0811

1-(4-methoxybenzyl)-5-nitro-1H-indole (21d)

Synthesized according to the general procedure E, starting from 5-nitro-1H-indole (**20**) and commercially available 1-(bromomethyl)-4-methoxybenzene. The intermediate was obtained in 64% yield as a dark yellow solid. ^{1}H NMR ($CDCl_3$, 400 MHz): δ: 3.80 (s, 3H, C*H*$_3$); 5.32 (s, 2H, C*H*$_2$); 6.73 (d, 1H, aryl, *J* = 4.0 Hz); 6.88 (d, 2H, aryl, *J* = 8.2 Hz); 7.09 (d, 2H, aryl, *J* = 8.3 Hz); 7.31-7.35 (m, 2H, aryl); 8.10 (d, 1H, aryl, *J* = 8.6 Hz); 8.62 (s, 1H, aryl). HR-MS *m/z*: calcd for $C_{16}H_{15}N_2O_3$, [$(M+H)^+$]: 283.1077; found 283.1085

1-(4-(trifluoromethyl)benzyl)-1H-indol-5-amine (22a)

Synthesized form **21a** using general procedure B. The intermediate was obtained in 93% yield as an off-white solid. ^{1}H NMR ($CDCl_3$, 400 MHz): δ: 3.71 (bs, 2H, N*H*$_2$); 5.32 (s, 2H, C*H*$_2$); 6.43 (d, 1H, aryl, *J* = 3.7 Hz); 6.67 (d, 1H, aryl, *J* = 8.4 Hz); 7.00-7.09 (m, 3H, aryl); 7.18 (d, 2H, aryl, *J* = 8.6 Hz); 7.55 (d, 2H, aryl, *J* = 8.6 Hz). HR-MS *m/z*: calcd for $C_{16}H_{14}F_3N_2$, [$(M+H)^+$]: 291.1104; found 291.1111

1-(4-(methoxymethoxy)benzyl)-1H-indol-5-amine (22b)

Synthesized form **21b** using general procedure B. The intermediate was obtained in 91% yield as a grey solid.^{1}H NMR ($CDCl_3$, 400 MHz): 3.48 (s, 3H, C*H*$_3$); 5.16 (s, 2H, C*H*$_2$), 5.21 (s, 2H, C*H*$_2$); 6.36 (d, 1H, aryl, J= 3.9 Hz); 6.66 (d, 1H, aryl, J= 7.9 Hz); 6.96-7.00 (m, 3H, aryl); 7.06-7.12 (m, 4H, aryl); HR-MS *m/z*: calcd for $C_{17}H_{19}N_2O_2$, [$(M+H)^+$]: 283.1441; found 283.1498

1-(4-fluorobenzyl)-1H-indol-5-amine (22c)

Synthesized form **21c** using general procedure B. The intermediate was obtained in 94% yield as a dark grey solid. ^{1}H NMR ($CDCl_3$, 400 MHz) δ: 3.50 (bs, 2H, N*H*$_2$); 5.24 (s, 2H, C*H*$_2$); 6.38 (d, 1H, aryl, *J* = 4.1 Hz); 6.65 (d, 1H, aryl, *J* = 8.4 Hz); 6.97-7.10 (m, 7H, aryl). HR-MS *m/z*: calcd for $C_{15}H_{14}FN_2$, [$(M+H)^+$]: 241.1136; found 241.1144

1-(4-methoxybenzyl)-1H-indol-5-amine (22d)

Synthesized form **21d** using general procedure B. The intermediate was obtained in 92% yield as a brown solid. ^{1}H NMR ($CDCl_3$, 400 MHz) δ: 3.03 (bs, 2H, N*H*$_2$); 3.79 (s, 3H, C*H*$_3$); 5.20 (s, 2H, C*H*$_2$); 6.36 (d, 1H, aryl, *J* = 3.8 Hz); 6.65 (d, 1H, aryl, *J* = 8.6 Hz); 6.85 (d, 2H, aryl, *J* = 8.4 Hz); 6.96 (s, 1H, aryl); 7.05-7.12 (m, 4H, aryl). HR-MS *m/z*: calcd for $C_{16}H_{17}N_2O$, [(M+H)$^+$]: 253.1335; found 253.1344

N-(1-(4-(trifluoromethyl)benzyl)-1H-indol-5-yl)heptanamide (23a)

Synthesized from **22a** and heptanoyl chloride following general procedure D. The final product was obtained in 80% yield as a white solid that crystallizes in n-hexane/diethyl ether. ^{1}H NMR ($CDCl_3$, 400 MHz) δ: 0.92 (t, 3H, C*H*$_3$, *J* = 6.5 Hz); 1.34-1.44 (m, 6H, 3 C*H*$_2$); 1.73-1.79 (m, 2H, C*H*$_2$); 2.39 (t, 2H, C*H*$_2$, *J* = 7.6 Hz); 5.38 (s, 2H, C*H*$_2$); 6.56 (d, 1H, aryl, *J* = 2.7 Hz); 7.15-7.23 (m, 6H, aryl); 7.56 (d, 2H, aryl, *J* = 8.0 Hz); 7.90 (s, 1H, N*H*);. ^{13}C NMR ($CDCl_3$, 100 MHz) δ: 14.0; 22.5; 25.8; 29.0; 31.6; 37.8; 49.8; 102.4; 109.6; 113.2; 116.4; 125.8; 126.8; 129.0; 130.5; 133.6; 141.5; 171.5. ^{19}F NMR ($CDCl_3$, 376.3 MHz) δ: -62.61 (s, 3F, C*F*$_3$). HR-MS *m/z*: calcd for $C_{23}H_{26}F_3N_2O$, [(M+H)$^+$]: 403.1992; found 403.2003; [(M+Na)$^+$]: 425.1811; found 425.1820

N-(1-(4-(methoxymethoxy)benzyl)-1H-indol-5-yl)heptanamide (23b)

Synthesized from **22b** and heptanoyl chloride following general procedure D. The final product was obtained in 76% yield as a grey wax that was not crystallized. ^{1}H NMR ($CDCl_3$, 400 MHz): 0.92 (t, 3H, C*H*$_3$, J = 6.6 Hz); 1.28-1.43 (m, 6H, 3 C*H*$_2$); 1.72-1.80 (m, 2H, C*H*$_2$); 2.38 (t, 2H, C*H*$_2$, J= 7.6 Hz); 3.48 (s, 3H, C*H*$_3$); 5.16 (s, 2H, C*H*$_2$), 5.24 (s, 2H, C*H*$_2$); 6.50 (d, 1H, aryl, J= 3.0 Hz); 6.96 (d, 2H, aryl, J= 8.6 Hz); 7.05 (d, 2H, aryl, J= 8.6 Hz); 7.11 (d, 1H, aryl, J=3.0 Hz); 7.19-7.22 (m, 2H, aryl); 7.30 (s, 1H, aryl); 7.85 (s, 1H, N*H*). ^{13}C NMR ($CDCl_3$, 100 MHz) δ: 14.1; 22.5; 25.8; 29.0;

31.6; 37.8; 49.7; 56.0; 94.4; 101.7; 109.8; 112.9; 116.1; 116.5; 128.1; 128.9; 129.0; 130.4; 130.7; 133.7; 156.7; 171.2. HR-MS *m/z*: calcd for $C_{24}H_{31}N_2O_3$ [(M+H)$^+$]: 395.2329; found 395.2391

N-(1-(4-fluorobenzyl)-1H-indol-5-yl)cyclohexanesulfonamide (23c)

Synthesized from **22c** and cyclohexanesulfonyl chloride following general procedure C. The final product was obtained in 71% yield as an off-white solid that crystallizes in n-hexane/ethyl acetate ^{1}H NMR ($CDCl_3$, 400 MHz) δ: 1.19-1.29 (m, 3H, C*H*$_2$); 1.61-1.68 (m, 3H, C*H*$_2$); 1.86-1.88 (m, 2H, C*H*$_2$); 2.19-2.22 (m, 2H, C*H*$_2$); 2.95-3.03 (m, 1H, C*H*); 5.29 (s, 2H, C*H*$_2$); 6.41 (s, 1H, N*H*); 6.55 (d, 1H, aryl, *J* = 2.8 Hz); 7.00-7.04 (m, 2H, aryl); 7.08-7.13 (m, 3H, aryl). 7.16 (d, 1H, aryl, *J* = 3.2 Hz); 7.22 (d, 1H, aryl, *J* = 8.7 Hz); 7.56 (d, 1H, aryl, *J* = 1.7 Hz). ^{13}C NMR ($CDCl_3$, 100 MHz) δ: 25.09; 25.11; 26.4; 49.7; 59.3; 102.0; 110.3; 115.3; 115.7; 115.9; 118.1; 128.5; 128.6; 129.0; 129.2; 129.4; 132.84; 132.88; 134.4; 161.1; 163.5. ^{19}F NMR ($CDCl_3$, 376.3 MHz) δ: -115.82 (s, 1F, C*F*). HR-MS *m/z*: calcd for $C_{21}H_{24}FN_2O_2S$, [(M+H)$^+$]: 387.1537; found 387.1548; [(M+Na)$^+$]: 409.1356; found 409.1362

N-(1-(4-methoxybenzyl)-1H-indol-5-yl)cyclohexanesulfonamide (23d)

Synthesized from **22d** and cyclohexanesulfonyl chloride following general procedure C. The final product was obtained in 65% yield as dark grey solid that crystallizes in n-hexane/ethyl acetate ^{1}H NMR ($CDCl_3$, 400 MHz): δ: 1.20-1.28 (m, 3H, C*H*$_2$); 1.58-1.68 (m, 3H, C*H*$_2$); 1.87-1.90 (m, 2H, C*H*$_2$); 2.19-2.22 (m, 2H, C*H*$_2$); 2.95-3.02 (m, 1H, C*H*); 3.80 (s, 3H, C*H*$_3$); 5.26 (s, 2H, C*H*$_2$); 6.21 (s, 1H, N*H*); 6.53 (d, 1H, aryl, *J* = 3.0 Hz); 6.86 (d, 2H, aryl, *J* = 8.6 Hz); 7.06-7.11 (m, 3H, aryl); 7.16 (d, 1H, aryl, *J* = 3.0 Hz); 7.26 (d, 1H, aryl, *J* = 8.8 Hz); 7.55 (d, 1H, aryl, *J* = 2.0 Hz). ^{13}C NMR ($CDCl_3$, 100 MHz) δ: 25.1; 26.4; 49.9; 55.3; 59.2; 101.7; 110.5; 114. 2; 115.3; 118.0; 128.3; 128.7; 129.06; 129.16; 129.4; 134.5; 159.2. HR-MS *m/z*: calcd for $C_{22}H_{27}N_2O_3$, [(M+H)$^+$]: 399.1737; found 399.1745; [(M+Na)$^+$]: 421.1556; found 421.1566

3,3-dimethyl-N-(1-(4-(trifluoromethyl)benzyl)-1H-indol-5-yl)butanamide (24a)

Synthesized from **22a** and 3,3-dimethylbutanoyl chloride following general procedure D. The final product was obtained in 74% yield as a white solid that crystallizes in n-hexane/diethyl ether. ^{1}H NMR ($CDCl_3$, 400 MHz): δ: 1.13 (s, 9H, C*H*$_3$); 2.24 (s, 2H, C*H*$_2$); 5.35 (s, 2H, C*H*$_2$); 6.54 (d, 1H, aryl, *J* = 3.0 Hz); 7.10-7.20 (m, 6H, aryl*);* 7.54 (d, 2H, aryl, *J* = 8.1 Hz); 7.88 (s, 1H, N*H*). ^{13}C NMR ($CDCl_3$, 100 MHz) δ: 29.9; 31.3; 49.7; 51.6; 102.4; 109.6; 113.1; 113.3; 116.5; 125.7; 126.8; 128.9; 129.0; 130.1; 130.5; 130.6; 133.6; 141.6; 170.1. ^{19}F NMR ($CDCl_3$, 376.3 MHz) δ: -61.85 (s, 3F, C*F*$_3$). HR-MS *m/z*: calcd for $C_{22}H_{24}F_3N_2O$, [$(M+H)^+$]: 389.1835; found 389.1901

N-(1-(4-hydroxybenzyl)-1H-indol-5-yl)heptanamide (24b)

Compound **23b** was dissolved in a mixture of solution of TFA in DCM (15% v:v) and stirred at room temperature for 1.5h. The reaction was then diluted with DCM and extracted with a saturated solution of $NaHCO_3$ and brine. The organic phase was dried over anhydrous Na_2SO_4, filtered and evaporated under vacuum. After purification of the crude product, **24b** was obtained in 87% yield as a white solid that crystallizes from n-hexane/ethyl acetate. ^{1}H NMR (CD_3OD, 400 MHz): 0.93 (t, 3H, C*H*$_3$, *J* = 6.6 Hz); 1.30-1.43 (m, 4H, C*H*$_2$); 1.68-1.75 (m, 2H, C*H*$_2$); 2.37 (t, 2H, C*H*$_2$, *J* = 7.6 Hz); 4.87 (s, 2H, C*H*$_2$); 6.42 (d, 1H, aryl, *J* = 3.0 Hz); 6.71 (d, 2H, aryl, *J* = 8.4 Hz); 6.99 (d, 2H, aryl, *J* = 8.4 Hz); 7.16-7.20 (m, 2H, aryl); 7.26 (d, 1H, aryl, *J* = 8.8 Hz); 7.77 (s, 1H, aryl). ^{13}C NMR (CH_3OD, 100 MHz) δ: 13.0; 22.2; 25.7; 28.7; 31.4; 36.6; 49.1; 100.8; 109.5; 112.9; 115.0; 115.9; 128.0; 128.7; 128.9; 130.2; 133.8; 156.5; 173.3. HR-MS *m/z*: calcd for $C_{22}H_{26}N_2O_2$ [$(M+H)^+$]: 351.2067; found 351.2073

N-(1-(4-(trifluoromethyl)benzyl)-1H-indol-5-yl)palmitamide (25a)

Synthesized from **22a** and palmithoyl chloride following general procedure D. The final product was obtained in 66% yield as a white wax that did not crystallize. ^{1}H NMR ($CDCl_3$, 400 MHz): δ: 0.90 (t, 3H, C*H*$_3$, *J* = 7.0 Hz); 1.28-1.42 (m, 24H, C*H*$_2$); 1.73-1.80 (m, 2H, C*H*$_2$); 2.38 (t, 2H, C*H*$_2$, *J* = 7.6 Hz); 5.38 (s, 2H, C*H*$_2$), 6.56 (d, 1H, aryl, *J* = 3.0 Hz); 7.14-7.23 (m, 6H, aryl); 7.56 (d, 2H, aryl, *J* = 8.1 Hz); 7.89 (s, 1H, N*H*); ^{13}C NMR ($CDCl_3$, 100 MHz) δ: 14.1; 22.7; 25.8; 29.33; 29.36; 29.4; 29.5; 29.66; 29.68; 29.70; 31.9; 37.8; 49.8; 102.4; 109.6; 113.1; 116.3; 125.8; 125.8; 126.8; 128.96; 129.03; 130.6; 133.6; 141.5; 171.3. ^{19}F NMR ($CDCl_3$, 376.3 MHz) δ: -62.54 (s, 3F, C*F*$_3$). HR-MS *m/z*: calcd for $C_{33}H_{44}F_3N_2O$, [$(M+H)^+$]: 529.3400; found 529.3392

N-(1-(4-(trifluoromethyl)benzyl)-1H-indol-5-yl)cyclohexanesulfonamide (26a)

Synthesized from **22a** and cyclohexanesulfonyl chloride following general procedure C. The final product was obtained in 69% yield as a grey solid that crystallizes in n-hexane/ethyl acetate. ^{1}H NMR ($CDCl_3$, 400 MHz): δ: 1.20-1.28 (m, 3H, C*H*$_2$); 1.58-1.68 (m, 3H, C*H*$_2$); 1.87-1.91 (m, 2H, C*H*$_2$); 2.20-2.23 (m, 2H, C*H*$_2$); 2.95-3.02 (m, 1H, C*H*); 5.39 (s, 2H, C*H*$_2$); 6.24 (s, 1H, N*H*); 6.58 (d, 1H, aryl, *J* = 2.7 Hz); 7.08 (d, 1H, aryl, *J* = 8.7 Hz); 7.17-7.22 (m, 5H, aryl); 7.58 (d, 2H, aryl, *J* = 8.7 Hz). ^{13}C NMR ($CDCl_3$, 100 MHz) δ: 25.1; 26.4; 49.9; 59.4; 102.4; 110.2; 115.4; 118.3; 125.85; 125.88; 125.92; 126.9; 129.19; 129.22; 129.50; 130.0; 130.3; 134.4; 141.2. ^{19}F NMR ($CDCl_3$, 376.3 MHz) δ: -61.89 (s, 3F, C*F*$_3$). HR-MS *m/z*: calcd for $C_{22}H_{24}F3N_2O_2S$, [$(M+H)^+$]: 437.1505; found 437.1513; [$(M+Na)^+$]: 459.1325; found 459.1333

2-cyclohexyl-N-(1-(4-(trifluoromethyl)benzyl)-1H-indol-5-yl)ethane-1-sulfonamide (27a)

Synthesized, following general procedure C, from **22a** and 2-cyclohexylethane-1-sulfonyl bromide. The final product was obtained in 64% yield as an off-white solid that crystallizes in n-hexane/ethyl acetate.^{1}H NMR ($CDCl_3$, 400 MHz): δ: 0.85-0.93 (m, 2H, C*H*$_2$); 1.11-1.33 (m, 4H, C*H*$_2$); 1.63-1.78 (m, 7H, C*H* and 3 C*H*$_2$); 3.05-3.09 (m, 2H, C*H*$_2$), 5.30 (s, 2H, C*H*$_2$); 6.48 (s, 1H, N*H*); 6.55 (d, 1H,

aryl, *J* = 3.1 Hz), 7.01 (t, 2H, aryl, *J* = 8.6 Hz); 7.07-7.12 (m, 3H, aryl); 7.17 (d, 1H, aryl, *J* = 3.1 Hz); 7.22 (d, 1H, aryl, *J* = 8.7 Hz); 7.56 (d, 1H, aryl, *J* = 1.6 Hz). ^{13}C NMR ($CDCl_3$, 100 MHz) δ: 26.0; 26.3; 30.7; 32.8; 36.6; 48.9; 49.7; 102.1; 110.4; 115.7; 115.83; 115.89, 118.4; 128.4; 128.5; 128.7; 129.2; 129.5; 132.9; 134.6; 161.1; 163.5. ^{19}F NMR ($CDCl_3$, 376.3 MHz) δ: -62.01 (s, 3F, C*F*$_3$). HR-MS *m/z*: calcd for $C_{24}H_{28}F_3N_2O_2S$, [$(M+H)^+$]: 465,1818; found 465.1820

2-(butylamino)-N-(1-(4-(trifluoromethyl)benzyl)-1H-indol-5-yl)acetamide (28a)

Intermediate **22a** was reacted with chloroacetyl chloride following the general procedure D. After work up the obtained 2-chloro-N-(1-(4-(trifluoromethyl)benzyl)-1H-indol-5-yl)acetamide crystallized from DCM at 0°C and, upon filtration, was used without further purification. 2-chloro-N-(1-(4-(trifluoromethyl)benzyl)-1H-indol-5-yl)acetamide (1.0 eq) was then dissolved in DMF and added with 2.6 equivalents of potassium tert-butoxyde and 2.6 equivalents of n-butylamine. The reaction was stirred under reflux overnight. Then water was added and the mixture was extracted four times with DCM. The organic phases were collected, dried over anhydrous Na_2SO_4, filtered and concentrated *in vacuo*. After purification by flash chromatography, final product **28a** was obtained in 57% yield as a white solid that crystallized from n-hexane/ethyl acetate.

2-chloro-N-(1-(4-(trifluoromethyl)benzyl)-1H-indol-5-yl)acetamide:

^{1}H NMR ($CDCl_3$, 400 MHz): 4.15 (s, 2H, CH_2), 5.30 (s, 2H, CH_2), 6.50 (d, 1H, aryl, J= 3.7 Hz), 7.08-7.19 (m, 5H, aryl); 7.48 (d, 2H, aryl, J= 8.0 Hz); 7.82 (s, 1H, aryl); 8.19 (bs, 1H, NH). HR-MS m/z: calcd for $C_{18}H_{14}ClF_3N_2O$, [(M+H)+]: 367.0820; found 367.0824

2-(butylamino)-N-(1-(4-(trifluoromethyl)benzyl)-1H-indol-5-yl)acetamide

^{1}H NMR (CH_3OD, 400 MHz): 1.03 (t, 3H, CH_3 , *J* = 7.3 Hz); 1.42-1.51 (m, 2H, CH_2); 1.71-1.79 (m, 2H, CH_2), 3.12 (t, 2H, CH_2 , *J* = 8.0 Hz); 3.99 (s, 2H, CH_2) 5.50 (s, 2H, CH_2), 6.54 (d, 1H, aryl, *J* = 2.9 Hz), 7.22-7.29 (m, 5H, aryl); 7.36 (d, 1H, aryl, *J* = 2.9 Hz); 7.59 (d, 2H, aryl, *J* = 8.0 Hz); 7.90 (s, 1H, N*H*). ^{13}C NMR (CD_3OD, 100 MHz) δ: 12.5; 19.4; 27.7; 48.2; 49.0; 101.5; 109.6; 112.6; 115.5;

125.1; 126.9; 129.0; 129.5; 129.8; 133.9; 142.7; 162.9. ^{19}F NMR ($CDCl_3$, 376.3 MHz) δ: -61.33 (s, 3F, CF_3). HR-MS *m/z*: calcd for $C_{22}H_{24}F_3N_3O$ [$(M+H)^+$]: 404,1944; found 404,2000

2-(butyl(methyl)amino)-N-(1-(4-(trifluoromethyl)benzyl)-1H-indol-5-yl)acetamide (29a)

Compound **28a** (1.0 eq) was dissolved in dry methanol and the solution was added with 1.5 equivalents of formaldehyde. The reaction was stirred at room temperature under positive nitrogen pressure overnight. Then, 3 equivalents of $NaBH_4$ were added and the reaction mixture was stirred for further 3h. Water was added to quench the excess of hydride, and the aqueous solution was extracted four times with DCM. The organic phases were washed with brine, dried over anhydrous Na_2SO_4, filtered and concentrated. Purification by flash chromatography gave **29a** in 81% yield as a white solid that crystallized from n-hexane/ethyl acetate. ^{1}H NMR ($CDCl_3$, 400 MHz): 0.88 (t, 3H, CH_3, *J* = 7.2 Hz); 1.30-1.38 (m, 2H, CH_2); 1.42-1.49 (m, 2H, CH_2); 2.59 (t, 2H, CH_2, *J* = 7.5 Hz); 3.40 (s, 3H, CH_3); 4.52 (s, 2H, CH_2); 5.30 (s, 2H, CH_2), 6.49 (d, 1H, aryl, *J* = 3.1 Hz), 7.06-7.13 (m, 4H, aryl); 7.30-7.32 (m, 1H, aryl); 7.47 (d, 2H, aryl, *J* = 8.2 Hz); 7.60 (d, 1H, aryl, *J* = 2.0 Hz). ^{13}C NMR ($CDCl_3$, 100 MHz) δ: 13.9; 20.4; 30.2; 49.8; 54.9; 57.4; 72.2; 102.5; 109.9; 113.3; 116.2; 125.8; 126.8; 128.8; 129.3; 130.2; 134.0; 141.4; 170.2. ^{19}F NMR ($CDCl_3$, 376.3 MHz) δ: -62.14 (s, 3F, CF_3). HR-MS *m/z*: calcd for $C_{23}H_{26}F_3N_3O$ [$(M+H)^+$]: 418,2101; found 418,2114.

N-(5-oxo-5,6,7,8-tetrahydronaphthalen-2-yl)heptanamide (31)

Intermediate **31** was synthesized in 84% yield, using 6-amino-3,4-dihydronaphthalen-1(2H)-one (**30**) and heptanoyl chloride as starting materials and following the general procedure D. ^{1}H NMR ($CDCl_3$, 400 MHz) δ: 0.90 (t, 3H, CH_3, J= 9.8 Hz); 1.27-1.27 (m, 6H, 3 CH_2); 1.69-1.78 (m, 2H, CH_2); 2.08-2.17 (m, 2H, CH_2); 2.40 (t, 2H, CH_2, J= 12.1 Hz); 2.64 (t, 2H, CH_2, J= 12.1 Hz); 2.94 (t, 2H, CH_2, J= 8.5 Hz), 7.23 (d, 1H, aryl, J= 11.6 Hz); 7.62 (bs, 1H, N*H*); 7.76 (s, 1H, aryl), 8.00 d (1H, H-4, J=11.5 Hz) HR-MS *m/z*: calcd for $C_{17}H_{24}NO_2$, [$(M+H)^+$]:274.1802; found 274.1810

N-(5-hydroxy-5,6,7,8-tetrahydronaphthalen-2-yl)heptanamide (32)

Alcohol **32** was synthesized in 90% yield by reduction of the ketone precursor **31** as already described.[13] ^{1}H NMR ($CDCl_3$, 400 MHz) δ: 0.90 (t, 3H, C*H*$_3$, J= 9.5 Hz); 1.28-1.36 (m, 6H, 3 C*H*$_2$); 1.68-1.76 (m, 4H, 2 C*H*$_2$); 1.95-2.00 (m, 2H, C*H*$_2$); 2.36 (t, 2H, C*H*$_2$, J= 11.7 Hz); 2.65-2.86 (m, 2H, C*H*$_2$); 4.76 (t, 1H, H-5, J=3.6 Hz); 7.18 (bs, 1H, N*H*); 7.24 (d, 1H, aryl, J= 11.4 Hz); 7.36-7.39 (m, 2H, aryl), HR-MS *m/z*: calcd for $C_{17}H_{26}NO_2$, [(M+H)$^+$]:276.1958; found 276.1949.

(Z)-N-(5-(4-(trifluoromethyl)benzylidene)-5,6,7,8-tetrahydronaphthalen-2-yl)heptanamide (33a)

Final compound **32a** was synthesized from **31** as described by Ulmschneider et al.[13] After purification, **32a** was isolated in 32% yield as a white solid that crystallized from petroleum ether. The geometry of the double bond was assigned by bidimensional NMR experiments (please see supplementary material file). ^{1}H NMR ($CDCl_3$, 400 MHz): δ: 0.91 (t, 3H, C*H*$_3$, J=6.8 Hz); 1.28-1.40 (m, 8H, 3 C*H*$_2$); 1.68-1.76 (m, 2H, C*H*$_2$); 1.99-2.05 (m, 2H, C*H*$_2$); 2.34 (t, 2H, C*H*$_2$, J=7.6 Hz); 2.52-2.55 (m, 2H, C*H*$_2$); 2.90 (t, 2H, C*H*$_2$, J=6.6 Hz); 6.39 (s, 1H, C_{sp2}*H*); 6.81-6.84 (m, 1H aryl); 7.03 (d, 1H aryl, J=8.5 Hz); 7.08 (s, 1H, N*H*); 7.33 (d, 2H, aryl, J= 8.2 Hz); 7.46 (d, 2H, aryl, J=8.2 Hz); 7.55 (s, 1H, aryl). ^{13}C NMR ($CDCl_3$, 100 MHz) δ: 14.0; 22.5; 23.9; 25.6; 28.9; 29.7; 31.6; 34.9; 37.9; 116.1; 119.6; 122.4; 125.1; 125.7; 127.9; 128.3; 129.2; 129.5; 130.3; 137.4; 139.8; 140.2; 142.5; 171.3; ^{19}F NMR ($CDCl_3$, 376.3 MHz) δ: -62.51 (s, 3F, C*F*$_3$). HR-MS *m/z*: calcd for $C_{25}H_{29}F_3NO$, [(M+H)$^+$]: 416.2193; found 416.2198;

(E)-N-(5-(4-(trifluoromethyl)benzylidene)-5,6,7,8-tetrahydronaphthalen-2-yl)heptanamide (33b)

Final compound **32b** was synthesized from **31** as described by Ulmschneider et al.[13] After purification, **32a** was isolated in 51% yield as a white solid that crystallized from petroleum ether.

The geometry of the double bond was assigned by bidimensional NMR experiments (please see supplementary material file). ^{1}H NMR ($CDCl_3$, 400 MHz): δ: 0.92 (t, 3H, C*H*$_3$, J=6.7 Hz); 1.28-1.43 (m, 8H, 3 C*H*$_2$); 1.72-1.79 (m, 2H, C*H*$_2$); 1.82-1.89 (m, 2H, C*H*$_2$); 2.38 (t, 2H, C*H*$_2$, J=7.6 Hz); 2.76-2.80 (m, 2H, C*H*$_2$); 2.85 (t, 2H, C*H*$_2$, J= 6.2 Hz); 7.00 (s, 1H, C_{sp2}*H*); 7.19 (s, 1H, N*H*); 7.31 (d, 1H, aryl, J=8.5 Hz); 7.46 (d, 3H, aryl, J=7.8 Hz); 7.62 (d, 2H, aryl, J= 8.2 Hz); 7.68 (d, 1H, aryl, J= 8.6 Hz) ^{13}C NMR ($CDCl_3$, 100 MHz) δ: 14.0; 22.5; 23.5; 25.6; 28.0; 28.9; 30.4; 31.6; 37.9; 117.7; 119.7; 121.3; 123.0; 125.2; 125.7; 128.0; 128.3;129.5; 131.7; 137.5; 138.9; 139.2; 141.8; 171.4; ^{19}F NMR ($CDCl_3$, 376.3 MHz) δ: -62.37 (s, 3F, C*F*$_3$). HR-MS *m/z*: calcd for $C_{25}H_{29}F_3NO$, [$(M+H)^+$]: 416.2193; found 416.2201

N-(5-(4-(trifluoromethyl)benzyl)-5,6,7,8-tetrahydronaphthalen-2-yl)heptanamide (34)

Compounds **33b** (1.0 eq) was dissolved in methanol and added with a catalytic amount of Pd/C 10% and ammonium formate (10.0 eq). The reaction was refluxed under stirring. After 40 minutes, the mixture was cooled to room temperature and filtered through celite. The resulting solution was evaporated and reconstituted in DCM. The organic phase was washed with water (three times) and brine (two times) before being dried over anhydrous Na_2SO_4, filtered and concentrated at the rotary evaporator. After purification, product **34** was obtained in 86% yield as a white was unable to crystallize. $[\alpha]^{25}_D$: +11.0 ± 0.03 (c = 0.05, MeOH). ^{1}H NMR ($CDCl_3$, 400 MHz): δ: 0.92 (t, 3H, C*H*$_3$, J=6.8 Hz); 1.28-1.42 (m, 6H, 3 C*H*$_2$); 1.56-1.78 (m, 5H, C*H*$_2$); 1.81-1.92 (m, 1H, C*H*); 2.36 (t, 2H, C*H*$_2$, J=7.86Hz); 2.72-2.83 (m, 3H, C*H*$_2$ and C*H*); 3.04-3.15 (m, 2H, C*H*$_2$); 7.10-7.14 (m, 2H, aryl and N*H*); 7.23-7.25 (m, 1H, aryl); 7.31 (d, 2H, aryl, J= 8.0 Hz); 7.35 (s, 1H, aryl); 7.57 (d, 2H, aryl, J=8.0 Hz); ^{13}C NMR ($CDCl_3$, 100 MHz) δ: 14.0; 19.2; 22.5; 25.6; 26.8; 28.9; 29.8; 31.6; 37.8; 39.0; 43.1; 117.5; 120.3; 123.0; 125.16; 125.19; 125.5; 125.4; 128.2; 128.5; 129.1; 129.5; 135.7; 135.9; 137.9; 145.0; 171.3; ^{19}F NMR ($CDCl_3$, 376.3 MHz) δ: -62.21 (s, 3F, C*F*$_3$). HR-MS *m/z*: calcd for $C_{25}H_{31}F_3NO$, [$(M+H)^+$]: 418.2352; found 418.2361;

Structures preparation.

Molecules were sketched using the Maestro GUI [44] and then submitted to the ligprep utility [45] to generate low-energy 3D structures from each input molecule, with various ionization states and tautomers at a pH range of 6–8. For each molecule, the state with the lowest state penalty was retained for the following studies. Compounds were studied for their conformational landscape using MacroModel.[46] The "Mixed torsional/Low mode sampling method" was employed, using the automatic setup of the search variables, with the torsion sampling set to extended; the maximum number of steps was set to 5000 and 200 per molecule and rotatable bond, respectively. Conformers in an energy window of 82 kJ/mol were saved, discarding the redundant ones (cutoff of maximum atom deviation=0.5Å). Minimization of conformers was performed using the Polak−Ribiere conjugate gradient method, using a maximum of 2500 minimization step and a 0.05 J/(Å mol) gradient convergence threshold. OPLS3 [45] was used as force-field. No implicit solvation model was used.

Pharmacophore modeling.

The data sets used for the pharmacophores development are reported in table S3. Ligand conformations from the above reported conformational searches were used as input. Hypotheses A, B and C were developed using Phase [20] to find the best alignment and common features. Hypothesis were required to match at least half of the active molecules and to have a number of feature ranging between 3 and 7, with at least a hydrogen bond donor. For each training set, the best ranked model (by Phase Hypo Score) was retained, finally obtaining models A, B and C. Model D was built on the basis of the latter three models. Models B and C were both superimposed to model A by the shared features Ar1, Ar2, HY1, HBA and HBD. The three models were then merged to get the coordinates of features HY2 and HY3 from models B and C, respectively, while features HY1, Ar1, Ar2, HBA and HBD were inherited from model A.

Dihedral scans of linker moieties.

Dihedral scans reported in figure S1 were performed using Macromodel.[46] Linker moieties were capped using methyl groups. Dihedral angles were scanned from 0° to 360° with an increment of 10° and each rotamer was minimized, freezing the studied dihedral, through the Polak−Ribiere conjugate gradient method, using a maximum of 2500 minimization step and a 0.05 J/(Å mol) gradient convergence threshold. OPLS3 [47] was used as force-field. For the molecules endowed with a second NH group (indicated with an asterisk in figure S1) a two coordinates scan was employed to find the absolute minimum for each dihedral angle. Molecular surfaces reported in Table S1 were calculated on the global minimum of each linker molecule. Electrostatic potential and electron densities were calculated using single-point DFT calculations (B3LYP/6-31G**) in vacuum, through the Jaguar software.[48] SCF spin treatment was set to automatic and grid density was set to medium. Accuracy level was set to quick and initial guesses for the molecular orbitals were constructed from atomic orbitals. SCF convergence (DIIS scheme) criteria were set as follows: maximum iterations=48; energy convergence=$5*10^{-5}$ E_h; RMS density matrix change=$5*10^{-6}$; SCF level shift 0.2 E_h

Homology modeling.

The sequence of human Kv7.2 (Swiss-Prot accession code O43526.2) was downloaded from the NCBI sequence database), and the region of our interest (residues 219-325) was extracted and aligned, using ClustalW,[49] to the CryoEM structure of Xenopus KCNQ1 channel (PDB id: 5VMS[50] – Score: 152 bits – Expect: 1e-44 – Identities: 70/112 – Positives 88/112 – Gaps: 5/112). $Kv7.2_{219-325}$ was modeled, as a homo-tetramer, by homology with the biological assembly 1 of 5VMS, using the energy-based method implemented in Prime.[51] Side chains were optimized, with the exception of those belonging to conserved residues, whose rotamers were retained from the template structure. Residues not obtained from the templates were minimized. Residue deletions caused by query gaps were closed. No further optimization was carried on.

Photochemical Stability assay.

Compounds were dissolved in DMSO and then diluted in buffered aqueous solutions at pH 7.4 to a final concentration of 1 mM, 10 μM and 1 μM. 1cm quartz cells, filled with the above mentioned solutions were irradiated under natural daylight, or maintained at 37°C and irradiated by an UV lamp at 365 and 264 nm wavelength or an artificial daylight D65 lamp (Philips, Amsterdam, Nederland) inside a black box UV analyser. Control samples were maintained at 37°C and wrapped by aluminium foils to avoid light exposure. At predetermined intervals aliquots were withdrawn and analysed by HPLC (see below) in order to assess the concentration decrease of the starting materials.

***In vitro* drug metabolism using human liver microsomes**

2 μL of Retigabine, **23a** and **24a** (1 mM) were incubated with 183 μL of 100 mM phosphate buffer (pH 7.4), and 5 μL of 20 mg/mL pooled human liver S9 fractions (Thermo Fisher Scientific, Bremen, Germany). After pre-incubation in water bath for 5 min, the mixture was incubated with 10 μL of the 20 mM NADPH at 37°C for 60 min in a Thermomixer comfort (Eppendorf, Hamburg, Germany). For the measurement of uridine glucuronide transferases (UGT) activity, before the incubation with NADPH, were added to the reaction mixture 5 mM of the uridine 5'-diphospho-alpha-D-glucuronic acid (UDPGA), 50 micrograms of alamethicin/mg of microsomial protein and 1 mM MgCl. For the measurement of N-acetyl transferases (NAT) activity, before the incubation with NADPH, were added to the reaction mixture 2 mM of dithiothreitol, 60 micrograms of sulfamethazine/mg of microsomial protein, 4.5 mM of acetyl DL-carnitine, 0.1 Units/mL of carnitine acetyltransferase. The mixture were incubated at 37°C for 60 min. The reactions were stopped by the addition of 200 μL of the ice-cold methanol and then samples were centrifuged at 10,000 rpm at 25°C for 5 min (Eppendorf microcentrifuge 5424, Hamburg, Germany). The supernatants were collected and injected in RP-UHPLC-DAD

The control at 0 min was obtained by addition of the organic solvent immediately after incubation with microsomes. As the positive control were used testosterone, 7-hydroxycoumarin and p-amino benzoic acid while the negative control was prepared by incubation up to 60 min without NADPH. The extent of metabolism is expressed as a percentage of the parent compound turnover using the following equation:

$$\% \text{ Parent compound turnover} = 100 - \left[\frac{\text{concentration at 60 min}}{\text{concentration at 0 min}} \times 100\right]$$

Analytical instrumentations and conditions

HPLC analysis

UHPLC analyses were performed on a Nexera UHPLC system (Shimadzu, Kyoto, Japan) consisting of a CBM-20A controller, two LC-30AD pumps, a DGU-20 A_{5R} degasser, an SPD-M20A photo diode array detector, a CTO-20AC column oven, a SIL-30AC autosampler.

The separation was carried out on a Kinetex™ C18 150 × 2.1 mm × 2.6 μm (100 Å) column (Phenomenex, Bologna, Italy). The optimal mobile phase consisted of 0.1% TFA/H_2O *v/v* (A) and 0.1% TFA/ACN *v/v* (B). Analysis was performed in gradient elution as follows: 0–13.0 min, 5–65% B; 13–14.0 min, 65–95% B; 14–15.0 min, isocratic to 95% B; 15–15.01 min, 95–5% B; then three minutes for column re-equilibration. Flow rate was 0.5 mL min^{-1}. Column oven temperature was set to 45°C. Injection volume was 7 μL of sample. The following PDA parameters were applied: sampling rate, 12.5 Hz; detector time constant, 0.160 s; cell temperature, 40°C. Data acquisition was set in the range 190–800 nm and chromatograms were monitored at 254 nm. To avoid overlapping of the compounds peak with the acetonitrile bump, derivatives **33a** and **33b** were analyzed using a Kinetex™ C8 150 × 2.1 mm × 2.6 μm (100 Å) column (Phenomenex, Bologna, Italy) using the following gradient elution: 0.01-13.00 min, 5-65% B; 13.01-14.00 min 65-95% B; 14.01-15.00 min, 95% isocratic B; and finally 5 minutes for column re-equilibration.

The calibration curves of were obtained in a concentration range of 10-0.6 μM with five concentration levels and triplicate injection of each level were run. Peak areas were plotted against corresponding concentrations and the linear regression was used to generate calibration curve (**retigabine**: y = 0.00012x + 0.16116, R^2 = 0.9995; **8a** y = 0.00008x + 0.03642, R^2 = 0.9993; **13a** y = 0.00008x + 0.06438, R^2 = 0.9995; **13d** y = 0.00007x + 0.09685, R^2 = 0.9994; **23a**: y = 0.00005x + 0.03559, R^2 = 0.9999; **23c** y = 0.00008x + 0.08246, R^2 = 0.9996; **24a**: y = 0.00005x + 0.07188, R^2 = 0.9998).

HPLC/MS analysis

HPLC/MS analyses were conducted interfacing the UHPLC system described above with an IT-TOF hybrid mass spectrometer (Ion Trap-Time of Flight) equipped with an electrospray source (ESI) (Shimadzu, Kyoto, Japan). The LC-MS/MS data were processed by the LCMSsolution® software (Version 3.50.346, Shimadzu). In detail, the analysis were conducted using a Kinetex® EVO C18 150 × 2.1 mm (100 Å) column, having a 2.6 μm core shell particulate (Phenomenex, Bologna, Italy). The flow of the mobile phases was set at 0.5 mL/min and the oven temperature was set at 45°C. The injection volume was 2 μL. The analysis were carried out employing as mobile phase: A) 10mM $HCOONH_4$ in H_2O (pH=6.3) and B) ACN using the following elution gradient: 0.01-20.00 min, 5-95% B; 20.01-22.00 min, 95% isocratic B; and finally 5 minutes for column re-equilibration. Data acquisition was set in the range 190–800 nm and chromatograms were monitored at 254 nm and 550 nm. MS detection was operated in positive ionization mode with the following parameters: 1.75 kV; CDL (curve desolvation line) temperature, 250°C; block heater temperature, 250°C; nebulizing gas flow (N_2), 1.5 L/min; drying gas pressure, 98 kPa. Full scan MS data were acquired in the range of 150–2000 m/z (ion accumulation time, 25 ms; IT, repeat = 3). MS/MS experiments were conducted in data dependent acquisition, precursor ions were acquired in the range 150–2000 m/z; peak width, 3 Da; ion accumulation time, 50 ms; CID energy, 55%; collision gas, 50%; repeat = 1; execution trigger (BPC) intensity, at 70% stop level.

GC/MS analysis

GC-MS analysis were performed on Shimadzu GC-2010 Plus gas chromatograph coupled to a 2010 Plus single quadrupole mass spectrometer (Shimadzu Corp., Kyoto, Japan). Chromatographic separation was carried out on an CP-Sil 8 CB fused silica capillary GC column (30 m × 0.25 mm i.d, 1.0 μm film thickness, Agilent, Santa Clara, CA). The operating conditions of GC were: Helium (purity > 99.9999%) was used as carrier gas at linear velocity of 39 cm/s, 2 μL of sample was injected in splitless mode via autosampler (AOC-20s), and injector temperature (AOC-20i) was 280 °C. Oven temperature was programmed as follows: started from 100 °C (hold for 1 min), increased to 320 °C at the rate of 6 °C/min (hold for 2 min). The mass spectrometer was operated in electron-impact mode with 70 eV electrons. Interface and ion source temperatures were set at 320 °C and 200 °C, respectively. The quadrupoles were operated in scan mode over the *m*/*z* range of 35–600 m/z with a solvent cut time of 2.9 min. The complete GC program duration was 40 min.

Cell Culture and Transient Transfection.

Channel subunits were expressed in Chinese Hamster Ovary (CHO) cells by transient transfection, using plasmids containing cDNAs encoding human Kv7.1, Kv7.2, Kv7.3, and Kv7.4, all cloned in pcDNA3.1 vector. According to the experimental protocol, these plasmids were expressed individually or in combination, together with a plasmid-expressing enhanced green fluorescent protein (Clontech, Palo Alto, CA) used as a transfection marker. Total cDNA in the transfection mixture was kept at 4 μg. CHO cells were grown in 100-mm plastic Petri dishes in Dulbecco's modified Eagle's medium containing 10% fetal bovine serum, nonessential amino acids (0.1 mM), penicillin (50 U/ml), and streptomycin (50 mg/ml) in a humidified atmosphere at 37°C with 5% CO_2. At 24 hours before transfection, the cells were plated on glass coverslips coated with poly-L-lysine, and were transfected on the next day with the appropriate cDNA using Lipofectamine 2000 (Life Technologies), according to the manufacturer's protocol. Electrophysiologic experiments were performed 24 hours after transfection.

Whole-cell electrophysiology.

Currents from CHO cells were recorded at room temperature (20–22°C) using the whole-cell configuration of the patch-clamp technique, with glass micropipettes of 3-5 MΩ resistance. During the recording, constant perfusion of extracellular solution was maintained. The extracellular solution contained (in mM): 138 NaCl, 2 $CaCl_2$, 5.4 KCl, 1 $MgCl_2$, 10 glucose, and 10 HEPES, at pH 7.4, with NaOH. The pipette (intracellular) solution contained (in mM): 140 KCl, 2 $MgCl_2$, 10 EGTA, 10 HEPES, 5 Mg^{2+}-ATP, at pH 7.3-7.4, with KOH. Current were recorded using an Axopatch-200A amplifier, filtered at 5 kHz, and digitized using a DigiData 1440A (Molecular Devices). The pCLAMP software (version 10.2) was used for data acquisition and analysis (Molecular Devices). To evaluate the activity of each compound on Kv7.2 currents, the cells were clamped at -80 mV and currents were elicited by 3-s voltage ramps from -80 mV to +20 mV in the presence and absence of each compound.

The ΔV values, calculated as membrane potentials at which currents reached 20% of their peak value for controls and after drug exposure, were plotted versus log(concentration) of the compound, fitted to a four parameter logistic equation and EC_{50} values were calculated with SigmaPlot (version 12.3). Indicated EC_{50} values are the mean of at least three independent experiments ± standard deviation (SD).

CMC determination using fluorescence spectroscopy

A stock solution of compounds 23a and 24a and retigabine was prepared in DMSO. These solutions were, then, diluted in 0.9% w/v NaCl to obtain the tested concentrations in the range 0.7-100 μM. Residual DMSO was below 0.1% v/v in all tested concentration. Pyrene (Sigma Aldrich, Italy) was used as fluorescent probe. Pyrene spectra in presence of different concentrations of these compounds were recorded in the range between 200 nm and 700 nm with a 2.5 nm slits after excitation at 334 nm. Each recorded spectrum was the sum of ten acquisition. Analyses were performed at 25 °C using a Fluorescence Spectrometer LS 55 (PerkinElmer, Waltham, USA) equipped with a thermostatic bath

(HAAKE C25P). The ratio of peak intensity I (λ=372 nm) and peak intensity III (λ=383 nm) of the emission spectrum of pyrene was plotted against concentrations. Data were the mean ± standard deviation of at least three independent measurements.

Statistical analysis

Statistically significant differences in electrophysiological data were evaluated with the Student t-test, or with ANOVA followed by the Student- Newman-Keuls test when multiple groups were compared, with the threshold set at $P < 0.05$. Data were analyzed using the Sigma Plot 12.3 for Windows (Systat Software Inc, San Jose, CA). Values are expressed as the mean ± standard deviation of at least 3 cells recorded in at least 2 independent transfections as the mean ± standard deviation of three independent measurements

ASSOCIATED CONTENT

The Supporting Information is available free of charge on the ACS Publications website at DOI:

Figure S1. Relative potential energies for the rotation of the bond connecting the hydrogen bond donor group to the hydrogen bond acceptor; **Table S1:** Relative electrostatic potential and relative electron densities surfaces of the linker moieties N-X; **Table S2:** Effect of tested compounds on ramp-evoked currents of Kv 7.2; **Figure S2**. CMC fluorescence measurements for **23a**, **24a** and retigabine; **Figure S3:** Effect of retigabine and 23a on homomeric Kv7.1 channels; **Figure S4**. Superimposition of models B (solid spheres) and C (transparent spheres); **Table S3:** Training sets of models A, B and C; **Figure S5**. UHPLC profile of a retigabine batch after 6h visible light irradiation**; Figure S6.** Full scan, MS/MS and predicted structure of a retigabine photoxidative byproduct**; Figure S7.** Retigabine GC/MS profile; **Figure S8**. Overlapping HPLC traces of a 4-fluorobenzaldehyde standard solution

and a photodegraded retigabine batch; **Figure S9.** MS/MS profile for unknown compound #1 and the corresponding putative molecular structures; Figure **S10**. HPLC, GC and MS profile for compoud **8a** after the photodegradation assay. **Figures S11-S12**. Blank RP-HPLC trace of the analytical method used for purity determination; **NMR spectra** of synthesized compounds, **RP-HPLC traces** of synthesized compounds (pdf). **Molecular Formula Strings** (CSV file)

AUTHOR INFORMATION

Corresponding Authors

* Pietro Campiglia, pcampiglia@unisa.it

* Maurizio Taglialatela, mtaglial@unina.it

Author Contributions

The manuscript was written through contributions of all authors. All authors have given approval to the final version of the manuscript. # These authors contributed equally.

Funding Sources

The present work was also supported by the Telethon Foundation (grant number GGP15113) to MT, the Italian Ministry for University and Research (MIUR) (PRIN 2017ALCR7C) to MT, MVS and MM, MIUR (Projects Scientific Independence of Researchers 2014 RBSI1444EM and PRIN 2017YH3SXK) to FM, the University of Naples "Federico II" and Compagnia di San Paolo in the frame of Program STAR "Sostegno Territoriale alle Attività di Ricerca" (project number 6-CSPUNINA-120) to FM, and the Italian Ministry of Health (Project GR-2016-02363337) to MVS.

ACKNOWLEDGMENT

NVIDIA Corporation is gratefully acknowledged for its support with the donation of the Tesla K40 GPU used for this research. The authors thank Prof. Thomas J. Jentsch (Max-Delbrück-Center for

Molecular Medicine, Berlin, Germany) for Kv7.2, Kv7.3, Kv7.4, and Kv7.5 cDNAs in pcDNA3.1; Prof. Mark Shapiro (University of Texas Health Science Center, San Antonio, TX) for Kv7.5 cDNA in pcDNA3zeo; and Dr. Eckhard Ficker (Rammelkamp Center, Cleveland, OH) for Kv7.1 cDNA.

ABBREVIATIONS USED

DIPEA, diisopropylethylamine. TEA, triethylamine. CHO, Chinese hamster ovary cells. RET, retigabine. APCI, atmospheric pressure chemical ionization. RP-HPLC, reverse phase-HPLC. PDA, photodiode array. MOMCl, methoxymethyl chloride. ACN, acetonitrile. HEPES, 4-(2-hydroxyethyl)-1-piperazineethanesulfonic acid; EGTA, ethylene glycol tetraacetic acid.

REFERENCES

1. Kwan, P.; Brodie, M.J., Early identification of refractory epilepsy. *N Engl J Med* **2000**, *342*, 314-319

2. Soldovieri, M. V.; Miceli, F.; Taglialatela, M., Driving with no brakes: molecular pathophysiology of Kv7 potassium channels. *Physiology (Bethesda)* **2011,** *26* (5), 365-376.

3. Miceli, F.; Soldovieri, M.V.; Ambrosino, P.; Manocchio, L.; Mosca, I.;, Taglialatela, M., Pharmacological targeting of neuronal Kv7.2/3 channels: a focus on chemotypes and receptor sites. *Curr Med Chem* **2018,** *25* (23), 2637-2660.

4. Main, M. J.; Cryan, J. E.; Dupere, J. R.; Cox, B.; Clare, J. J.; Burbidge, S. A., Modulation of KCNQ2/3 potassium channels by the novel anticonvulsant retigabine. *Mol Pharmacol* **2000,** *58* (2), 253-262.

5. (a) Kim, R. Y.; Yau, M. C.; Galpin, J. D.; Seebohm, G.; Ahern, C. A.; Pless, S. A.; Kurata, H. T., Atomic basis for therapeutic activation of neuronal potassium channels. *Nat Commun* **2015,** *6*,

8116; (b) Schenzer, A.; Friedrich, T.; Pusch, M.; Saftig, P.; Jentsch, T. J.; Grotzinger, J.; Schwake, M., Molecular determinants of KCNQ (Kv7) K+ channel sensitivity to the anticonvulsant retigabine. *J Neurosci* **2005,** *25* (20), 5051-5060; (c) Wuttke, T. V.; Seebohm, G.; Bail, S.; Maljevic, S.; Lerche, H., The new anticonvulsant retigabine favors voltage-dependent opening of the Kv7.2 (KCNQ2) channel by binding to its activation gate. *Mol Pharmacol* **2005,** *67* (4), 1009-1017.

6. Barrese, V.; Miceli, F.; Soldovieri, M. V.; Ambrosino, P.; Iannotti, F. A.; Cilio, M. R.; Taglialatela, M., Neuronal potassium channel openers in the management of epilepsy: role and potential of retigabine. *Clin Pharmacol* **2010,** *2*, 225-236.

7. Zhou, P.; Zhang, Y.; Xu, H.; Chen, F.; Chen, X.; Li, X.; Pi, X.; Wang, L.; Zhan, L.; Nan, F.; Gao, Z., P-retigabine: an N-propargyled retigabine with improved brain distribution and enhanced antiepileptic activity. *Mol Pharmacol* **2015,** *87* (1), 31-38.

8. Jankovic, S.; Ilickovic, I., The preclinical discovery and development of ezogabine for the treatment of epilepsy. *Expert Opin Drug Discov* **2013,** *8* (11), 1429-1437.

9. (a) Kumar, M.; Reed, N.; Liu, R.; Aizenman, E.; Wipf, P.; Tzounopoulos, T., Synthesis and evaluation of potent KCNQ2/3-specific channel activators. *Mol Pharmacol* **2016,** *89* (6), 667-677; (b) Bock, C.; Link, A., How to replace the lost keys? Strategies toward safer KV7 channel openers. *Future Med Chem* **2019,** *11* (4), 337-355.

10. (a) Manville, R.W.; Abbott, G.W., Ancient and modern anticonvulsants act synergistically in a KCNQ potassium channel binding pocket. *Nat Commun* **2018,** *9* (1), 3845; (b) Manville, R.W.; Abbott, G.W., In silico re-engineering of a neurotransmitter to activate KCNQ potassium channels in an isoform-specific manner. *Commun Biol* **2019**, *2*, 401; (c) Liu, R.; Tzounopoulos, T.; Wipf, P. Synthesis and Optimization of Kv7 (KCNQ) Potassium Channel Agonists: The Role of Fluorines in Potency and Selectivity. *ACS Med Chem Lett* **2019**, *10* (6), 929-935.

11. Vernier, J.M.; Chen, H.; Song, J. Derivatives of 5-Amino-4,6-Disubstituted Indole and 5-Amino-4,6-Disubstituted Indoline as Potassium Channel Modulators. WO2009023677, 2009; Valeant Pharmaceuticals (US)

12. (a) Fang, Z.; Song, Y.; Zhan, P.; Zhang, Q.; Liu, X., Conformational restriction: an effective tactic in 'follow-on'-based drug discovery. *Future Med Chem* **2014,** *6* (8), 885-901; (b) Hempel, R.; Schupke, H.; McNeilly, P. J.; Heinecke, K.; Kronbach, C.; Grunwald, C.; Zimmermann, G.; Griesinger, C.; Engel, J.; Kronbach, T., Metabolism of retigabine (D-23129), a novel anticonvulsant. *Drug Metab Dispos* **1999,** *27* (5), 613-622.

13. Ulmschneider, S.; Muller-Vieira, U.; Klein, C. D.; Antes, I.; Lengauer, T.; Hartmann, R. W., Synthesis and evaluation of (pyridylmethylene)tetrahydronaphthalenes/-indanes and structurally modified derivatives: potent and selective inhibitors of aldosterone synthase. *J Med Chem* **2005,** *48* (5), 1563-1575.

14. (a) Wang, L.; Qiao, G.-H.; Hu, H.-N.; Gao, Z.-B.; Nan, F.-J., Discovery of novel retigabine derivatives as potent KCNQ4 and KCNQ5 channel agonists with improved specificity. *ACS Med Chem Lett* **2019**, *10* (1), 27-33; (b) Hu, H-N.; Zhou, P-Z.; Chen, F.; Li, M.; Nan, F-J.; Gao, Z-B., Discovery of a retigabine derivative that inhibits KCNQ2 potassium channels. *Acta Pharmacol Sin* **2013**, *34*(10), 1359-1366.

15. Tatulian, L.; Delmas, P.; Abogadie, F. C.; Brown, D. A., Activation of expressed KCNQ potassium currents and native neuronal M-type potassium currents by the anti-convulsant drug retigabine. *J Neurosci* **2001,** *21* (15), 5535-5545.

16. Wickenden, A. D.; Yu, W.; Zou, A.; Jegla, T.; Wagoner, P. K., Retigabine, a novel anti-convulsant, enhances activation of KCNQ2/Q3 potassium channels. *Mol Pharmacol* **2000,** *58* (3), 591-600.

17. (a) Martire, M.; Castaldo, P.; D'Amico, M.; Preziosi, P.; Annunziato, L.; Taglialatela, M., M channels containing KCNQ2 subunits modulate norepinephrine, aspartate, and GABA release from hippocampal nerve terminals. *J Neurosci* **2004**, *24*, 592-597. (b) Blom, S.M.; Schmitt, N.; Jensen, H.S., Differential effects of ICA-27243 on cloned K(V)7 channels. *Pharmacology* **2010**, *86*, 174-181.

18. (a) Winnik, F.M., Photophysics of preassociated pyrenes in aqueous polymer solutions and in other organized media. *Chem Rev* **1993**, *93* (2), 2587-614; (b) Salonen, A.; Knyazev, A; von Bandel,

N.; Degrouard, J.; Langevin, D.; Drenckhan, W., A Novel Pyrene-Based Fluorescing Amphiphile with Unusual Bulk and Interfacial Properties. *ChemPhysChem* **2011**, *12* (1), 150-160.

19. (a) Padilla, K.; Wickenden, A.D.; Gerlach, A.C.; McCormack, K., The KCNQ2/3 selective channel opener ICA-27243 binds to a novel voltage-sensor domain site. *Neurosci Lett* **2009**, *465*, 138-142. (b) Wang, A.W.; Yang, R.; Kurata, H.T., Sequence determinants of subtype-specific actions of KCNQ channel openers. *J Physiol* **2017**, *595*, 663-676.

20. (a) Dixon, S. L.; Smondyrev, A. M.; Knoll, E. H.; Rao, S. N.; Shaw, D. E.; Friesner, R. A., PHASE: a new engine for pharmacophore perception, 3D QSAR model development, and 3D database screening: 1. Methodology and preliminary results. *J Comput Aid Mol Des* **2006,** *20* (10-11), 647-671; (b) Dixon, S. L.; Smondyrev, A. M.; Rao, S. N., PHASE: a novel approach to pharmacophore modeling and 3D database searching. *Chem Biol Drug Des* **2006,** *67* (5), 370-372.

21. Manville, R. W.; Papanikolaou, M.; Abbott, G. W., Direct neurotransmitter activation of voltage-gated potassium channels. *Nat Commun* **2018,** *9* (1), 1847.

22. Dousa, M.; Srbek, J.; Radl, S.; Cerny, J.; Klecan, O.; Havlicek, J.; Tkadlecova, M.; Pekarek, T.; Gibala, P.; Novakova, L., Identification, characterization, synthesis and HPLC quantification of new process-related impurities and degradation products in retigabine. *J Pharm Biomed Anal* **2014,** *94*, 71-76.

23. Meyer, A.; Fischer, K., Oxidative transformation processes and products of para-phenylenediamine (PPD) and para-toluenediamine (PTD)—a review. *Environ Sci Eur* **2015,** *27* (1), 11.

24. Groseclose, M. R.; Castellino, S., An investigation into retigabine (ezogabine) associated dyspigmentation in rat eyes by MALDI imaging mass spectrometry. *Chem Res Toxicol* **2019,** *32* (2), 294-303.

25. (a) Lai, J.; Chang, L.; Yuan, G., I_2/TBHP Mediated C−N and C−H bond cleavage of tertiary amines toward selective synthesis of sulfonamides and β-arylsulfonyl enamines: the solvent effect on reaction. *Org Lett* **2016**, *18*, 3194−3197; (b) Gong, J.L.; Qi, X.; Wei, D.; Feng, J.B.; Wu X.F.,

Oxidative cleavage of benzylic C–N bonds under metal-free conditions. *Org Biomol Chem* **2014**, *12*, 7486–7488; (c) Yang, Z.K.; Xu, N.X.; Wang, C.; Uchiyama, M., Photoinduced C(sp_3)-N bond cleavage leading to the stereoselective syntheses of alkenes. *Chem Eur J* **2019**, *25*, 5433 – 5439

26. (a) Boger, D. L.; Zarrinmayeh, H., Regiocontrolled nucleophilic addition to selectively activated p-quinone diimines: alternative preparation of a key intermediate employed in the preparation of the CC-1065 left-hand subunit. *J Org Chem* **1990,** *55* (4), 1379-1390; (b) Boger, D. L.; Coleman, R. S., Total synthesis of (+)-CC-1065 and ent-(-)-CC-1065. *J Am Chem Soc* **1988,** *110* (4), 1321-1323.

27. Hubbard, T. D.; Murray, I. A.; Perdew, G. H., Indole and tryptophan metabolism: endogenous and dietary routes to Ah receptor activation. *Drug Metab Dispos* **2015,** *43* (10), 1522-1535.

28. Lewis, D. F.; Jacobs, M. N.; Dickins, M., Compound lipophilicity for substrate binding to human P450s in drug metabolism. *Drug Discov Today* **2004,** *9* (12), 530-537.

29. (a) Borlak, J.; Gasparic, A.; Locher, M.; Schupke, H.; Hermann, R., N-Glucuronidation of the antiepileptic drug retigabine: results from studies with human volunteers, heterologously expressed human UGTs, human liver, kidney, and liver microsomal membranes of Crigler-Najjar type II. *Metab Clin Exp* **2006,** *55* (6), 711-721; (b) Perez, H. L.; Boram, S. L.; Evans, C. A., Development and validation of a quantitative method for determination of retigabine and its N-acetyl metabolite; overcoming challenges associated with circulating labile N-glucuronide metabolites. *Anal Methods* **2015,** *7* (2), 723-735.

30. Jentsch, T. J.; Schroeder, B. C.; Kubisch, C.; Friedrich, T.; Stein, V., Pathophysiology of KCNQ channels: neonatal epilepsy and progressive deafness. *Epilepsia* **2000,** *41* (8), 1068-1069.

31. Munro, G.; Dalby-Brown, W., Kv7 (KCNQ) channel modulators and neuropathic pain. *J Med Chem* **2007,** *50* (11), 2576-2582.

32. Wainger, B. J.; Kiskinis, E.; Mellin, C.; Wiskow, O.; Han, S. S.; Sandoe, J.; Perez, N. P.; Williams, L. A.; Lee, S.; Boulting, G.; Berry, J. D.; Brown, R. H., Jr.; Cudkowicz, M. E.; Bean, B.

P.; Eggan, K.; Woolf, C. J., Intrinsic membrane hyperexcitability of amyotrophic lateral sclerosis patient-derived motor neurons. *Cell Rep* **2014,** *7* (1), 1-11.

33. (a) Korsgaard, M. P.; Hartz, B. P.; Brown, W. D.; Ahring, P. K.; Strobaek, D.; Mirza, N. R., Anxiolytic effects of Maxipost (BMS-204352) and retigabine via activation of neuronal Kv7 channels. *J Pharmacol Exp Ther* **2005,** *314* (1), 282-292; (b) Dencker, D.; Dias, R.; Pedersen, M. L.; Husum, H., Effect of the new antiepileptic drug retigabine in a rodent model of mania. *Epilepsy Behav* **2008,** *12* (1), 49-53; (c) Delmas, P.; Brown, D. A., Pathways modulating neural KCNQ/M (Kv7) potassium channels. *Nat Rev Neurosci* **2005,** *6* (11), 850-862.

34. (a) Lange, W.; Geissendorfer, J.; Schenzer, A.; Grotzinger, J.; Seebohm, G.; Friedrich, T.; Schwake, M., Refinement of the binding site and mode of action of the anticonvulsant Retigabine on KCNQ K+ channels. *Mol Pharmacol* **2009,** *75* (2), 272-280; (b) Manville, R. W.; Abbott, G. W., Gabapentin is a potent activator of KCNQ3 and KCNQ5 potassium channels. *Mol Pharmacol* **2018,** *94* (4), 1155-1163.

35. Kalappa, B. I.; Soh, H.; Duignan, K. M.; Furuya, T.; Edwards, S.; Tzingounis, A. V.; Tzounopoulos, T., Potent KCNQ2/3-specific channel activator suppresses in vivo epileptic activity and prevents the development of tinnitus. *J Neurosci* **2015,** *35* (23), 8829-8842.

36. (a) Surur, A. S.; Bock, C.; Beirow, K.; Wurm, K.; Schulig, L.; Kindermann, M. K.; Siegmund, W.; Bednarski, P. J.; Link, A., Flupirtine and retigabine as templates for ligand-based drug design of KV7.2/3 activators. *Org Biomol Chem* **2019,** *17***,** 4512-4522**;** (b) Bock, C.; Surur, A. S.; Beirow, K.; Kindermann, M. K.; Schulig, L.; Bodtke, A.; Bednarski, P. J.; Link, A., Sulfide analogues of flupirtine and retigabine with nanomolar KV 7.2/KV 7.3 channel opening activity. *ChemMedChem* **2019,** *14* (9)**,** 952-964.

37. Musella, S.; di Sarno, V.; Ciaglia, T.; Sala, M.; Spensiero, A.; Scala, M. C.; Ostacolo, C.; Andrei, G.; Balzarini, J.; Snoeck, R.; Novellino, E.; Campiglia, P.; Bertamino, A.; Gomez-Monterrey, I. M., Identification of an indol-based derivative as potent and selective varicella zoster virus (VZV) inhibitor. *Eur J Med Chem* **2016,** *124*, 773-781.

38. Bertamino, A.; Iraci, N.; Ostacolo, C.; Ambrosino, P.; Musella, S.; Di Sarno, V.; Ciaglia, T.; Pepe, G.; Sala, M.; Soldovieri, M. V.; Mosca, I.; Gonzalez-Rodriguez, S.; Fernandez-Carvajal, A.; Ferrer-Montiel, A.; Novellino, E.; Taglialatela, M.; Campiglia, P.; Gomez-Monterrey, I., Identification of a potent tryptophan-based TRPM8 antagonist with in vivo analgesic activity. *J Med Chem* **2018**, 61 (14), 6140–6152

39. Quast, H.; Ross, K.-H.; Philipp, G.; Hagedorn, M.; Hahn, H.; Banert, K., Syntheses and 15N NMR spectra of iminodiaziridines - ring-expansions of 1-aryl-3-iminodiaziridines to 1H- and 3aH-benzimidazoles, 2H-indazoles, and 5H-dibenzo[d,f][1,3]diazepines. *Eur J Org Chem* **2009,** 23, 3940-3952.

40. Plsikova, J.; Janovec, L.; Koval, J.; Ungvarsky, J.; Mikes, J.; Jendzelovsky, R.; Fedorocko, P.; Imrich, J.; Kristian, P.; Kasparkova, J.; Brabec, V.; Kozurkova, M., 3,6-Bis(3-alkylguanidino)acridines as DNA-intercalating antitumor agents. *Eur J Med Chem* **2012,** *57*, 283-295.

41. Bertamino, A.; Ostacolo, C.; Ambrosino, P.; Musella, S.; Di Sarno, V.; Ciaglia, T.; Soldovieri, M. V.; Iraci, N.; Fernandez Carvajal, A.; de la Torre-Martinez, R.; Ferrer-Montiel, A.; Gonzalez Muniz, R.; Novellino, E.; Taglialatela, M.; Campiglia, P.; Gomez-Monterrey, I., Tryptamine-based derivatives as transient receptor potential melastatin type 8 (TRPM8) channel modulators. *J Med Chem* **2016,** *59* (5), 2179-2191.

42. Thuo, M. M.; Reus, W. F.; Nijhuis, C. A.; Barber, J. R.; Kim, C.; Schulz, M. D.; Whitesides, G. M., Odd-even effects in charge transport across self-assembled monolayers. *J Am Chem Soc* **2011,** *133* (9), 2962-2975

43. Madabhushi, S.; Jillella, R.; Sriramoju, V.; Singh, R., Oxyhalogenation of thiols and disulfides into sulfonyl chlorides/bromides using oxone-KX (X = Cl or Br) in water. *Green Chem.* **2014,** *16* (6), 3125-3131

44. Maestro, S. R.-. *Schrödinger, LLC*, New York, NY, 2018.

45. LigPrep, S. R.-. *Schrödinger, LLC,*, New York, NY, 2018.

46. MacroModel, S. R.-. *Schrödinger, LLC*, New York, NY, 2018.

47. Jorgensen, W. L.; Maxwell, D. S.; TiradoRives, J., Development and testing of the OPLS all-atom force field on conformational energetics and properties of organic liquids. *J Am Chem Soc* **1996,** *118* (45), 11225-11236.

48. Bochevarov, A.D.; Harder, E.; Hughes, T.F.; Greenwood, J.R.; Braden, D.A.; Philipp, D.M.; Rinaldo, D.; Halls, M.D.; Zhang, J.; Friesner, R.A., Jaguar: A high-performance quantum chemistry software program with strengths in life and materials sciences. *Int. J. Quantum Chem.*, **2013**, 113(18), 2110-2142.

49. Thompson, J. D.; Higgins, D. G.; Gibson, T. J. CLUSTAL W: improving the sensitivity of progressive multiple sequence alignment through sequence weighting, position-specific gap penalties and weight matrix choice. *Nucleic Acids Res* **1994**, 22 (22), 4673−4680.

50. Sun, J.; MacKinnon. R., Cryo-EM structure of a KCNQ1/CaM complex reveals insights into congenital long QT syndrome. *Cell* **2017**, 169 (6), 1042-1050.e9

51. (a) Jacobson, M. P.; Pincus, D. L.; Rapp, C. S.; Day, T. J. F.; Honig, B.; Shaw, D. E.; Friesner, R. A., A hierarchical approach to all-atom protein loop prediction. *Proteins* **2004,** *55* (2), 351-367; (b) Jacobson, M. P.; Friesner, R. A.; Xiang, Z. X.; Honig, B., On the role of the crystal environment in determining protein side-chain conformations. *J Mol Biol* **2002,** 320 (3), 597-608.

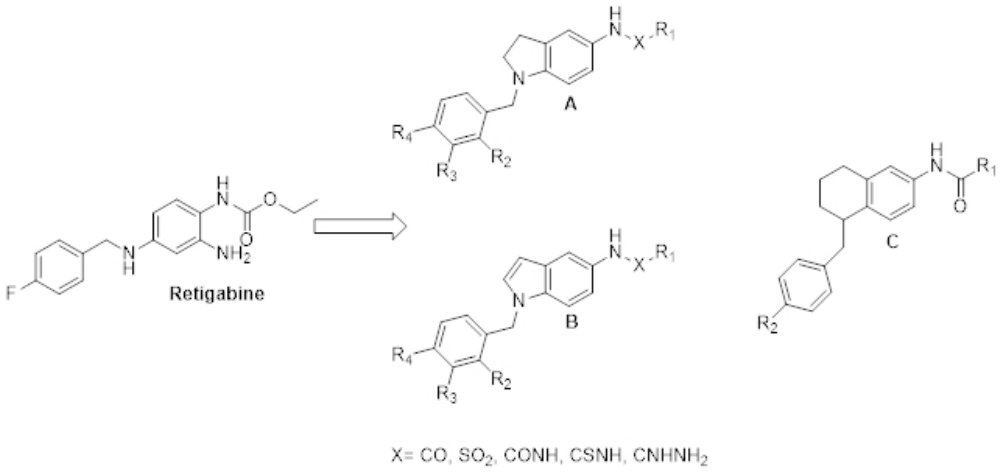

Figure 1. Structures of retigabine and its newly synthesized analogues

54x25mm (300 x 300 DPI)

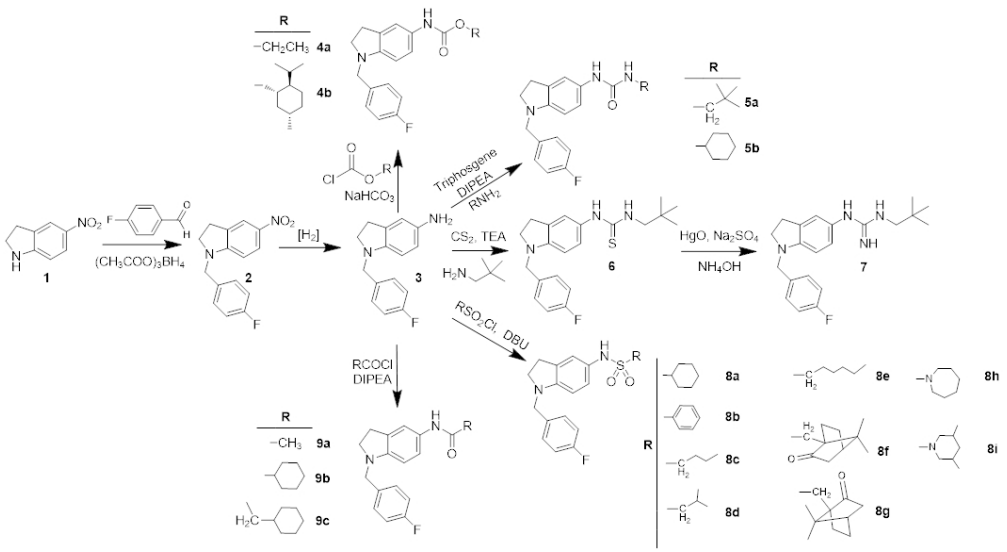

Scheme 1: Synthesis of 1-(4-fluorobenzyl)-5-substituted indoline derivatives 4a-b, 5a-b, 6, 7, 8a-i and 9a-c.

89x48mm (300 x 300 DPI)

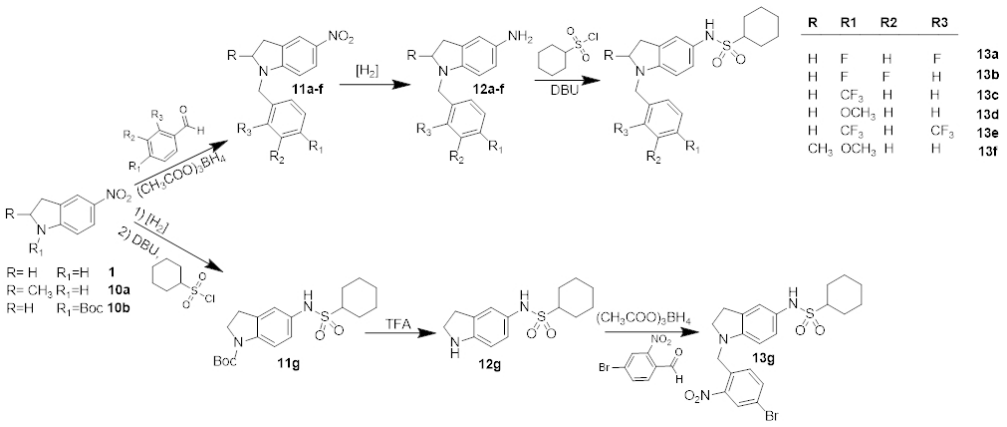

Scheme 2: Synthesis of 1-benzyl-5-cyclohexanesulfonamido indoline derivatives 13a-g.

85x35mm (300 x 300 DPI)

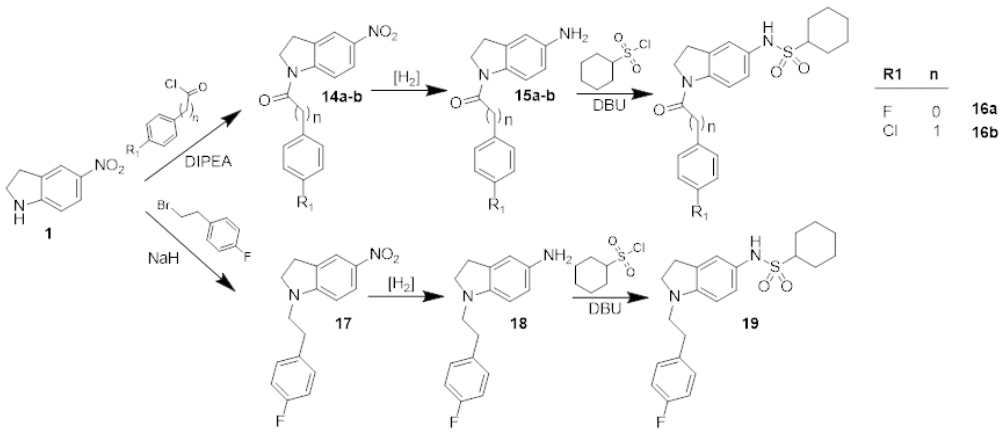

Scheme 3: Synthesis of 1-acyl-5-cyclohexanesulfonamido (16a-b) and 1-alkyl-5-cyclohexanesulfonamido (19) indoline derivatives.

72x31mm (300 x 300 DPI)

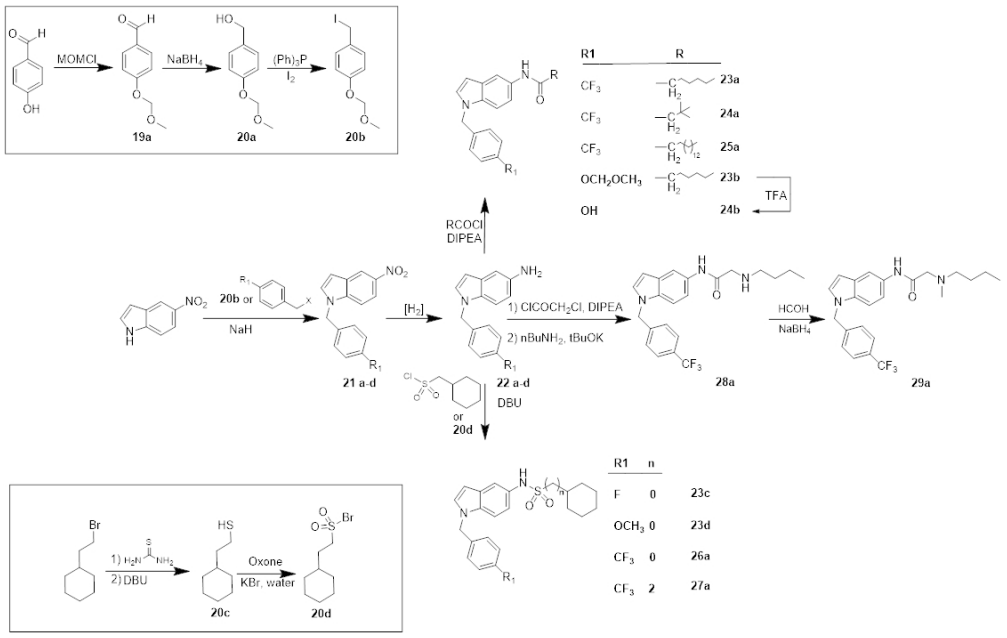

Scheme 4: Synthesis of 1-benzyl-5-amido (23a-25a, 23b-24b, 28a-29a) and 1-benzyl-5-cyclohexanesulfonamido (23c-23d, 26a-27a) indole derivatives.

95x60mm (300 x 300 DPI)

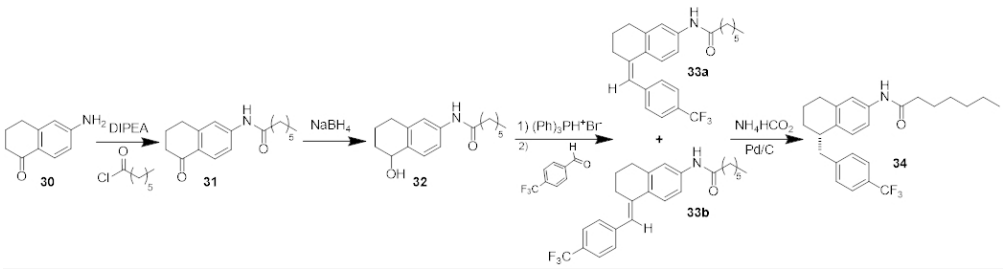

Scheme 5: Synthesis of (R,S)-N-(5-(4-(trifluoromethyl)benzyl)-5,6,7,8-tetrahydronaphthalen-2-yl)heptanamide (34).

88x23mm (300 x 300 DPI)

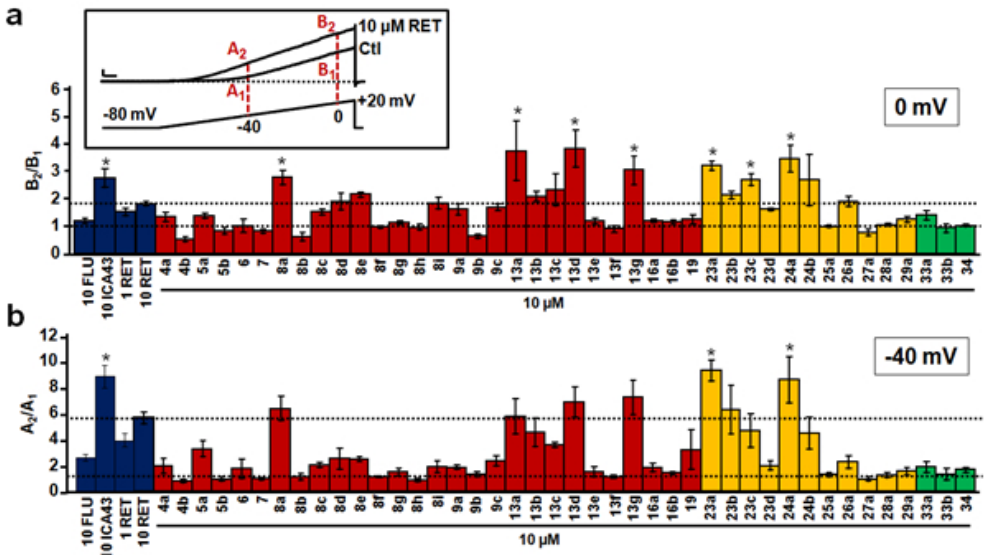

Figure 2. Effect of synthesized compounds on Kv7.2 current in comparison with retigabine. a-b. Representation of the ratio between current amplitude in the presence (A2, B2) and absence (A1, B1) of each of the indicatedcompounds (10 µM) calculated at 0 mV (a) and at -40 mV (b). The inset shows the protocol used to evaluate drug activity on Kv7.2 currents. Current scale, 400 pA; time scale, 0.2 s. Histograms are colored according to the following scheme: blue represents available Kv7 activators, such as retigabine (RET) at 1 and 10 µM, Flupirtine (FLU) at 10 µM, and ICA27243 (ICA43) at 10 µM; red represents indoline derivatives, yellow represents indole derivatives and green represents tetrahydronaphthalene derivatives. Each data point is expressed as the mean ± standard error of the mean (SEM) of at least 3 cells recorded in at least 2 independent transfections; the precise number of cells included in the analysis for each compound is specified in Table S2. * indicates values significantly different ($p < 0.05$) from retigabine (10 µM).

51x29mm (300 x 300 DPI)

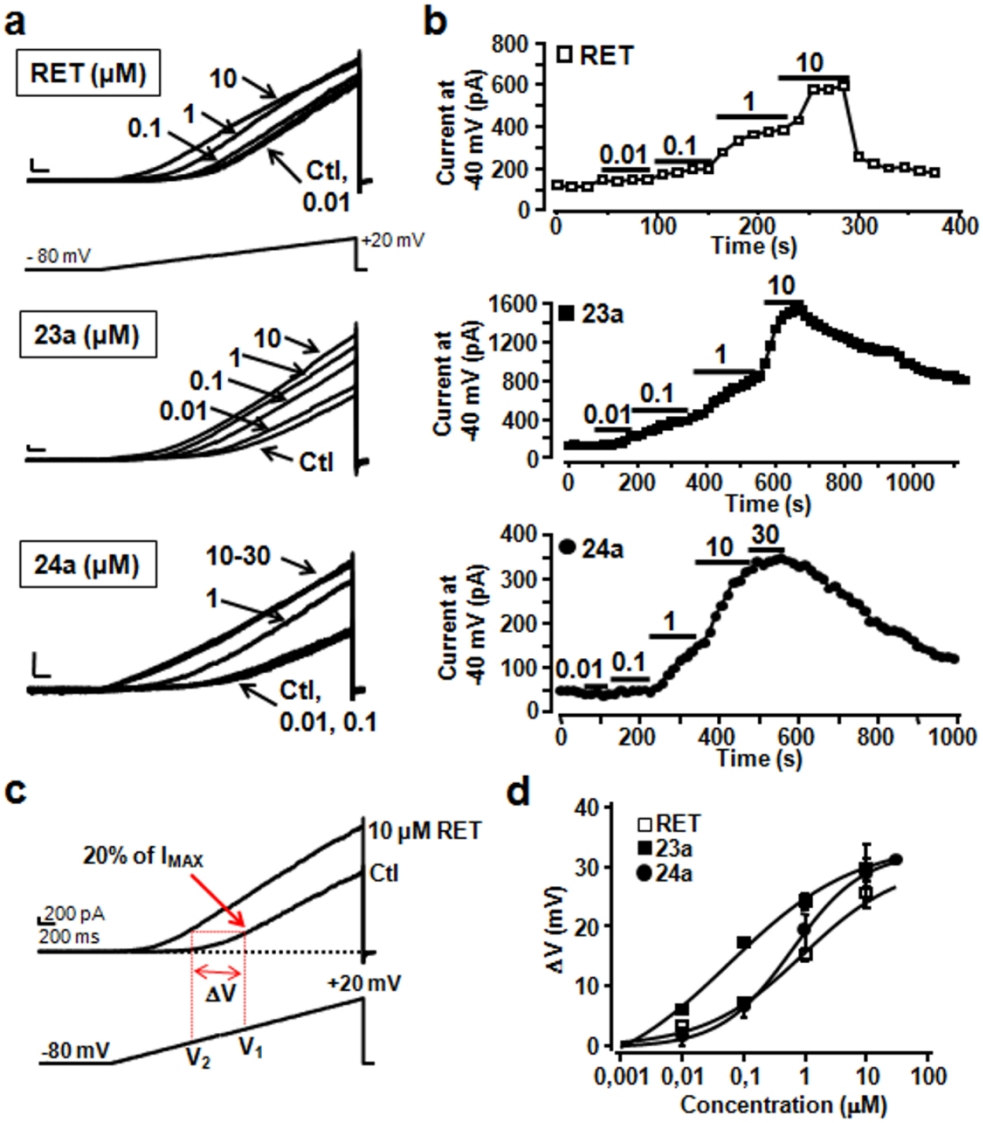

Figure 3. Effect of retigabine, 23a and 24a on ramp-evoked Kv7.2 current. a. Representative whole-cell current traces from Kv7.2 channels activated by the indicated ramp protocol recordedin control conditions and upon exposure to 0.01-10 μM retigabine (RET), 23a and 24a. b. Time courses of Kv7.2 current potentiation by retigabine (RET), 23a and 24a. The steady-state amplitudes of the peak currents at -40 mV were plotted as a function of time. The bars on top of the plot indicate the duration of drug application. Current scale, 200 pA; time scale, 0.2 s. c. Protocol used to calculate ΔV (V2-V1) at 20% of current peak value for controls (V1) and after RET exposure (V2). d. Dose-response curve for RET-, 23a-, and 24a-induced ΔV shift.

119x137mm (300 x 300 DPI)

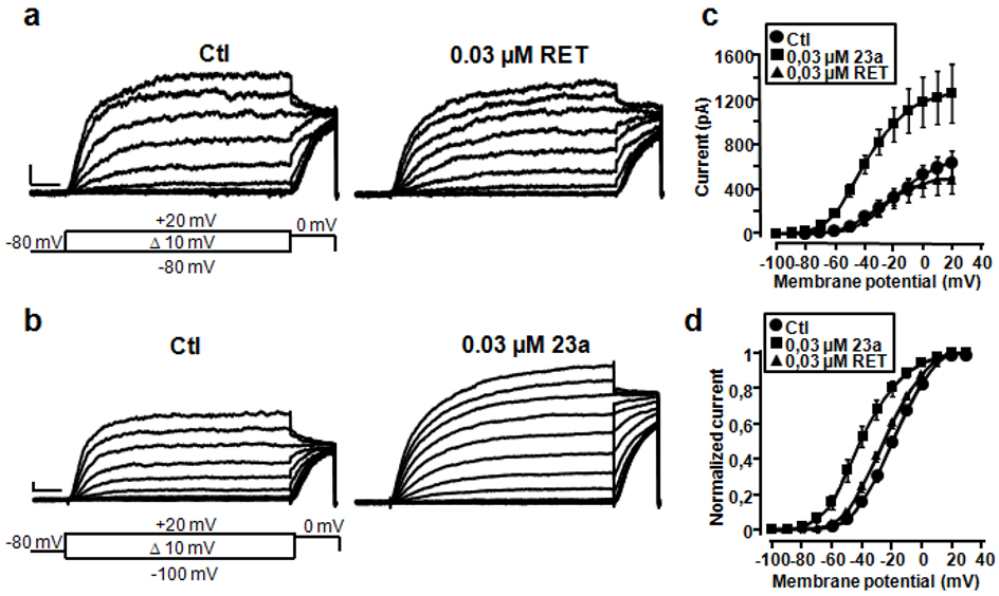

Figure 4. Effect of retigabine and 23a on the activation curve of Kv7.2 channels expressed in CHO cells. a-b. Representative macroscopic current traces recorded from a CHO cell expressing Kv7.2 homomeric channels in response to the indicated voltage protocol before (left) and after (right) application of 0.03 µM RET (a) and 23a (b). Current scale, 100 pA; time scale, 0.2 s. c. Current/voltage curves for Kv7.2 currents before and after application of RET or 23a. d.Normalized I/V curves for Kv7.2 currents before and after application of RET or 23a. Continuous lines represent fits of the experimental data to a double Boltzmann distribution.

80x49mm (300 x 300 DPI)

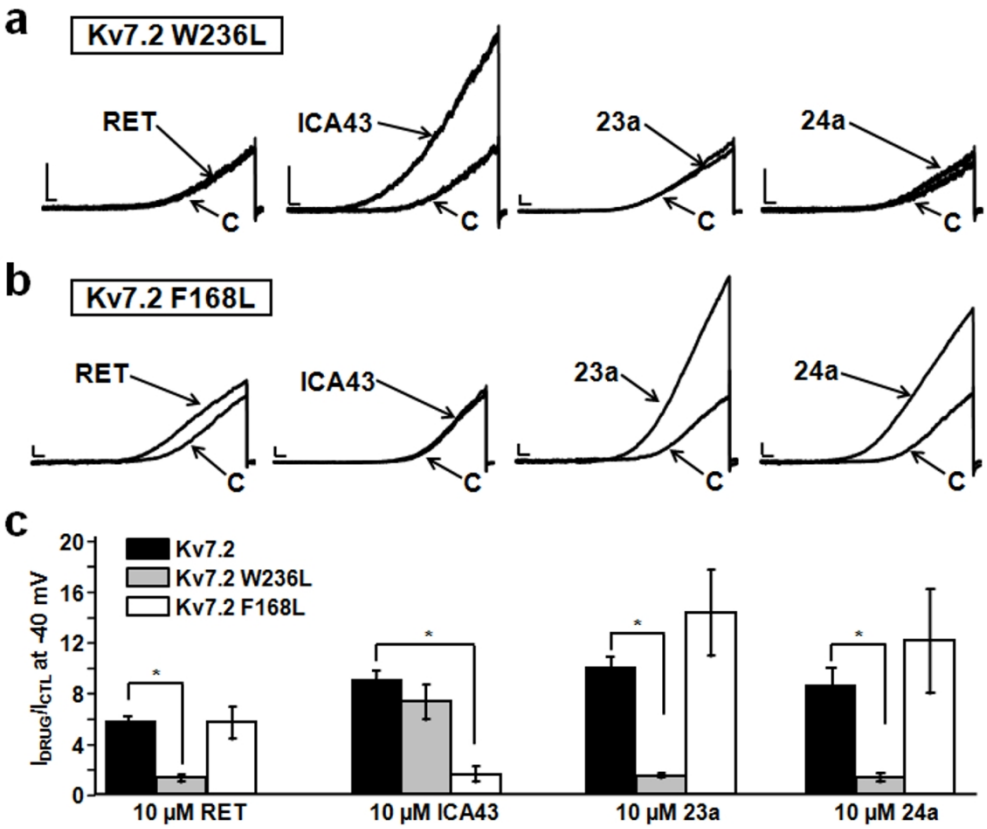

Figure 5. The W236 residue in Kv7.2 exerts a critical influence on 23a and 24a abilty to activate Kv7.2 currents. a-b. Representative traces of whole-cell ramp-evoked currents from Kv7.2 W236L (a) and Kv7.2 F168L (b) channels upon applicatio of 10 µM retigabine (RET), ICA 27243 (ICA43), 23a and 24a. c. Quantification of the effects of the indicated compounds on Kv7.2, W236L and Kv7.2 F168L currents; data are expressed as the ratio between current amplitude at -40 mV in the presence and absence of 10 µM drugs (IDRUG/ICTL). Each data point is expressed as the mean ± standard error of the mean (SEM) of at least 3 cells recorded in at least 2 independent transfections. * indicates values significantly different ($p < 0.05$) from respective controls.

119x99mm (300 x 300 DPI)

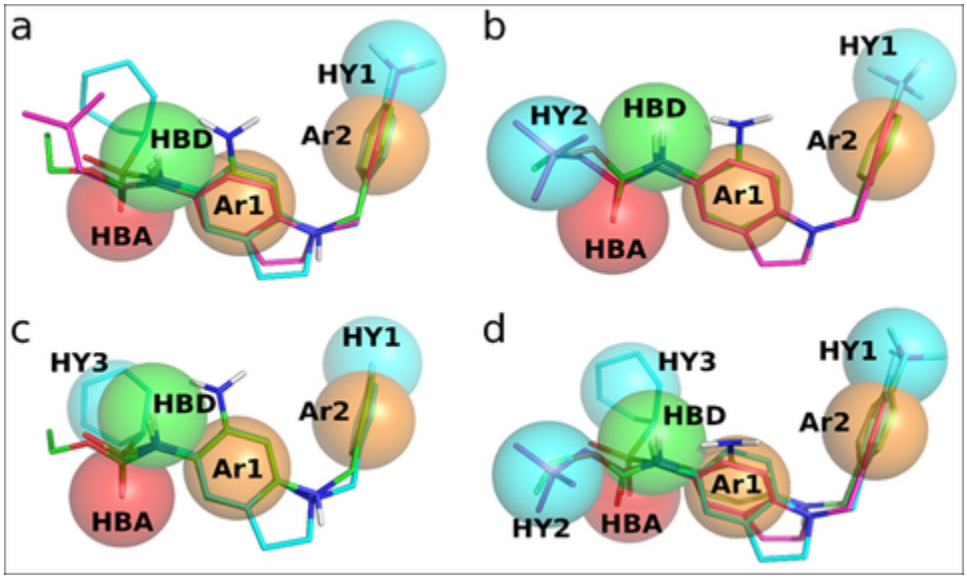

Figure 6. Pharmacophore models developed on the basis of our novel Kv7 channel activators. Pharmacophore features are color-coded as follows: Hydrophobic (HY – cyan), Aromatic (Ar – orange), Hydrogen Bond Donor (HBD – green), Hydrogen Bond Acceptor (HBA – red). Panel a) Model A with compounds 24a and 8a depicted in magenta and cyan sticks, respectively. Panel b) Model B with compound 24a depicted in magenta sticks. Panel c) Model C with compound 8a depicted in cyan sticks. Panel d) Model D with compounds 24a and 8a depicted in magenta and cyan sticks, respectively. Retigabine is depicted as reference, in every panel, in green sticks.

40x24mm (300 x 300 DPI)

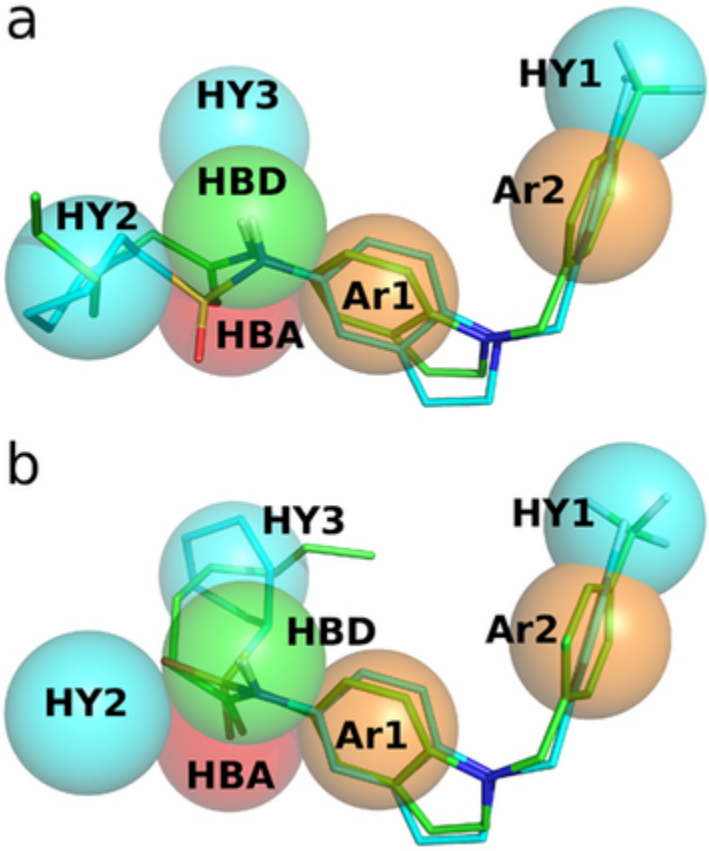

Figure 7. Compounds 23a (green sticks) and 8a (cyan sticks) fitting feature HY2 (panel a) and HY3 (panel b). Pharmacophore features are color-coded as follows: Hydrophobic (HY – cyan), Aromatic (Ar – orange), Hydrogen Bond Donor (HBD – green), Hydrogen Bond Donor (HBD – green).

30x36mm (300 x 300 DPI)

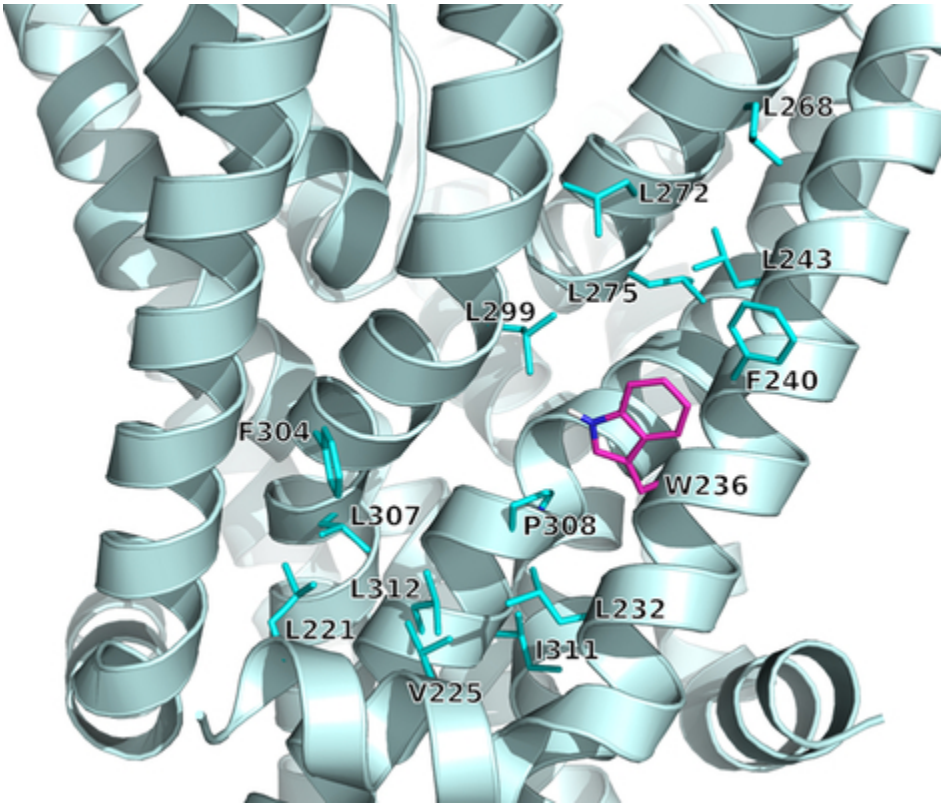

Figure 8. Kv modulators binding region modeled by homology with the CryoEM structure of Xenopus KCNQ1 channel (PDB id: 5vms). W236 (magenta sticks) is surrounded by several hydrophobic residues (cyan sticks) that could host chemical features HY1 and HY2/3.

39x33mm (300 x 300 DPI)

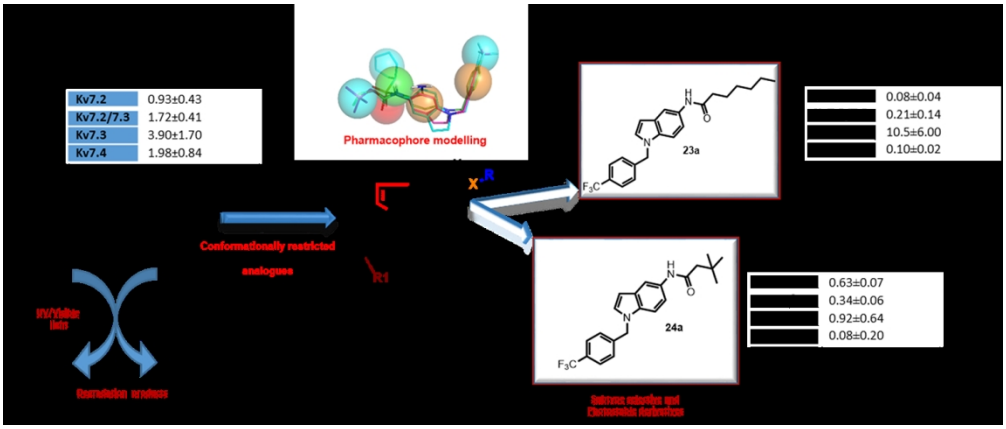

Table of contents graphic

131x55mm (300 x 300 DPI)